Connectivity and Regional Distribution of Constituent Cells of the Mammalian Locomotor Central Pattern Generator

by

Anna Lorraine Griener

A thesis submitted in partial fulfillment of the requirements for the degree of

Doctor of Philosophy

Centre for Neuroscience
University of Alberta

Abstract

The mammalian spinal cord contains a network of neurons capable of generating the rhythm and coordinating the complex motor pattern which underlies overground locomotion. This network, called the locomotor central pattern generator (CPG), can operate in isolation from afferent input and descending drive from higher centres of the central nervous system. Historically, investigations of the interneurons which comprise the locomotor CPG have relied on blind recording from spinal interneurons of the adult cat or the neonatal rodent. Molecular genetic approaches have recently been adopted to classify spinal cord interneurons into a defined set of cardinal populations based on shared embryonic origin.

Work presented in this thesis investigates the network composition of the neonatal mouse locomotor CPG. First, the firing behaviour, distribution, and morphology of unidentified locomotor-related lamina VII interneurons is examined to elucidate the general organizational principles governing the CPG. Second, using a unique TgDbx1^{Cre}; ROSA26^{EFP}; Dbx1^{LacZ} transgenic mouse model, the genetically-defined V0 and dI6 interneurons are investigated. Overall our findings demonstrate that within the spinal cord there is a differential distribution and network interconnectivity between interneurons which serve distinct functions. Among the unidentified rhythmically active lamina VII interneurons, putative rhythm generating (pRG) cells are located more medially and extend short processes towards nearby interneurons whereas putative pattern forming (pPF) cells are found laterally and extend long processes in the direction of the lateral motor pools. Investigation of the diversity between the $V0_V$ and $V0_D$ subpopulations indicates each population uses a distinct neurotransmitter, is differentially innervated by primary afferent, and follows unique synaptic pathways to contralateral motorneurons. The difference between the

activity of $V0_V$ and $V0_D$ interneurons during fictive locomotion leads us to hypothesize that $V0_V$ cells are primarily responsible for left-right coordination while $V0_D$ cells may serve a critical role in the integration of sensory information. Examination of the dI6 population indicates they are a predominantly commissural interneuron population, though premotor dI6 cells target motorneurons bilaterally. Rhythmically active dI6 interneurons located in lamina VII show firing behaviour consistent with a role in either rhythm generation or pattern formation, with the pPF dI6 cells preferentially situated laterally. As our hypothetically premotor pPF dI6 cells fire predominantly in phase with their local ventral root and we find little evidence to support an exclusively inhibitory nature, our results suggest that an excitatory population of dI6 interneurons may exist and thus further examination of the neurotransmitter phenotype is necessary. The present examination of spinal interneurons illuminates the manner in which the lumbar spinal cord is elegantly organized to execute the complex generation of locomotor activity.

Preface

All of the research conducted in this thesis was performed in accordance with the Canadian Council on Animal Care (CCAC) and approved by the Animal Welfare Committee at the University of Alberta. Protocol # 507 Title: "Analysis of the role of genetically-defined interneurons in the development and operation of the locomotor CPG". 2007-present.

Chapter 2 of this thesis has been published as Griener A, Dyck J, Gosgnach S. (2013) Regional distribution of putative rhythm-generating and pattern-forming components of the mammalian locomotor CPG. Neurosci. 250: 644-50. Dr. Dyck provided assistance with preliminary concept development. I was responsible for care and husbandry of the transgenic mouse colony, collection and analysis of all data, and assisted Dr. Gosgnach in experimental design, optimization, and composition of the manuscript.

The data for Chapters 3 and 4 of this thesis were collected from the same experimental animals by analyzing several different neuronal subtypes. Chapter 3 of this thesis has been published as Griener A, Zhang W, Kao H, Wagner C, Gosgnach S. (2015) Probing diversity within subpopulations of locomotor-related V0 interneurons. Dev Neurobiol. 75:1189-1203. Chapter 4 is expected to be submitted for publication in late 2016. For these projects I was responsible for care and husbandry of the transgenic mouse colony, performed viral and tracer applications to map axonal projections, harvested/prepared tissue for immunohistochemistry, carried out electrophysiological recordings and designed/refined/carried out tissue clearing protocols. Wei Zhang performed much of the immunohistochemistry and collected images. Henry Kao designed the custom MatLab analysis program used to analyze distribution. Christine Wagner assisted with cell counts/localization. For these projects I assisted Dr. Gosgnach with optimization of the experiments. While Dr. Gosgnach was primarily responsible for writing the manuscript that comprises chapter 3, I wrote chapter 4 independently.

Acknowledgments

I would first like to thank my Supervisor Dr. Simon Gosgnach for providing me with the opportunity to pursue my doctoral degree. I am grateful for the knowledge you shared, all of your help in the lab, and the creativity and optimism with which you guided my research. It is also my pleasure to thank the members of my Supervisory Committee, Dr. Greg Funk and Dr. Kelvin Jones. You each have an obvious enthusiasm for research and love of mentoring that have made it a pleasure to learn from you. I sincerely thank all three of you for your guidance and support throughout my studies.

Thank you to all of the experts who agreed to participate in my Candidacy Exam and Thesis Defence. I am grateful for the time and efforts of Dr. Bradley Kerr, Dr. Clayton Dickson, Dr. Declan Ali, and Dr. Ying Zhang.

I have had the great privilege of working with many enthusiastic young researchers whose intelligence, optimism, and humour have shortened the many long hours in the lab. I would like to extend my sincere and personal thanks to Dr. Ann Revill, Dr. Vishaal Rajani, Tucaauê Alvares, and Vivian Biancardi. I am endlessly impressed by the expertise and talent of Wei Zhang, without whom this thesis would not have been possible.

On a personal note, I am indebted to the uplifting support and motivation from my many great friends particularly Janet Montgomery, Dr. Stephanie Magnan, Jason Bondarevich and Jocelyn and Amanda Schielke-Ellis. My parents, Joanne and Glenn, my brothers, Matthew and Tom, their lovely wives, Lindsay and Abby, my hoard of loud and cheery nephews and my precious niece have all provided me with unfailing support and continuous encouragement, and for that I am grateful. Finally, I owe my deepest debt of gratitude to my loving husband, Ross Wilson. Without your steadfast support in the face of the challenges this program presented I would not have made it to the end.

Thank you.

Table of Contents

Chapter 1 – General Introduction 1
1.1 Introduction 2
1.2 Rationale for Researching the Locomotor CPG 3
1.3 Neural Connectivity in the Feline Hindlimb Locomotor CPG 4
1.3.1 Preparations used to study locomotion in the cat 4
1.3.2 Spinal interneurons identified via input from sensory receptors 6
1.3.3 Spinal interneurons mediating presynaptic inhibition 19
1.4 Neural Connectivity in the Murine Hindlimb CPG 20
1.4.2 Network architecture defined using wildtype rodents 21
1.4.3 Incorporation of molecular genetics into the study of the Locomotor CPG 28
1.4.4 Ventral Spinal Interneuron Populations 29
1.4.5 Dorsal Spinal Populations 46
1.5 Comparison of genetically and functionally defined spinal interneurons 55
1.6 Conceptual models of the locomotor CPG 58
1.7 Conclusion 63
Chapter 2 - Regional distribution of rhythm generating and pattern forming components of the mammalian locomotor CPG. 65
2.1 Abstract 66
2.2 Introduction 67
2.4 Results 72
2.5 Discussion 75
2.6 References 79
2.7 Figures 84
Chapter 3 – Probing diversity within subpopulations of locomotor-related V0 interneurons. 88
3.1 Abstract 89
3.2 Introduction 90
3.3 Materials and Methods 91
3.4 Results 95
3.5 Discussion 103
3.6 References 110
3.7 Figures 117

Chapter 4 – Anatomical and electrophysiological characterization of dI6 interneurons in the neonatal mouse spinal cord. 127
4.1 Abstract 128
4.2 Introduction 129
4.3 Materials and Methods 131
4.4 Results 136
4.5 Discussion 149
4.6 References 162
4.7 Figures 171
Chapter 5 – General Discussion 183
5.1 Summary 183
5.2 Discussion & Future Directions 183
References 190

List of Tables

Table 3.1. Distribution of all V0 interneurons as well as ventral and dorsal subpopulations in the mouse lumbar spinal cord

Table 4.1 Distribution of dI6 interneurons in the TgDbx1^{Cre}; R26^{EFP}; Dbx1^{lacZ} neonatal mouse spinal cord

List of Figures

Chapter 2

Figure 1. *Activity of RG and PF cells during ipsilateral non-resetting deletions of fictive locomotion.*

Figure 2. *Regional distribution of PF and RG cells.*

Figure 3. *Morphological characteristics of PF and RG cells.*

Chapter 3

Figure 1. *Distribution of V0 subpopulations in the lumbar spinal cord.*

Figure 2. *$V0_D$ cells are glycinergic.*

Figure 3. *$V0_D$ cells receive primary afferent input.*

Figure 4. *Serononergic innervation of $V0_V$ and $V0_D$ cells.*

Figure 5. *V0 cells project axons towards contralateral motoneurons.*

Figure 6. *V0 cells lateral to the central canal are active at all fictive locomotor frequencies*.

Chapter 4

Figure 1. *Distribution of dI6 interneurons in the mouse spinal cord*.

Figure 2. *dI6 interneurons receive primary afferent and descending serotonergic input*.

Figure 3. *The majority of dI6 interneurons are commissural*.

Figure 4. *dI6 interneurons form mono- and disynaptic contacts on flexor and extensor motorneurons bilaterally.*

Figure 5. *A minority of dI6 interneurons are glycinergic*.

Figure 6. *Firing behaviour and location of putative RG and PF dI6 interneurons*.

Figure 7. *Morphological reconstruction of pRG and pPF dI6 interneurons*.

List of Abbreviations

5-HT – 5-hydroxytryptamine (serotonin)

aCIN – ascending commissural interneuron

adCIN – bifurcating (ascending and descending) commissural interneuron

aCSF – artificial cerebrospinal fluid

AMPA – α-amino-3-hydroxy-5-methylisoxazole-4-proprionate

BMP – bone morphogenetic protein

ChAT – choline acetyltransferase

CIN – commissural interneuron

CNS – central nervous system

CNQX – 6-cyano-7-nitroquinoxaline-2,3-dione

CPG – central pattern generator

DA – dopamine

daCSF – dissecting artificial cerebrospinal fluid

dCIN – descending commissural interneuron

DTA – dyptheria toxin A

E0.5 – E18.5 – embryonic day 0.5 – 18.5

EMG – electromyogram

ENG – electroneurogram

EPSC – excitatory postsynaptic current

EPSP – excitatory postsynaptic potential

FP – fluorescent protein

FRA – flexion reflex afferent

GABA – γ-aminobutyric acid

GAD65/67 – glutamic acid decarboxylase 65/67

GC – gastrocnemius muscle

GTO – Golgi tendon organ

IPSC – inhibitory postsynaptic current

IPSP – inhibitory postsynaptic potential

L-DOPA – L - 3,4 – dihydroxyphenylalanine

L1 – L6 – first lumbar to sixth lumbar

MLR – mesencephalic locomotor region

NMDA – *N*-methyl-D-aspartate

P0 – P21 – postnatal day 0 to 21

PAD – primary afferent depolarization

pPF – putative pattern forming

pRG – putative rhythm generating

PRV-152 – pseudorabies virus 152

raCSF – recording artificial cerebrospinal fluid

RC – Renshaw cell

SCI – spinal cord injury

sCIN – segmental commissural interneuron

Shh – sonic hedgehog

SP – superficial peroneal nerve

T1 – T13 – first thoracic to thirteenth thoracic

TA – tibialis anterior muscle

TS – triceps surae muscle

TTX – tetrodotoxin

UBG – unit burst generator

vAChT – vesicular acetylcholine transporter

vGluT1-3 – vesicular glutamate transporter 1 - 3

viaat – vesicular inhibitory amino acid transporter

Chapter 1 – General Introduction

1.1 Introduction

It is becoming increasingly apparent that the true power of the central nervous system rests not in the neurons *per se*, but rather arises from the vast and intricate web of connectivity which binds the cells together. Orchestrated activity within circuits of neurons yields an array of highly complex behaviours which could not be achieved by neurons working in isolation. In mammals, many rhythmic motor movements, including breathing, whisking, and chewing, are coordinated by specialized neural circuits termed Central Pattern Generators (CPGs). The defining feature of a CPG is its intrinsic ability to generate and sustain rhythmic output in the absence of phasic external drive. The constituent CPG neurons, appropriately connected and acting in concert, are all that is required to evoke and harmonize the activity of many muscles into one elegant movement.

The rhythmic muscle contractions driving locomotion result from activity in the locomotor CPG, a neural network contained entirely within the spinal cord. Just over a century ago, Sherrington was among the first to show that complex stepping movements could be elicited in spinal cord transected animals following sensory stimulation (Sherrington, 1910). Soon thereafter, Brown recorded rhythmic flexor-extensor alternation in a spinalized and deafferented animal, thereby demonstrating that sensory input was dispensable for rhythm generation (Brown, 1911). This showed that the spinal cord, independent of descending and sensory input, contained all of the necessary elements to generate rhythmic locomotor activity. This foundational experiment focused all further research regarding the structure and operation of the locomotor CPG onto the cells of the spinal cord.

Work presented in this thesis builds upon this body of knowledge by examining general organizational principles of locomotor-related spinal interneurons. The

morphology, connectivity, and regional distribution of functionally and genetically defined spinal interneurons were examined with the objective of understanding the cellular architecture of the mammalian locomotor CPG.

1.2 Rationale for Researching the Locomotor CPG

In addition to addressing how the activity of neural networks generates complex motor behavior, the primary impetus for understanding the cellular origin of walking in animals is to understand the mechanism of walking in humans and, as a corollary, to develop interventions for individuals with locomotor impairments. Many key features of overground locomotion observed in quadrupedal animals are common to bipedal locomotion in humans (reviewed in Guertin, 2014). However, the existence of a spinally restricted CPG in humans is difficult to prove as spinal network elements cannot be completely isolated from descending and sensory inputs. In human infants, before 1 year of age the motor cortex and descending motor tracts are sufficiently immature that the spinal CPG can be studied in relative isolation (reviewed by Yang et al., 2004). Standing babies on a moving treadmill or tilting their bodies forward while supporting their weight can evoke stepping movements. In adults, patients with clinically complete spinal cord injuries can generate complex stepping patterns in the absence of descending control (reviewed by Harkema, 2001). In both populations the methods for eliciting locomotion and the reflex responses to sensory stimulation are qualitatively similar to those observed in animal models, and it thus stands to reason that the underlying neural networks are conserved from quadrupeds to humans. A thorough understanding of the composition and operation of the mammalian locomotor CPG is thus invaluable toward developing interventions and restoring function after injury to the human central nervous system.

Classically, spinal networks controlling walking were explored in the adult cat. More recently, research has shifted towards the newborn mouse. Work in both species has yielded significant insights into the organization of the mammalian CPG, however the shift in model and associated discrepancy of experimental methodologies has led to a disconnection between functionally-defined spinal interneurons in the cat, and genetically-defined interneurons in the mouse. The aim of the following literature review is to analyze the anatomical characteristics and cellular connectivity of interneuron populations defined in each preparation in order to identify commonalities that would suggest a shared identity.

1.3 Neural Connectivity in the Feline Hindlimb Locomotor CPG

1.3.1 Preparations used to study locomotion in the cat

During overground walking in intact animals, locomotor activity can be measured using electromyogram (EMG) recording from limb muscles. Such studies provide significant information about the output of the locomotor CPG as a whole, particularly with respect to the pattern and timing of activation of individual muscles (Engberg & Lundberg, 1969, English, 1978). Activity in flexor and extensor muscles correspond to the swing and stance phases of locomotion, respectively.

Considerable insight into the neural control of locomotion in mammals has been achieved through experiments using the decerebrate or spinal cord transected cat preparations. At the cost of isolating the brainstem and spinal cord from higher brain circuits, the decerebrate preparation allows for the experimental manipulation of the locomotor networks in adult animals. Removal of the cerebral cortices occurs via transection through the brainstem (reviewed by Whelan, 1996). Depending on the

level of the lesion, when placed on a moving treadmill the decerebrate cat may begin to walk spontaneously in response to sensory input from the moving limbs. Alternatively, stimulation of the mesencephalic locomotor region (MLR) may be required to elicit locomotion. The MLR is a small area in the pons including regions of the pedonculopontine and cuneiform nuclei (Shik et al., 1966). With increasing intensity of MLR stimulation, spinal networks convert the tonic descending drive into different locomotor gaits, increasing in speed from walking to trotting to galloping. In spinal cord transected cats, the spinal locomotor CPG can be studied in isolation from higher CNS structures. In these cats, administration of the noradrenaline precursor L-3,4-dihydroxyphenylalanine (L-DOPA) with a monoamine oxidase inhibitor results in bouts of alternating flexor-extensor activity following hindlimb afferent stimulation (see Lundberg, 1979). Both the decerebrate and spinal preparations allow investigation of the locomotor CPG without confounding effects of anaesthetics.

In order to obtain intracellular recordings from spinal neurons, the animal must be immobilized. In immobilized preparations, rather than recording locomotor activity directly from flexor and extensor muscles, electroneurogram (ENG) recording from the efferent nerves provides a measure of *fictive* locomotor activity. The efferent output measured using such a preparation shares many of the key features of locomotion recorded using EMG from moving muscles including bilateral alternation and the appropriate sequential recruitment of diverse hindlimb muscles (see Rossignol, 1996). As they allow for simultaneous study of individual spinal neurons and global network output, the paralyzed decerebrate and spinal cord transected cat preparations have been mainstays of locomotor CPG research.

1.3.2 Spinal interneurons identified via input from sensory receptors

Due to the readily accessible nature of peripheral sensory receptors, classical studies of spinal cord architecture defined interneuron populations via their response to afferent input and the reflex pathways they subserve. Distinct reflex pathways can be activated by varying the modality of mechanical stimulus applied to a limb or the intensity of electrical stimulus applied to a nerve. Careful observation of the resulting activity in interneurons and motorneurons provides insight into the nature of connections between cells. First order interneurons are defined by their monosynaptic input from sensory afferents. Last order interneurons are defined by their monosynaptic output to motorneurons, and are thus also called premotor interneurons. Cells interposed between the two are classified as second order, third order, etc., based on the number of synapses intervening from the sensory afferent. Excitatory or inhibitory postsynaptic potentials (EPSPs or IPSPs, respectively) recorded from downstream targets reveal the neurotransmitter phenotype of a population. This method of function-based classification was applied in studies of the feline lumbar spinal cord and led to the establishment of numerous interneuron populations. Confounding this approach is the considerable convergence and divergence of synaptic information conveyed by multiple reflex pathways. Interneurons defined by their dominant role in a given reflex arc may also be involved in other spinal circuits. Nevertheless, this approach defined canonical interneuron populations and revealed fundamental information about the neural architecture of the mammalian spinal cord.

The interaction between spinal reflexes and locomotion is evidenced by the phase-dependent reversal of some reflexes, the suppression or emergence of reflex pathways at the onset of locomotion, and the delay or advancement of stance-swing phase switching in response to afferent stimuli. Given this functional interplay, it stands to reason that physical connections must exist between reflex and locomotor

circuitries, be it in the form of shared constituent neurons and/or synaptic contacts between discrete interneuron populations. Therefore studying the locomotor-related activity of interneuron populations defined by their input from proprioceptors provides a means of elucidating the network composition of the locomotor CPG.

1.3.2.1 Interneurons mediating reflexes from Ia Afferents

Ia afferents are large diameter, myelinated fibres originating in the muscle spindle. They convey information regarding muscle fibre length, rate of change in length, and are sensitive to high frequency vibration. Activation of Ia afferents evokes the monosynaptic reflex, which reveals one of the simplest spinal pathways. Also called the stretch, myotactic, or tendon jerk reflex, this reflex is characterized by a compensatory shortening of a muscle in response to muscle stretch. The increase in length is signaled by spindle primary endings through Ia afferents to the spinal cord wherein the Ia afferents excite the α-motorneurons of homonymous and heteronymous muscles.

In addition to direct effects on motorneurons, Ia afferents elicit longer latency reflexes through diverse spinal interneurons. In the cat, interneurons with monosynaptic input from Ia afferents originating in hindlimb muscles are located throughout the lumbar enlargement in laminae V, VI, VII and VIII (reviewed in Jankowska, 1992). As Ia afferents are the largest, fastest conducting and have the lowest activation threshold of all sensory fibres, these spinal pathways can readily be studied in isolation.

The sensitivity of the locomotor CPG to change in muscle length is well documented. The position of the limb, signalled via primary afferent receptors in the hip flexors, is of particular importance in regulating locomotor activity. Artificially stretching the hip flexors during treadmill locomotion initiates flexion (Hiebert et al.,

1996). The locomotor rhythm can also be entrained by experimentally manipulating the position of the hip joint (Kriellaars et al., 1994). Indeed, it has been proposed that during walking, full extension of the hip provides one of the primary sensory stimuli required to allow phase switching to flexion (Grillner & Rossignol, 1978). Because these stimuli change speed of locomotion and alter the output of all muscles of the limb it is presumed that their effects are due to direct interaction with the locomotor CPG.

Ia Inhibitory Interneurons

Ia inhibitory interneurons (IaINs) mediate the reciprocal inhibition of antagonist motorneurons following activation of Ia muscle spindle afferents (Eccles et al., 1956, Hultborn et al., 1971). They are located ventrally in lamina VII in close proximity to their homonymous motor nuclei (Hultborn et al., 1971). IaINs extend long ipsilaterally restricted axons which either ascend or descend in the lateral or ventral funiculi across many segments. It has been shown that axon collaterals extend into the motor nuclei of multiple antagonist muscles. As their name implies, IaINs are exclusively inhibitory and evoke strychnine-sensitive IPSPs in their target neurons, indicating a glycinergic phenotype (Curtis, 1959).

The only afferent terminals to contact IaINs are those of the Ia muscle spindle afferents, with individual IaINs receiving convergent input from several synergist muscles (Hultborn et al., 1971, 1976). Within the spinal cord, IaINs receive polysynaptic excitatory input from interneurons interposed in the Flexion Reflex Afferent pathway (see later Section 1.3.2.4). Spinal inhibition of IaINs derives from two main sources: other IaINs and Renshaw Cells. Inhibition between IaINs occurs between functionally opposed subpopulations; in other words, IaINs receiving Ia afferents from a given muscle will inhibit IaINs contacted by Ia afferents from the

antagonist muscle. The post-synaptic targets are quite restricted as other IaINs appear to be the only interneuron target of IaINs (Hultborn et al., 1976).

At rest, IaINs are tonically active (Hultborn et al., 1971). During MLR-evoked fictive locomotion in the paralyzed decerebrate preparation, Ia inhibitory interneurons become rhythmically active in phase with motorneurons supplied by the same Ia afferent (Feldman & Orlovsky, 1975). The reciprocal nature of the connections between functionally opposed motorneurons initially implicated IaINs in evoking flexor-extensor alternation. Subsequent analysis indicated that IaINs are active after the onset of activity in their 'source' muscle and are thus not responsible for driving flexor-extensor alternation (Pratt & Jordan, 1987). Instead, recent analysis has suggested that the locomotor CPG drives motorneurons of a given muscle in parallel with the IaINs which inhibit its antagonist (Geertsen et al., 2011). Thus IaINs contribute to hyperpolarization of motorneurons during their inactive locomotor phase, but are not fundamentally responsible for generating the locomotor rhythm.

1.3.2.2 Interneurons mediating reflexes from Ib Afferents

Ib afferents are large diameter, myelinated fibres originating in the Golgi Tendon Organ (GTO) and provide information regarding the tension within a muscle. Typically the threshold for activation of Ib afferents is slightly higher than that of Ia afferents and the conduction velocity is slightly lower. Due to these similarities, it is often difficult to distinguish between effects mediated by Ia *versus* Ib afferents. Interneurons contacted by Ib terminals are located in laminae V, VI, dorsal VII, and VIII (reviewed in Jankowska, 1992).

Ib Inhibitory Interneurons and Ib Interneurons

Group I non-reciprocal inhibition refers to the di- and trisynaptic inhibition of homonymous and synergist α-motorneurons paired with trisynaptic excitation of

antagonist motorneurons that occurs following activation of the GTO (reviewed in Jankowska, 1992). Formerly described as autogenic inhibition or the inverse myotactic reflex, several classes of spinal interneurons can be identified and the connections between them can be mapped through careful investigation of this reflex. The disynaptic component is mediated by Ib inhibitory interneurons (IbINs). IbINs are located in lamina VI and dorsally within lamina VII. They are glycinergic premotor interneurons with ipsilaterally restricted axons (Curtis 1959, 1968, Rudomin et al., 1990). Oligosynaptic Ib effects are mediated by the broader population of Ib interneurons. These interneurons are located within the same laminae as IbINs and similarly evoke ipsilateral responses. In contrast, Ib interneurons can be excitatory or inhibitory, utilizing glutamate, GABA, or glycine. While not all Ib interneurons make monosynaptic contacts onto motorneurons, both excitatory and inhibitory premotor Ib interneurons exist.

Reflex responses to Ib afferent input occur across a broad array of target motorneurons and can thus bind together activity in many muscle groups. In contrast to the restricted nature of Ia afferent effects about a single joint, responses to Ib afferents of a particular muscle can be recorded from most motor pools of the ipsilateral limb. Furthermore, individual Ib interneurons receive convergent input from many Ib afferents, including those originating in extensors, and flexors. Functionally, there is a clear bias towards extensor effects. Stimulation of Ib afferents from extensor muscles yields potent disynaptic inhibition of extensors and trisynaptic excitation of flexors. Conversely, similar treatment applied to flexors evokes only weak responses.

Although named for their dominant input from Ib afferents, Ib interneurons integrate synaptic input from a variety of sensory receptors. Primary muscle spindle afferents can activate Ib interneurons, including the IbINs. Given the similarity of threshold and conduction velocity it can be difficult to experimentally distinguish

between interneuronal responses evoked by Ia or Ib afferents. Group II, cutaneous, joint, and interosseous afferents can likewise activate Ib interneurons, however this occurs indirectly through 1-2 intervening spinal neurons. Mutual inhibition has been observed between Ib interneurons.

The reflex reversal involving the Ib pathway that occurs during locomotion is one of the most striking examples of the interplay between reflexes and the neural circuits of the locomotor CPG. During locomotion, rather than homonymous inhibition, Ib afferent stimulation instead causes an excitation of homonymous and synergist α-motorneurons. Several mechanisms account for this phenomenon. Generally, homonymous inhibition is reduced as group I non-reciprocal inhibition is suppressed during both phases of locomotion (Jankowska et al., 1981). Additionally, with the onset of locomotion a unique disynaptic excitatory reflex emerges. Both Ia and Ib afferents from extensor muscles elicit disynaptic excitation of extensor motorneurons, specifically during the extension phase (Guertin et al., 1995, Angel et al., 1996). The responsible interneuron is located in lamina VII of the lumbar enlargement and is rhythmically active, in phase with extension (Angel et al., 2005).

Group I sensory input can regulate the ongoing stepping activity. Stimulation of group I ankle extensor nerves during the flexion (swing) phase of locomotion causes a resetting to extension (stance) and shortens the period of both the step in which the stimulus was applied and the subsequent step. The early onset of extension occurs throughout all extensor muscles of the limb. This, together with the change in cycle period, implies that group I input directly effects the ongoing activity of the locomotor CPG (Guertin et al., 1995, Conway et al., 1987, McCrea, 2001). Similar stimulation of group I ankle extensor nerves during extension (stance) enhances extensor motorneuron output. In contrast to stimulation during flexion, the step-to-step cycle period is unaffected but rather the duty period for extension versus flexion is altered;

that is, flexion is shortened to compensate for the prolonged extension such that the onset of the subsequent step is not displaced. The consequence of flexor group I afferent stimulation is weaker than of extensor stimulation and is more variable between different muscles (McCrea, 2001).

Input from ankle extensor group I afferents has been suggested to serve a pivotal role in the transition from stance to swing in decerebrate cats walking on a treadmill (Duysens & Pearson, 1980). Specifically, sustained input from load sensitive afferents prevents the initiation of flexion. As aforementioned, preventing extension of the hip also inhibits the transition from stance to swing (Grillner & Rossignol, 1978). The behavioural consequence of these two pathways is that the limb will not be lifted until it has passed fully behind the animal's body and the weight has been transferred to the opposite limb.

1.3.2.3 Interneurons mediating reflexes from Group II Muscle Spindle Afferents

Secondary muscle spindle afferents provide information about muscle length, though unlike primary spindle afferents, they are largely insensitive to the rate of change. They possess myelinated, medium diameter axons and thus conduct more slowly than Ia and Ib afferents and are activated in the range of 2-5 times threshold of Ia afferents. While group II afferents do form monosynaptic contacts onto homonymous motorneurons, these connections appear to be functionally weak. Rather, their response is mediated primarily via spinal interneurons (Lundberg et al., 1977).

Following stimulation of the mixed peripheral nerve, the dominating response to group II spindle stimulation is inhibition of extensors and excitation of flexors, irrespective of the function of muscle of origin (Eccles & Lundberg, 1959, Holmqvist &

Lundberg, 1961, Wilson & Kato, 1965). To a lesser extent excitation of extensors does occur in some preparations.

Group II interneurons

Group II interneurons include those cells which receive monosynaptic input from group II muscle spindle afferents and in turn synapse directly onto motorneurons (Jankowska, 1992). In the cat, interneurons contacted by group II muscle afferent terminals are found in two locations: laminae IV-V of the dorsal horn, and laminae VI-VIII of the intermediate and ventral horns. However, interneurons of the dorsally located subpopulation do not make monosynaptic contact onto motorneurons and are thus not classified as Group II interneurons. Within Group II interneurons in laminae VI-VIII, the ventrally located cells are primarily commissural and synapse on contralateral motor neurons (Jankowska et al., 2002). The Group II interneuron population contains both excitatory and inhibitory neurons and can therefore mediate disynaptic EPSPs and IPSPs in motorneurons. Individual α-motorneurons often receive convergent input from many Group II interneurons.

Motorneurons are the obligate synaptic target of Group II interneurons, though abundant connectivity to other spinal neurons has been demonstrated (Jankowska, 1992). Group II interneurons extend axons which travel intersegmentally in the lateral and ventral funiculi. Axon collaterals branch off and arborize within laminae VII, VIII and IX, consistent with their targeting interneurons as well as motorneurons. Among the interneuron targets are other Group II interneurons. Interestingly, Group II interneurons mediate disynaptic IPSPs or EPSPs in ipsilaterally or contralaterally located Group II interneurons. Thus it appears that Group II interneurons include both excitatory and inhibitory commissural interneurons with branches to the ipsilateral motorneuron.

Group II interneurons have been shown to be co-excited by group II afferents of both flexors, and extensors. They can also be activated by group II afferents from muscles in the contralateral limb, though this occurs indirectly through an interposed interneuron. It has recently been suggested that genuine Group II interneurons located in the intermediate zone are synaptic targets of the interneurons contacted by group II muscle afferents in the dorsal horn (Jankowska et al., 2002). They are therefore interposed in di- and trisynaptic reflex pathways from group II afferents to motorneurons. Direct afferent input to this population is not limited to group II fibres; Ia and/or Ib afferents have been found to directly contact 60% of the Group II interneurons (Edgley & Jankowska, 1987). Joint, interosseous, and both low and high threshold cutaneous afferents provide additional monosynaptic input to some cells. Interneurons of other reflex pathways can also affect Group II interneurons. For instance, Ib interneurons can evoke IPSPs in Group II interneurons. Additionally, Group II interneurons receive excitation from interneurons of the FRA pathways. Consequently, Group II interneurons are poised to integrate information from several sensory modalities.

1.3.2.4 Interneuron of the Flexion Reflex Afferent pathway

The Flexion Reflex Afferents (FRAs) include group II and III muscle, joint, and cutaneous afferents (Eccles & Lundberg, 1959). In acute spinal cats, stimulation of the FRAs results in excitation of the ipsilateral flexors and contralateral extensors, coupled to inhibition of their respective antagonists. This patterned muscle response can be obtained through two alternate spinal pathways: 1) that which mediates early, short-latency reflexes, or 2) after L-DOPA administration, the pathway which mediates late, long-latency reflexes involving bouts of alternating flexor-extensor activity. With L-DOPA administration and the emergence of the long-latency responses, activity in the early reflex pathway is depressed. Interneurons involved in the late effects are of

particular interest to studies of the locomotor CPG as their reciprocal organization was initially lauded as evidence of the Half-Centre Model for locomotor rhythm generation (Jankowska et al., 1967*b*; discussed further in Section 1.6).

Strong mutual inhibition occurs between the long-latency FRA pathways transmitting excitation to ipsilateral flexors and the pathways transmitting excitation to extensors from contralateral FRAs (Jankowska et al., 1967*a*). That is, stimulation of contralateral FRAs inhibits excitatory transmission to ipsilateral flexors and conversely, stimulation of ipsilateral FRAs inhibits excitatory transmission of extensors by contralateral FRA pathways. This mutual inhibition occurs via an interneuron interposed between the FRAs and their target motorneurons. Putative interneurons mediating this inhibition were found in lamina VII; these neurons were either excited by ipsilateral and inhibited by contralateral FRA stimulation, or were excited by contralateral and inhibited by ipsilateral FRA stimulation. These strong mutual inhibitions between antagonists were offered as the neural correlate of Brown's theoretical half-centres (Jankowska et al., *1967b,* Brown, 1911).

Due to the diversity of afferent inputs as well as the complexity of the motor response they evoke (i.e., reactions on both sides of the spinal cord and between various antagonist motor pools) interneurons of the FRA pathways remain difficult to categorize and evaluate using blind electrophysiological approaches.

1.3.2.5 Interneurons mediating the Stumbling-Corrective Reaction

The stumbling-corrective reaction denotes a behaviour in which a walking cat will lift its paw up and over a contacted obstacle in order to avoid tripping. During treadmill locomotion in the chronic spinal cat, tactile stimuli applied to the dorsum of the paw evoke different responses depending on the locomotor phase. During swing, the mild sensory input produces excitation of knee flexors and inhibition of extensors

coupled with brief excitation of ankle extensors which together raise the paw and clear the obstacle. Following the brief excitation of ankle extensors, a period of sustained activation of ankle flexors ensues (Buford & Smith, 1993, Forssberg, 1979, Forssberg et al., 1977, Pratt et al., 1996, Prochazka et al., 1978, Wand et al., 1980). Conversely, the same sensory stimulus applied during the stance phase evokes excitation of extensors and inhibition of flexors, in a phenomenon referred to as the stumbling-preventive reaction. In the subsequent flexion phase, flexor motorneuron activity is increased (Buford & Smith, 1993, Forssberg, 1979).

Due in part to the complexity of the motor response, relatively little is known about the interneurons which underlie this reflex. During MLR-evoked fictive locomotion in the paralyzed, decerebrate cat, a stimulus applied to the superficial peroneal (SP) nerve during the flexion phase can provide a proxy of the stumbling-corrective reaction (Quevedo et al., 2005*a*). Intracellular recordings from motorneurons provide insight into the spinal circuits mediating this reflex (Quevedo et al., 2005*b*). At rest, SP stimulation causes inhibition of ankle flexor and extensor motorneurons. With the onset of locomotion, inhibition of extensors is suppressed, while that of flexors is enhanced. Additionally, in response to a stimulus train applied during flexion, ankle extensor motorneurons are depolarized through a spinal pathway consisting of 1 to 2 interneurons. Bifunctional muscles (knee flexors, hip extensors) are likewise depolarized. Ankle flexor motorneurons show a brief excitation which is rapidly overwhelmed by inhibition. These effects are mediated by short chains of ipsilaterally restricted interneurons which convey sensory input from the SP nerve to the appropriate motorneurons. To explain all of these findings the authors proposed a hypothetical model in which the SP nerve terminals contact 1) premotor excitatory interneurons, 2) excitatory interneurons which synapse onto the same premotor excitatory interneurons, and 3) constituent cells of the locomotor CPG. Two distinct

populations of inhibitory interneurons are proposed to underlie the inhibition of ankle flexors and extensors seen at rest. With the onset of locomotion, the CPG evokes opposing effects on each, inhibiting the population which suppresses ankle extensors and conversely exciting the population which suppresses ankle flexor motorneurons. Further exploration of this reflex pathway will necessitate characterization of the interneurons themselves.

1.3.2.6 Renshaw cells and recurrent inhibition

Recurrent inhibition presents another well characterized spinal circuit: Renshaw cells (RCs) receive cholinergic excitation from motor axon collaterals and in turn provide feedback inhibition to the homonymous and synergist α-motorneurons (Eccles et al., 1954). The inhibitory effects of RCs are mediated by both glycine and GABA as IPSPs recorded in α-motorneurons show strychnine- and bicuculline/picrotoxin-sensitive components (Cullheim & Kellerth, 1981). RCs are located close to the motorneurons, in lamina VII of the cat spinal cord (Carr et al., 1998), and extend axons within a few ipsilateral spinal segments (Jankowska & Lindstrom, 1971). In addition to targeting motorneurons, RCs inhibit other RCs, IaINs, and ventral spinocerebellar tract neurons. RCs provide parallel inhibition of the α-motorneurons and IaINs contacted by the same Ia afferents. This inhibition of tonically active IaINs results in the phenomenon of recurrent facilitation of antagonistic α-motorneurons.

The majority of the synaptic input onto RCs derives from motorneuron axon collaterals. Individual RCs receive cholinergic input from several synergist motorneurons, whereas input from antagonist muscles generally does not occur. A variety of spinal interneurons also target RCs. Mutual inhibition between RCs is well documented, with RCs receiving collaterals from extensor motorneurons predominantly inhibiting RCs excited by flexor motorneurons, and vice versa (Ryall 1981).

RCs do not receive monosynaptic afferent input but are indirectly sensitive to sensory input through spinal interneurons. Stimulation of cutaneous afferents and ipsilateral group II muscle afferents elicits polysynaptic excitation or inhibition of RCs (Ryall & Piercey, 1971, Piercey & Goldfarb, 1974, Wilson et al., 1964). Group III muscle afferents provide alternate polysynaptic excitation of RCs (Piercey & Goldfarb, 1974).

An early conceptual model explaining the neural mechanism of locomotor rhythm generation ascribed a pivotal role to RCs. The Miller & Scott model (1977) postulated that during the active locomotor phase an increase in RC-mediated recurrent inhibition would decrease the output of the dominant motorneuron pool. This would be coupled to recurrent facilitation of the antagonist motorneuron pool. This shift in excitability between motor pools was proposed to account for phase transitions during locomotion. Initially, this model was promising as it took into account known spinal synaptic pathways and the fact that RCs are rhythmically active during fictive locomotion. However, this model has since been discounted as closer examination of the behaviour of RCs has revealed their activity cannot support such a role. McCrea et al. (1980) demonstrated that RCs receiving primary input from flexor or extensor motorneurons fired preferentially during the flexor or extensor phases, respectively. However, burst onset in RCs occurs after the burst onset in the affiliated motorneuron. This demonstrates that RCs cannot be responsible for generating locomotor rhythm, but rather are rhythmic as a result of rhythmic input from motorneurons (Pratt & Jordan, 1987). Experiments blocking nicotinic acetylcholine receptors with mecamylamine, thereby silencing motorneuron input to RCs, failed to affect the locomotor drive potentials in motorneurons (Noga et al., 1987). Together this demonstrates that RCs cannot be responsible for locomotor rhythm generation.

1.3.3 Spinal interneurons mediating presynaptic inhibition

Attempts to understand the mechanisms of presynaptic inhibition provided another avenue towards defining the cellular architecture of the spinal cord. Presynaptic inhibition denotes a phenomenon first described by Frank and Fuortes as depression of the monosynaptic EPSP in extensor motorneurons following stimulation of the flexor muscle, without any change in the membrane properties of the motorneurons. Subsequent experiments have shown presynaptic inhibition is closely associated with primary afferent depolarization (PAD), wherein axo-axonic GABAergic synapses mediate a long-lasting reduction in neurotransmitter release from primary afferent terminals (reviewed in Rudomin & Schmidt, 1999). Activation of $GABA_A$ receptors on primary afferents results in Cl^- efflux, depolarization, and reduced Ca^{2+} influx, ultimately resulting in reduced neurotransmitter release. It is generally held that primary afferent depolarization is the mechanism responsible for presynaptic inhibition.

Presynaptic inhibition allows selective gating of sensory information arriving in the spinal cord. GABAergic axo-axonic synapses have been demonstrated on group Ia, Ib, II and large cutaneous primary afferent terminals (see Rudomin & Schmidt, 1999). Additionally, input from different afferent modalities elicits presynaptic inhibition of various sensory afferent types. This suggests incoming sensory information of diverse modalities can all be subjected to selective suppression as it arrives in the CNS. The spinal circuits mediating presynaptic inhibition remain poorly understood. Generally, the shortest pathway involves two spinal interneurons; the first-order excitatory interneuron receives afferent input and excites the GABAergic last-order interneuron which in turn evokes PAD in the target afferent (Jankowska et al., 1981). The last-order GABAergic PAD interneurons are located in laminae V and VI (Eccles et al., 1962).

Ia afferents from both flexors and extensors are subjected to PAD via Ia and Ib afferents originating predominantly from flexors. In the spinal cat, the Ia afferents to all ipsilateral motorneurons of the hindlimb are simultaneously subjected to PAD (Eccles et al., 1962). Ib afferents are subjected to PAD from both flexors and extensors and only via other Ib afferents. Group II afferents are subjected to PAD upon activation of group II muscle, cutaneous, and joint afferents and to a much lesser extent group I muscle afferents (see Jankowska & Riddell, 1998).

With the onset of locomotion, the spinal circuitry mediating presynaptic inhibition is altered. The excitability of Ia and Ib afferents from extensor muscles has been demonstrated to be cyclical and maximal during the flexor phase of locomotion, suggestive of cyclical modulation of PAD (Duenas & Rudomin, 1988). Intra-axonal recordings from Ia afferents have shown rhythmic PAD of Ia afferents (Gossard et al., 1996). In contrast, another report failed to show a relationship between the degree of depression of the Ia evoked motorneuron EPSP and the locomotor phase, but did demonstrate a tonic depression which appeared at the onset of MLR-evoked fictive locomotion (Gosgnach et al., 2000). Additionally, the effects of sensory input on presynaptic inhibition can be completely reorganized. For instance, at rest stimulation of cutaneous afferents increases PAD of Ib afferents (Rudomin et al., 1983), whereas during locomotion the same stimulus attenuates it (Duenas & Rudomin, 1993).

1.4 Neural Connectivity in the Murine Hindlimb CPG

1.4.1 *In vitro* neonatal rodent spinal cord

The introduction of the neonatal rodent *in vitro* isolated spinal cord preparation precipitated a major shift in the field of locomotor research. In this preparation, the intact spinal cord of a newborn rodent, complete with hindlimb roots, is dissected into oxygenated artificial cerebrospinal fluid (aCSF) where it remains viable for several hours. Suction electrodes are placed on the ventral roots to record spinal motor output, thereby allowing measurement of network response to various electrical and/or pharmacological stimuli. To study the locomotor CPG, suction electrodes are placed on the flexor related (i.e. second lumbar, L2) and extensor related (i.e. fifth lumbar, L5) ventral roots. Stable fictive locomotion is characterized by rhythmic ventral root bursting which alternates 1) between ipsilateral flexor and extensor roots (i.e. iL2-iL5) and 2) between the right and left sides of the spinal cord (i.e. rL2 – lL2 and rL5 – lL5). Robust fictive locomotion can be evoked pharmacologically by bath application of *N*-methyl-D-aspartate (NMDA) and serotonin (5-hydroxytryptamine, 5-HT), often with dopamine (DA). Alternately, electrical stimulation of the dorsal roots, cauda equina or brainstem can elicit bouts of fictive locomotor activity. While early approaches utilized neonatal rats, as molecular genetic approaches were incorporated into the study of the locomotor CPG the mouse ultimately became the most prevalent model. The major criticism of this preparation is the limitation to newborn and therefore functionally immature spinal cords. Nevertheless, due to the stability and longevity of fictive locomotion as well as the ease with which the intrinsic networks can be manipulated, the isolated neonatal rodent spinal cord preparation allowed for considerable insight into the spinal production of locomotor output.

1.4.2 Network architecture defined using wildtype rodents

Nature of locomotor rhythm generation

Isolation of the spinal cord from higher CNS structures and peripheral inputs allowed directed investigation into the cellular origin of the locomotor rhythm. The

initial description of the *in vitro* spinal cord preparation used the excitatory amino acid receptor agonist NMDA to evoke locomotion (Kudo & Yamada, 1987). Subsequent studies have demonstrated the additional importance of numerous neuromodulators including acetylcholine, dopamine, noradrenaline and serotonin (Cowley & Schmidt, 1997). Bath application of fast inhibitory neurotransmitter antagonists to locomotor preparations failed to abolish rhythmic activity and it therefore appears that rhythm generation must occur via purely excitatory mechanisms (Bonnot et al., 2002, Bracci et al., 1996, Kjaerulff & Kiehn 1997, Kremer & Lev-Tov, 1997).

A major criticism of bath application of pharmacological agents to activate the locomotor CPG is that all spinal neurons, not just constituents of the CPG are exposed to the drugs. To mitigate spurious activation of unrelated neurons, electrical approaches can be used to elicit fictive locomotion. Trains of electrical stimuli applied to a lumbar dorsal root can evoke bouts of rhythmic locomotor-like activity characterized by flexor-extensor and left-right alternation which persist beyond the cessation of the stimulus (Marchetti et al., 2001, Bonnot et al., 2002). Electrical stimulation of sacro-caudal afferents can also provide appropriate stimulation to evoke fictive locomotor-like output from the lumbar CPG (Lev-Tov et al., 2000). Alternately, electrical stimuli applied to the ventral surface of the medulla or pons can elicit locomotion in isolated brainstem-spinal cord preparations (Zaporozhets et al., 2004). The locomotor related output elicited via electrical stimulation typically displays a much shorter period but does not last as long as drug induced fictive locomotion. Thus, while electrical stimulation via brainstem or sensory inputs may present a more physiologically relevant model than prolonged exposure to neuroactive drugs, the latter is widely used for practical reasons.

Boundaries of the rodent Locomotor CPG

Following pharmacologically induced fictive locomotion, examination of uptake of the activity-dependent dye sulphorhodamine 101 revealed clusters of labelled interneurons bilaterally distributed around the central canal and in the intermediate grey throughout the lumbar enlargement (Kjaerulff et al., 1994). Confirming the amenability of the *in vitro* preparation to invasive experimentation, partitioning and lesioning studies were performed to delineate the anatomical boundaries of the locomotor CPG. Well-coordinated fictive locomotion can be obtained following NMA/5-HT application caudal to a Vaseline barrier placed at T13 (Cazalets et al, 1995) or in isolated spinal cord preparations sectioned at an anterior boundary of T12 (Kjaerulff & Kiehn, 1996). Successive horizontal and sagittal transecting within the lumbar enlargement demonstrated that dorsal and lateral grey matter are likewise dispensable for generating fictive locomotion (Kiehn & Kjaerulff, 1996). Hence, in the neonatal rodent the core of the hindlimb locomotor CPG is contained within the ventro-medial aspect of the T12-L6 segments.

Location of the core rhythm generating elements

Transverse sectioning within the lumbar enlargement indicated the ability to generate rhythm is broadly distributed throughout the caudal thoracic and lumbar spinal segments. Bath application of NMDA/5-HT to separate T13-L1 and L2-L6 spinal segments evoked coordinated locomotor activity in both sections (Kiehn & Kjaerulff, 1996). NMDA-induced alternation of ankle flexors and extensors can be recorded from the neonatal rat following acute isolation and hemisection of the L4-L5 segments (Kudo & Yamada, 1987). This is in accordance with observations in the cat wherein L-DOPA administration can induce ankle flexor-extensor alternation following acute isolation of the L6-S1 segments (Grillner & Zangger, 1979).

The dispersed rhythm generating ability of the spinal cord does not imply that the locomotor CPG is a homogenous entity; rather network elements contained within

the rostral segments have greater rhythmogenic capacity. Bath application of NMA/5-HT to the T13-L2 segments induces rhythmic locomotor-like activity in L2 and L5 ventral roots, however drug application caudal to L2 produces only increased tonic activity in L5 roots (Cazalets et al., 1995). Moreover, while either the T13-L1 or the L2-L6 tissue blocks can generate locomotor activity, coordinated rhythmic activity was less reliably induced, the period was greater, and burst amplitude was lower in the caudal portion suggesting that it has a weaker ability to generate rhythm (Kiehn & Kjaerulff, 1996). The excitability gradient persists in the adult rodent as destruction of rostral lumbar grey matter via kainate injection causes a significantly greater impairment to overground locomotion than a similar injection performed more caudally (Magnuson et al., 2005).

In addition to greater rhythm generating ability, network elements located in rostral segments appear to exert a unidirectional control over caudally located elements. Increasing excitation within the rostral CPG network, either by increasing the concentration of NMA or extracellular K^+ in the solution bathing the L1-L2 segments, caused a significant decrease in the period of ongoing locomotor activity (Bertrand & Cazalets, 2002). In contrast, the same manipulations applied caudal to L2 failed to change the locomotor period. This implies an asymmetry in the locomotor CPG whereby rostrally located elements have exclusive control over speed. The lack of reciprocal control implies caudally located CPG elements cannot access the mechanisms regulating the speed of locomotion. During drug-induced fictive locomotion, partial transection through the L3 segment abolishes rhythmic activity in the ipsilateral L5 ventral root, despite continued locomotor activity in bilateral L2 and contralateral L5 roots (Kjaerulff & Kiehn 1996, Bertrand & Cazalets, 2002). Coordinated rhythmic activity is maintained in the L5 ventral root on the unlesioned side when only a small lateral bridge containing the lateral funiculus is spared (Kjaerulff

& Kiehn, 1996). This suggests that the rhythmic activity from the rostral CPG elements is transmitted ipsilaterally towards caudally located cells. Loss of L5 output with little effect on L2 activity implies a primary directionality to the information transmission from rostral to caudal. Additionally, as maintained connectivity from network elements in the contralateral L5 segment are insufficient to rescue rhythmic motor output, descending input from rostral CPG elements appears to be more important to generating motor output than input from contralateral CPG circuits.

Numerous studies have suggested that rhythm generation occurs via unilaterally constrained circuitry. Stable, rhythmic bursting characterized by flexor-extensor alternation can be elicited following complete mid-sagittal transection of the spinal cord (Whelan et al., 2000, Bonnot et al., 2002, Hinckley et al., 2005). Interestingly, the locomotor period is significantly longer in hemisected than in intact spinal cords. This slowing of the rhythm cannot be accounted for solely by mechanical trauma caused by the hemisection, as a similar phenomenon was found following unilateral bath application of locomotor agonists in bilaterally intact spinal cords (Kjaerulff & Kiehn, 1997).

Commissural interneurons

Coordination of activity between the left and right sides of the spinal cord necessitates neurons whose axons cross the midline and synapse onto contralateral CPG elements. This key anatomical feature defines a broad population of CPG interneurons known as commissural interneurons (CINs). Based on their projections along the rostro-caudal axis, CINs are subdivided into intrasegmental (sCIN), and intersegmental ascending (aCIN), descending (dCIN), or bifurcating (ascending and descending, adCIN) groups (Eide et al., 1999, Stokke et al., 2002).

Axons of intrasegmental CINs remain within the same spinal segment as their cell body and have been proposed to coordinate the activity between homonymous motorneurons on the left and right sides of the spinal cord (Quinlan & Kiehn, 2007). The sCINs include both excitatory and inhibitory interneurons and effect contralateral motorneurons via both mono- and polysynaptic pathways. Coordination across the spinal cord appears to be mediated by 1) monosynaptic excitation of contralateral motorneurons by glutamatergic sCINs, 2) monosynaptic inhibition by glycinergic/GABAergic sCINs, and 3) polysynaptic inhibition by glutamatergic sCINs acting on inhibitory premotor interneurons located ipsilaterally to the target motorneurons (Kjaerulff & Kiehn 1997, Quinlan & Kiehn, 2007, Nishimaru et al., 2006). The inhibitory premotor interneurons include RCs and IaINs (Nishimaru et al., 2006).

Intersegmental CINs are defined by axons that project at least two spinal segments away from the soma. Descending CINs have been proposed to bind synergies across the spinal cord (Butt et al., 2002, Butt & Kiehn 2003). During drug-induced fictive locomotion a significant proportion of dCINs located in the L2 segment are rhythmically active, though they are preferentially active either in or out of phase with the ipsilateral L2 ventral root. Examination their effect on L4 motorneurons indicates dCINs are a mixed excitatory and inhibitory population. From this it was proposed that dCINs that fire during flexion excite contralateral extensor motorneurons or inhibit contralateral flexor motorneurons. Conversely, dCINs that fire out of phase with the flexor-related root excite contralateral flexor motorneurons or inhibit contralateral extensor motorneurons. Thus, dCINs reinforce the coupling of flexors on one side of the body with extensors on the other side, while simultaneously impairing bilateral co-activation of pairs of flexors or extensors.

L2-located dCINs fire either in phase with their ipsilateral L2 ventral root, or out of phase, though in-phase dCINs tend to be located more ventrally than out of phase

dCINs (Butt et al., 2002). Furthermore, they suggested that rhythmicity of in phase dCINs was due predominantly to excitatory synaptic inputs, whereas rhythmicity in out of phase dCINs was due primarily to inhibitory inputs (Butt et al, 2002). In neither group did it seem likely that intrinsic membrane properties were involved in rhythm generation in these cells.

The manner of connections to motor neurons and the action during locomotion and at rest were used to further divide the dCINs into functional sub-populations (Butt & Kiehn, 2003). One sub-population, termed switch cells, is involved in polysynaptic, GABAergic inhibition of contralateral motor neurons at rest, but monosynaptic excitation during drug induced fictive locomotion (Butt & Kiehn, 2003). Three sub-populations had the same effect at rest and during fictive locomotion. Two were monosynaptically connected; one causing strychnine-sensitive hyperpolarizing potentials, and one causing AP-5/CNQX-sensitive depolarizing potentials. The third sub-population caused hyperpolarizing potentials at a longer latency and was sensitive to both AP-5/CNQX and bicuculline, suggesting GABAergic inhibition via an intermediary excitatory synapse (Butt & Kiehn, 2003).

Experiments performed using the isolated spinal cords of neonatal wildtype rodents established much of our understanding of the principles governing the mode of operation of the locomotor CPG. Results of these experiments stipulated that the neurons underlying rhythm generation would be rhythmically active during locomotor tasks, excitatory, ipsilaterally projecting, and located in the ventro-medial spinal cord. Further advancements were hindered by the vast numbers of functionally unrelated interneurons heterogeneously distributed throughout the spinal cord. While gross morphological characteristics could be used to isolate particular interneurons of interest, a more refined approach was required for further investigation of the constituent CPG interneurons.

1.4.3 Incorporation of molecular genetics into the study of the Locomotor CPG

In recent years, a suite of molecular tools has been developed which opened the door for substantial and rapid progress into understanding the composition of the mammalian locomotor CPG. The foundational premise for these experiments posits that during embryogenesis, transcription factor expression regulates gene expression which defines cellular features such as migration pattern, axonal projection pattern, and neurotransmitter phenotype. Consequently it was proposed that cells which express the same transcription factors will share a cellular phenotype and therefore serve a common function in the mature spinal cord. Thus researchers sought to employ molecular genetics to divide the developing spinal cord into populations of functionally related cells.

Cellular differentiation during embryonic development is temporally and spatially orchestrated by morphogens, signaling proteins which regulate gene expression in downstream cells (reviewed in Lee & Jessell, 1999, Jessell, 2000, Briscoe & Ericson, 2001). Within the embryonic neural tube, initial cellular differentiation is regulated by the action of two signaling molecules: Sonic hedgehog (Shh), released ventrally from the notochord and floor plate, and bone morphogenetic proteins 4 & 7 (BMP-4/7) released from the overlying dorsal ectoderm. As each is a diffusible protein, two opposing and overlapping morphogen concentration gradients are established. Consequently, neural tube cells which share a position along the dorso-ventral axis develop in a common morphogen signalling milieu. This establishes unique transcription factor expression profiles within spatially delineated progenitor domains. Transcription factors induce further gene expression and cellular specialization, thus ensuring that cells which develop from common progenitor domain acquire common cellular characteristics. Once a cell has been directed down the appropriate developmental course, transcription factor expression declines. In the embryonic

mouse, 11 postmitotic populations emerge between embryonic days 9 to 11 (E9-11). These include 6 dorsal interneuron populations (dI1-dI6), 4 ventral interneuron populations (V0-V3) and motor neurons. Two late born populations of dorsal interneurons, dIL_A and dIL_B, emerge between E12.5-E13.5 (Gross et al., 2002, Muller et al., 2002). Each of these cardinal populations is defined by a distinct transcription factor expression profile.

Although it was initially believed that all cells arising from a common progenitor domain would serve a similar function in the adult, subsequent research has revealed this to be an oversimplification. Within each of the cardinal populations there is a significant degree of heterogeneity, often with discrete subpopulations serving different functions. Conversely, some functionally-defined interneuron populations have been shown to include cells derived from more than one progenitor domain. In spite of these shortcomings, molecular genetic approaches have proven invaluable by their ability to refine the vast numbers of intermingled spinal interneurons into experimentally tractable populations.

1.4.4 Ventral Spinal Interneuron Populations

As experiments in the wildtype rodent indicated that the rhythm generating core of the locomotor CPG is distributed throughout the ventro-medial aspect of the lumbar enlargement, research focussed predominantly on the ventrally derived spinal interneuron populations. Anatomical and electrophysiological characterization has been performed for each of the V0-V3 populations, thus allowing preliminary 'wiring diagrams' to be drawn. Genetic knock-out or silencing experiments have shown that locomotor rhythm persists following the loss of any individual population.

V0 Interneurons

Among the cardinal interneuron populations, the V0 interneurons were the first to be studied with respect to locomotion (Lanuza et al., 2004). While description of the locomotor phenotypes caused by abnormalities in the V0 population can allude to its role in the CPG, further studies are required to understand the intrinsic properties and firing behaviour of these cells. Chapter 3 of this thesis addresses anatomical characteristics of the two primary sub-populations of V0 interneurons, $V0_V$ and $V0_D$.

V0 interneurons are generated from the Dbx1-expressing *p0* progenitor domain (Pierani et al., 2001, Moran-Rivard et al., 2001, Lanuza et al., 2004). Expression of Pax7 and Dbx2 within the dorsally located progenitor cells in addition to transient expression of the homeodomain protein Evx1 within the ventrally located post-mitotic cells distinguishes the $V0_D$ and $V0_V$ subpopulations (Lanuza et al., 2004). An additional marginal subpopulation identified via Pitx2 expression has also been described (Zagoraiou et al., 2009). Initially arising at E11.5-E12, these neurons transiently express Evx1 and are thus of $V0_V$ origin.

Studies in the embryo indicate approximately two thirds of the total V0 population is inhibitory while one third is excitatory (Talpalar et al., 2013, Lanuza et al., 2004). Interestingly, this neurotransmitter profile coincides with the transcription factor profile, as $V0_D$ interneurons are GABAergic, whereas $V0_V$ are glutamatergic (Talpalar et al., 2013).

Immunohistochemistry indicates that $Pitx2^+$ V0 interneurons express either vesicular acetylcholine transporter (vAChT) with choline acetyltransferase (ChAT), or vesicular glutamate transporter 2 (vGluT2), thereby designating these cells as cholinergic ($V0_C$) or glutamatergic ($V0_G$), respectively (Zagoraiou et al., 2009).

V0 interneurons are generated just ventral to the sulcus limitans and migrate ventro-medially to settle in lamina VIII (Moran-Rivard et al., 2001, Pierani et al.,

2001). Both $V0_V$ and $V0_D$ interneurons project axons contralaterally (Pierani et al, 2001, Moran-Rivard et al., 2001, Lanuza et al., 2004). Injection of the retrograde trans-synaptic tracer pseudorabies virus 152 (PRV-152) into the gastrocnemius muscle resulted in virus-mediated labelling of V0 interneurons solely in the contralateral spinal cord (Lanuza et al., 2004).

The Pitx2-expressing V0 cells settle close to the central canal (Zagoraiou et al., 2009). The cholinergic $V0_C$ subpopulation is found in the upper lumbar segments, whereas the glutamatergic $V0_G$ is found caudally. In contrast to the ventral and dorsal subpopulations, these cells project ipsilaterally. Initial assessment of the cholinergic cells indicated $V0_C$ cells are the sole source of spinal C-boutons (Zagoraiou et al., 2009). Studies examining monosynaptically restricted retrograde virus transport across synapses have shown that cholinergic cells in lamina X form direct contacts on lumbar motorneurons (Stepien et al., 2010, Coulon et al., 2011). Findings between the two studies disagree on whether $V0_C$ cells target motorneurons solely within the ipsilateral spinal cord or whether they target motor nuclei bilaterally. While it is possible that this discrepancy results from the different viral tracers used by each experiment, it may also be the case that different motor pools show distinct cholinergic innervation as one study injected the virus into the quadriceps (Stepien et al., 2010) and the other injected into the triceps surae (Coulon et al., 2011). Cholinergic interneurons labelled following virus injection into the triceps surae were situated in lumbar segments rostral to the L4 segment in which the majority of TS motorneurons are situated (Coulon et al., 2011).

Investigation into the synaptic targets of other genetically-defined interneuronal populations has identified 'upstream' partners of the V0 cells. $Evx1^+$ $V0_V$ interneurons receive excitatory monosynaptic inputs from V2a interneurons (Crone et

al., 2008). Additionally, $V0_C$ interneurons receive inputs from V2b inhibitory interneurons (Zhang et al., 2014).

Role in Locomotion

The involvement of this genetically-defined population in locomotion was first suggested by increased c-fos expression in V0 cells following drug induced fictive locomotion in isolated spinal cords of $Dbx1^{LacZ/+}$ pups (Lanuza et al., 2004). Subsequent knock-out studies indicated a role in securing left-right alternation. Elimination of the entire V0 population disrupts coordination between left and right limbs, while sparing coupling between flexors and extensors. In isolated spinal cords of E18.5 $Dbx1^{lacZ/lacZ}$ embryos, alternation between left and right pairs of ventral roots is impaired with frequent episodes of synchrony interspersed with alternation, indicative of phase drifting (Lanuza et al., 2004). Elaboration of the available transgenic mouse lines allowed study of V0-related locomotor phenotypes in the adult. In the E1Ngn2::Cre;$Dbx1^{DTA}$ model, Dbx1-expressing cells are abolished exclusively from the spinal cord while higher respiratory centres are spared. Mutant mice live to maturity and lack left-right alternation throughout the spinal cord. The mice hop by advancing both forelimbs in synchrony followed by both hindlimbs (Talpalar et al., 2013).

A variety of transgenic lines have been employed to tease apart the relative contribution of each of the $V0_V$ and $V0_D$ subpopulations. Initial studies using the isolated spinal cords of E18.5 $Evx1^{tm/tm}$ embryos revealed no observable impairment caused by loss of the $V0_V$ cells (Lanuza et al., 2004). A recent report suggested that the subpopulations serve complementary roles but at different speeds (Talpalar et al., 2013). In isolated spinal cords of E18.5 Pax7::Cre;$Dbx1^{DTA}$ embryos in which $V0_D$ interneurons were selectively eliminated, fictive locomotion at intermediate

frequencies displayed mixed alternation and synchrony between pairs of L2 ventral roots, with synchrony between L5 roots. At high locomotor frequencies, L2 left-right alternation was normal. At very low frequencies locomotion could not be evoked. The role of the $V0_V$ subpopulation was examined using Vglut2::Cre;$Dbx1^{DTA}$ animals. Overground locomotion in juvenile mutant mice revealed frequency dependent impairments specifically in the hindlimbs. At low locomotor frequencies alternation was maintained, but at high locomotor frequencies a hopping gait occurred. From these observations, the authors conclude that $V0_D$ interneurons are recruited at low speeds to secure left-right alternation via inhibition. At high locomotor frequencies, excitatory $V0_V$ interneurons secure left-right alternation through their actions on inhibitory interneurons in the contralateral spinal cord. Both work in synergy at intermediate frequencies.

The only study to address the cellular activity of the V0 interneurons was restricted to the Pitx2-expressing cells (Zagoraiou et al., 2009). Intracellular recording from $Pitx2^+$ interneurons in the hemisected spinal cord preparation showed that $V0_C$ interneurons are rhythmically active during drug-induced fictive locomotion. However this activity was not due to intrinsic rhythm generation, but rather resulted from the barrage of EPSPs they received, in phase with their ipsilateral ventral root. The authors propose that during locomotion the $V0_C$ interneurons provide phasic neuromodulation to motorneurons. The locomotor impairments observed in the Dbx1 mutant mice are unlikely to result from the loss of the Pitx2-expressing cells.

V1 Interneurons

V1 interneurons arise from the *p1* progenitor cells, demarcated by Pax6/Dbx2/Nkx6.2 transcription factor expression (Burrill et al., 1997, Ericson et al., 1997). In the developing mouse embryo, postmitotic V1 cells transiently express the transcription factor En1 between E9.5-E16 (Ericson et al., 1997, Saueressig et al,. 1999).

During embryonic development all $En1^{+}$ V1 neurons express GABAergic markers (Saueressig et al., 1999, Sapir et al., 2004). In the adult mouse, the majority of V1 synapses on motorneurons display GlyT2 immunoreactivity, while significantly fewer express GAD67 (Alvarez et al., 2005). While the absence of ChAT or vGluT2-expressing V1 terminals in the adult conforms to the inhibitory phenotype defined in the embryo, the increase in glycinergic and decrease in GABAergic markers indicates that postnatally there is a maturation of the inhibitory nature of this population (Alvarez et al., 2005).

In newborn the mouse, V1 interneurons are found along the length of the spinal cord. Within the lumbar enlargement, they are distributed throughout the ventral horn, although most are located within the motor neuron pools in lamina IX or close to motorneurons in a band in lamina VII (Alvarez et al., 2005).

Early studies of developing V1 cells using the $En1^{lacZ}$ mouse embryo indicated they are a population of ipsilaterally projecting interneurons (Saueressig et al., 1999). Numerous studies indicate that motorneurons receive monosynaptic input from the V1 population. Soon after their birth (E10) these interneurons extend intra-segmentally restricted axons towards nearby motorneurons. Using a transgenic reporter line which labels the axons of V1 interneurons, significant contact from V1 cells onto the somata and proximal dendrites of motor neurons was demonstrated (Sapir et al., 2004). Recent studies report that by P15, V1-derived interneurons provide between 38-59%

of the total inhibitory input to hindlimb motorneurons in mice (Zhang et al., 2014). In addition to targeting motorneurons, uptake of reporter lectin in a transgenic conditional floxed-WGA reporter reveal V1 interneurons form synaptic connections onto other interneurons within the ventral spinal cord (Sapir et al., 2004). Among these targets are Renshaw cells, identified based on their location within the spinal cord, calbindin and gephryn immunoreactivity, and cholinergic inputs.

Role in Locomotion

No intracellular recordings have been performed on V1 interneurons, and therefore their significance to locomotor function must be extrapolated from observed locomotor phenotypes in mutant animals. To examine the functional role of the V1 spinal interneurons, the *in vitro* isolated neonatal mouse spinal cord preparation was used with two transgenic mouse lines in which the V1 cells were eliminated; the first was the Pax6-knockout ($Pax6^{-/-}$), in which V1 cells were re-specified into neighbouring cell types, and second was the $En1^{Cre};R26^{laczFlox/DTA}$ line in which V1 cells develop but subsequently die off due to dyptheria toxin A (DTA) production (Gosgnach et al., 2006). Using each model, the authors found that loss of V1 interneurons did not abolish the ability to generate locomotion, nor did it alter the patterns of left-right or flexor-extensor alternation. Interestingly, it did cause a significant slowing of the locomotor rhythm. To eliminate the possibility that the altered phenotype was due to impaired development of the locomotor CPG, acute silencing of the V1 interneurons using Allatostatin-receptor expression was also used to show a transient and reversible slowing of the locomotor rhythm when V1 interneurons were 'silenced' from the locomotor CPG.

V2 Interneurons

The *p2* progenitor domain, demarcated by Lhx3 expression, gives rise to the V2 interneuron population (Peng et al., 2007). This population has classically been divided into two subpopulations; the glutamatergic V2a which express the transcription factors Lhx3, Chx10 and Sox14 (Al-Mosawie et al., 2007, Hargrave et al., 2000, Lundfald 2007, Peng et al., 2007), and the inhibitory V2b, which lose Lhx3 expression but express GATA2 and GATA3 (Peng et al., 2007, Karunaratne et al., 2002). Recently, the transcription factor Sox1 has been suggested as a marker for a third subpopulation, V2c, which derives from V2b (Panayi et al., 2010), however beyond the fact of their existence, little information is available to characterize these interneurons.

V2a Subpopulation

By P0, V2a interneurons are located in a band in lamina VII, which spans the entire medial-lateral axis of the grey matter (Lundfald et al., 2007, Crone et al., 2008, Dougherty & Kiehn 2010). *In situ* hybridization for vGluT2 indicated that 80% of $Chx10^{+}$ V2a cells are glutamatergic (Lundfald et al., 2007). Conversely, *in situ* hybridization for GlyT2 revealed only a marginal population of glycinergic V2a cells (Lundfald et al., 2007). V2a interneurons represent a significant source of spinal excitation as, of the total population of glutamatergic cells in the ventral spinal cord, approximately 30% co-express Chx10 (Crone et al., 2008).

V2a interneurons project ipsilaterally in the spinal cords of embryonic and newborn mice (Lundfald et al., 2007). Within the spinal cord both motorneurons and interneurons are targets of the V2a population. Glutamatergic boutons of V2 interneurons were most densely located in laminae IX and VII, with few located in lamina VIII or in the dorsal spinal cord (Al-Mosawie et al., 2007). Reconstruction of biocytin-filled Chx10-EGFP interneurons revealed both locally projecting V2a interneurons with short processes restricted near the soma, as well as ascending,

descending, or both ascending and descending intersegmental interneurons (Dougherty & Kiehn, 2010). Of the biocytin-filled cells, the local interneurons extended axons into lamina VII whereas axonal branches of the intersegmental cells terminated in laminae VII, VIII, and/or the motor nuclei (Dougherty & Kiehn, 2010). Within the motor pool, glutamatergic V2 boutons are often found in close apposition to motorneuron somata (Al-Mosawie et al., 2007), suggesting they are among the premotor excitatory interneurons. Retrograde trans-synaptic tracing has demonstrated V2 interneurons are monosynaptically connected to quadriceps motorneurons (Stepien et al., 2010). While this study could not differentiate between V2a and V2b interneurons, it nevertheless demonstrates that the V2 interneurons are ipsilaterally located premotor interneurons.

The location of V2a terminals is suggestive of connectivity onto other CPG interneurons. Injection of fluorescent dextrans into the contralateral ventral spinal cord of transgenic mice showed that V2a directly contact commissural interneurons (Crone et al., 2008). Among the interneuron targets, glutamatergic V2a terminals made contact onto $Evx1^{+}$ $V0_{V}$ cells (Crone et al., 2008). It remains unclear whether V2a interneurons excite one another. There appears to be a lack of fast chemical synaptic transmission between V2a interneurons, however conflicting studies either support or refute the presence of electrical coupling (Zhong et al., 2010, Dougherty & Kiehn, 2010).

Immunohistochemical approaches have been used to demonstrate synaptic input onto V2 interneurons. Within the spinal cord, primary afferent terminals can be identified via their expression of the vesicular glutamate transporter 1 (vGluT1) protein (Oliveira et al., 2003). Large vGluT1 expressing boutons were found in close apposition to the somata and proximal dendrites of V2-derived interneurons (Al-Mosawie et al., 2007). While this study demonstrates V2 interneurons receive primary afferent input,

further investigation is required to fully define sensory innervation to each subpopulation.

Role in Locomotion

During drug induced fictive locomotion in a dorsal horn removed *in vitro* preparation, a proportion of $Chx10^{+}$ V2a interneurons are rhythmically active (Dougherty & Kiehn, 2010, Zhong et al., 2010). Rhythmically active V2a interneurons were found firing either in phase or out of phase with their local ventral root, that is, both during flexor- and extensor-related ventral root activity (Dougherty & Kiehn, 2010, Zhong et al., 2010). A further survey of Chx10-expressing interneurons using calcium imaging revealed no anatomical segregation of flexor- and extensor-related rhythmically active V2a interneurons (Zhong et al., 2010). It thus appears that V2a interneurons support rhythmic excitation without phase preference for extension or flexion. V2a interneurons themselves receive rhythmic excitation from the locomotor CPG. During drug induced fictive locomotion, V2a interneurons receive EPSPs in phase with their functionally related ventral root (Dougherty & Kiehn, 2010, Zhong et al., 2010). Little evidence is available to suggest they receive rhythmic inhibition, suggesting they are not under the control of a 'push-pull' mechanism.

Surprising given the ipsilateral restriction of their axonal projections, ablation of V2a interneurons leads to impairments in left-right coordination during fictive locomotion in the *in vitro* preparation (Crone et al., 2008, 2009). As V2a cell contact commissural interneurons, including the $V0_V$ subpopulation, it has been proposed that these defects result from a reduced excitatory drive to the commissural interneurons which bind together CPG elements located on the left and right sides of the spinal cord. Further study indicates that the severity of locomotor defects resulting from loss of the V2a cells is frequency dependent. In mature (P24-25) Chx10::DTA mice walking on a

treadmill, left-right alternation is replaced with synchrony, specifically at high speeds (Crone et al., 2009). In the isolated neonatal spinal cord, a greater proportion of V2a interneurons are rhythmically active at higher frequencies of drug or brainstem electrical stimulation evoked fictive locomotion (Zhong et al., 2010, 2011).

V2b Subpopulation

V2b cells show two distinct settling positions in the P0 spinal cord; one group settles around the central canal in lamina X, while the other group is distributed throughout lamina VII (Lundfald et al., 20007). Immunohistochemistry revealed that the majority of V2b interneurons in lamina VII are glycinergic while a smaller proportion is GABAergic (Lundfald et al., 2007). Conversely, within the group of neurons located in lamina X, V2b cells were primarily GABAergic and only a minimal portion were glycinergic (Lundfald et al., 2007). *In situ* hybridization for vGluT2 reveals a near complete absence of glutamatergic V2b cells in both laminae (Lundfald et al., 2007). Thus the V2b population are inhibitory.

As with the V2a cells, V2b interneurons project ipsilaterally (Lundfald et al., 2007). Their axons extend towards the ipsilateral motor nuclei as well as into the ventrolateral and/or the ventromedial fasciculi (Lundfald et al., 2007). Complementing the demonstration that the broader population of V2 interneurons are premotor interneurons (Stepien et al., 2010), V2b cells have been shown to form inhibitory synapses onto motorneurons. Early reports indicated that V2b cells account for only a small proportion (<10%) of the total inhibitory input onto hindlimb motorneurons (Al-Mosawie et al., 2007), however a more recent study has suggested that this proportion varies between motor pools from 23 to 41% (Zhang et al., 2014). This discrepancy may be due to different methodologies or may represent an increase in V2b-derived inhibition during development as the latter study addressed P15 mice, an age at which animals are capable of weight-bearing locomotion. Inhibitory V2b synapses have been

observed on $V0_C$ interneurons, as well as other undefined interneurons in laminae VII and VIII (Zhang et al., 2014).

Role in Locomotion

Consistent with their ipsilateral projections and inhibitory neurotransmitter profile, V2b interneurons are involved in securing flexor-extensor alternation during locomotion. Elimination of V2b interneuron output using $Gata3^{Cre}$:$R26^{floxstop\text{-}TeNT}$ transgenic mice revealed only a mild impairment of alternation between iL2-iL5 ventral roots during drug induced fictive locomotion in the isolated spinal cords of newborn mice (Zhang et al., 2014). Interestingly, alternating L2-L5 bursting was replaced with synchrony in the majority of hemisected spinal cords (Zhang et al., 2014). The preserved flexor-extensor alternation observed in some $Gata3^{Cre}$:$R26^{floxstop\text{-}TeNT}$ spinal cords prompted the suggestion that a supplemental population serves this function as well (Zhang et al., 2014). Loss of neurotransmission from both populations of ipsilaterally projecting inhibitory spinal interneuron populations (i.e., V1 and V2b) in $Gata3^{Cre}$;$En1^{Cre}$;$R26^{floxstop\text{-}TeNT}$ transgenic mice resulted in flexor-extensor synchrony in all isolated spinal cords tested (Zhang et al., 2014). In addition to shedding light on the spinal origin of flexor-extensor alternation, this finding refutes the dogmatic view that specific spinal functions are mediated by discrete genetically-defined populations.

V3 Interneurons

In the most ventral aspect of the developing neural tube, V3 interneurons arise from Nkx2.2/2.9 expressing *p3* progenitors (Briscoe et al., 1999; Goulding et al., 2002). Postmitotic V3 interneurons can be studied via their expression of the transcription factors *Sim1* (Briscoe et al., 1999, Goulding et al., 2002) and *Uncx* (Carcagno et al., 2014, Blacklaws et al., 2015). Recently, three functional subpopulations have been proposed based on the cellular properties of V3 interneurons

in the mature (P20-23) spinal cord (Borokowska et al., 2013). While there is no unique transcription factor to distinguish these subpopulations, settling position and distinct electrophysiological properties can be used to classify the studied cells. Following mitosis, V3 interneurons migrate dorsally and laterally away from the floor plate and by birth settle in clusters in the ventral spinal cord (lamina VIII), intermediate spinal cord (laminae VI, VII, X) and deep dorsal horn (laminae IV-V; Borowska et al., 2013, Blacklaws et al., 2015). The dorsal cluster only extends in the thoracic and upper lumbar segments, as far caudal as L3.

V3 spinal interneurons are exclusively excitatory, expressing vGluT2 at their terminals (Zhang et al., 2008). The majority of V3 interneurons project axons across the ventral midline into the contralateral spinal cord, while a minority of cells send axons either ipsilaterally or both ipsi- and contralaterally (Zhang et al., 2008, Blacklaws et al., 2015). At birth, commissural V3 interneurons with descending axons were restricted to the ventral spinal cord, while ascending V3 commissural interneurons were distributed throughout all three locales (Blacklaws et al., 2015).

To determine whether V3 interneurons make monosynaptic connections onto motor neurons, the retrograde trans-synaptic tracer PRV-152 was injected into hindlimb flexor and extensor muscles of newborn pups (Zhang et al., 2008). At 38-40 hours post-injection, GFP-labelled V3 interneurons were discovered, indicating the existence of synaptic connection onto motor neurons. Of the monosynaptically connected V3 interneurons, 80% were located contralateral to the infected motor neurons, consistent with the predominantly contralateral projection pattern of the population as a whole. V3 interneurons represent a significant source of spinal excitation to motorneurons as approximately 22% of the total glutamatergic contacts onto motor neurons derive from V3 interneurons (Zhang et al., 2008).

In addition to motorneurons, V3 interneurons target other locomotor-related spinal interneurons. In P0 $Sim1^{Cre}$ transgenic mice expressing an axonal GFP reporter, dense arborizations of V3 interneurons were observed throughout the ventral spinal cord with a near complete absence of axons in the dorsal spinal cord (Zhang et al., 2008). This distribution throughout areas of the spinal cord which contain the locomotor CPG is suggestive of extensive interconnectivity with other CPG cells. Other known targets of V3 interneurons include the Ia inhibitory interneurons, Renshaw Cells, Lim3-derived V2 interneurons, and other undefined commissural interneurons. Notably, V3 cells were shown to account for 24% of the glutamatergic inputs onto IaINs and 27% of the glutamatergic input onto Renshaw Cells.

Role in Locomotion

Initial inquiry into the specific locomotor function of the V3 interneurons indicated they act to stabilize the locomotor rhythm (Zhang et al., 2008). Elimination of their synaptic output resulted in increased variability of ENG bursts and caused an overall lengthening of the step cycle period during drug induced fictive locomotion in the isolated spinal cord. Moreover, isolated spinal cords were less likely to display rhythmic activity in response to either bath application of drugs or stimulation of the sensory afferents. As it was more difficult to evoke locomotor activity, it appears that in the absence of the V3 interneurons the locomotor CPG is less robust.

In a recent report, c-fos expression was used to determine whether V3 interneurons were active during either a treadmill or a swimming task in the mature mouse (Borowska et al., 2013). Following both locomotor challenges c-fos expression was increased in the ventral V3 subpopulation. In contrast, cells of the dorsal V3 subpopulation only showed increased c-fos expression following the weight bearing treadmill task, and not after swimming. This led the authors to conclude that distinct

subpopulations of V3 interneurons serve unique roles in the mature animal; dorsal V3 cells are involved in motor control via sensory processing, while ventral V3 cells are integral constituents of the locomotion CPG.

Hb9 Interneurons

Despite the limited number of cells, early enthusiasm surrounding their putative involvement in rhythm generation led to considerable research into the small population of Hb9 interneurons. Currently, the developmental origin of this population is unknown, though it is possible they are a specialized subset derived from one or more of the cardinal populations. They are identified via their expression of the transcription factor Hb9, a protein which serves a critical function in consolidation of motorneuron identity (Arber et al., 1999).

While sharing a transcription factor with motorneurons could predict a shared neurotransmitter phenotype, immunohistochemistry for ChAT demonstrated no cholinergic Hb9 interneurons (Hinckley & Ziskind-Conhaim, 2006). Rather, expression of vGluT2 in their terminals indicates they are exclusively glutamatergic (Hinckley et al., 2005, Wilson et al., 2005).

Small, medially located clusters of Hb9 interneurons are found in lamina VIII of the rostral segments of the lumbar enlargement (L1-L3; Hinckley et al., 2005, Wilson et al., 2005, Kwan et al., 2009). Overall there are very few Hb9 interneurons as in addition to their rostral restriction, there are relatively few cells per segment.

Axons of Hb9 interneurons project locally within the ipsilateral spinal cord (Hinckley et al., 2005, Wilson et al., 2005). It has been proposed that Hb9 interneurons mutually excite one another, possibly via both electrical and chemical synapses. Bouton-like varicosities of Neurobiotin filled Hb9 interneurons have been observed in close apposition to dendrites of other Hb9 interneurons (Hinckley et al.,

2005), however electrophysiological evidence into the functional significance of this is lacking. In TTX, synchronous firing among closely situated Hb9 interneurons can be abolished via carbenoxolone, an inhibitor of gap junctions (Wilson et al., 2007). Using paired intracellular recordings, bidirectional electrical coupling between Hb9 interneurons and/or other spinal interneurons has been demonstrated, as carbenoxolone-sensitive spikelets occur in a second cell following current injection to the first, and vice-versa (Hinckley & Ziskind-Conhaim, 2006, Wilson et al., 2007).

The question of whether Hb9 interneurons synapse directly onto motorneurons remains contentious. Initial reports were contradictory, with one group finding evidence of bouton-like varicosities in close apposition on motorneuron dendrites (Hinckley et al., 2005), while another group found no evidence for Hb9 projections into lamina IX (Wilson et al., 2005).

While their downstream targets remain vague, electrophysiological and immuno-histochemical studies provide a clearer understanding of the sources of synaptic input to this population. Hb9 interneurons receive direct input from primary afferents evidenced by abundant vGlut1-immunoreactive terminals observed in contact with Hb9 interneurons (Wilson et al., 2005, Hinckley et al., 2010). Stimulation of the L1 dorsal root at low intensities thought to recruit group I and II afferents evoked monosynaptic, CNQX-sensitive EPSCs in Hb9 interneurons (Hinckley et al., 2010). Stimulation of the L5 dorsal root evoked only polysynaptic effects in Hb9 interneurons; unsurprising given primary afferents do not project across segments in the spinal cord. Hb9 interneurons receive additional input from both excitatory and inhibitory spinal interneurons. Inhibitory glycinergic and GABAergic terminals, visualized respectively via GlyT2 and GAD67 immunoreactivity, and excitatory glutamatergic terminals, visualized via vGluT2 immunoreactivity, are all found close to Hb9 interneurons (Wilson et al., 2005). In addition to the monosynaptic response, dorsal root stimulation evoked

postsynaptic currents of polysynaptic latencies which were abolished via mephenesin application (Hinckley et al., 2010). Interestingly, L2 dorsal root stimulation evoked only EPSCs whereas L5 dorsal root stimulation evoked both EPSCs and IPSCs. Descending serotonergic systems likely exert a neuromodulatory effect on Hb9 interneurons as 5-HT immunoreactive fibres were found in close apposition to the medial cell clusters (Wilson et al., 2005).

Role in Locomotion

Although it has since been refuted, Hb9 interneurons were initially heralded as a putative rhythm generating kernel of the locomotor CPG. Such speculation was prompted by their glutamatergic phenotype, ipsilateral axonal projections, recurrent self-excitation, and intrinsic membrane properties (reviewed in Brownstone & Wilson, 2008). Unlike for the other genetically-defined interneuron populations, this question could not be resolved via knock-out experiments because loss of Hb9 adversely affects motorneuron development (Arber et al., 1999). However, upon careful examination of the timing of the onset of activity in Hb9 interneurons it was demonstrated that locomotor activity in the ventral root precedes that of the Hb9 interneurons, a finding incongruent their having a role in driving the locomotor rhythm (Kwan et al., 2009). Nevertheless, there exists considerable evidence that Hb9 interneurons are constituent cells of the locomotor CPG.

Following a 90-minute locomotor task, Fos expression was increased in the clusters of Hb9 interneurons (Wilson et al., 2005). In the *in vitro* neonatal spinal cord, several studies using intracellular recording and calcium imaging during fictive locomotion have demonstrated Hb9 interneurons are rhythmically active in phase with the ipsilateral flexor related ventral root (Kwan et al., 2009). This rhythm results at least in part from rhythmic excitatory input as intracellular recordings in the

hemisected spinal cord revealed a significant increase in the number of incoming EPSCs during the ipsilateral flexor-related L2 burst (Hinckley et al., 2005). Interestingly, the same study did not report any phase related change in the occurrence of IPSCs. While this may show that rhythm results from purely excitatory mechanisms, it is possibly an experimental artefact resulting from hemisecting the spinal cord. Nevertheless, given their glutamatergic phenotype and recurrent self-excitation, the Hb9 population may be involved in reinforcement of the ongoing flexor activity.

1.4.5 Dorsal Spinal Populations

Although the core of the locomotor CPG is located in the ventral aspect of the spinal cord, dorsally located spinal neurons are physiologically relevant to proper hindlimb control. Considerably less information is available regarding the dorsally derived populations. Often, the origin and physical characteristics have been defined, but the function of the populations has not been studied. Given the extensive characterization of sensory control of locomotion available from the feline model, further understanding of these dorsal populations is imperative to bridge the gap which currently exists in the locomotor literature.

During embryonic development in the mouse, there are two phases of dorsal interneuron genesis; the first yields dorsal interneuron populations 1 through 6 (dI1-dI6) between embryonic day 10-11.5 (E10-E11.5) while two late populations, dIL_A and dIL_B arise between E12-E13.5 (Gross et al., 2002, Muller et al., 2002). Class A dorsal populations rely on Wnt signalling from the roof plate and include the dI1-dI3 interneurons. Class B dorsal populations develop independently of Wnt signalling and are identified via Lbx1 expression. These include dI4-dI6 as well as the two late born populations.

Class A Dorsal Interneurons

dI1 Interneurons

Immediately ventral to the roof plate, the dI1 population develops from the Atoh1-expressing *dp1* progenitor domain (Helms & Johnson, 1998). Post-mitotically all dI1 cells express Brn3a (Gowan et al., 2001, Muller et al., 2002). Upon further diversification, two subtypes arise which express either Lhx9, or Lhx2 with low levels of Lhx9.

After leaving the cell cycle, dI1 cells migrate ventrally and settle in the deep dorsal horn (Bermingham et al., 2001). Laterally located cells extend axons ipsilaterally and are thus termed $dI1_i$ whereas medially located dI1 cells extend axons contralaterally and are termed $dI1_c$. Distinction based on location and projection pattern is congruent with transcription factor expression profile, as laterally located $dI1_i$ cells express Lhx9 alone and medially located $dI1_c$ cells express high Lhx2 and little Lhx9 (Wilson et al., 2008).

Neurons of the dI1 population make up part of the spinocerebellar tracts (SCTs) with $dI1_c$ and $dI1_i$ subpopulations forming the ventral and dorsal subdivisions, respectively (Bermingham et al., 2001, Miesegaes et al., 2009). Additionally, within the cervical and thoracic spinal cord, dI1 interneurons form the rostral SCT. As the cerebellum is critically involved in motor learning and execution of smooth and accurate movements (reviewed in Ito, 2002), it seems likely that the dI1 interneurons, by relaying proprioceptive information as the SCTs, serve an important role in motor control.

dI2 Interneurons

Ventral to the *dp1* progenitor domain, *Neurog1* and *Neurog2* demarcate the *dp2* progenitor domain, cells of which differentiate into dI2 interneurons. This population expresses the transcription factors Lhx1/5, Brn3a, and Foxd3 (Gowan et al., 2001, Gross et al., 2002, Muller et al., 2002). dI2 interneurons migrate into the intermediate and ventral horns (Gross et al., 2002). They develop into glutamatergic relay interneurons that project contralaterally and send sensory information to higher brain centres (Gowan et al., 2001, Bermingham et al., 2001).

dI3 Interneurons

Proceeding further ventrally, expression of the transcription factor Ascl1 demarcates the *dp3-dp5* progenitor domains. Low levels of *Pax7* help define the *dp3* domain which give rise to the dI3 interneurons (Muller et al., 2002). Post-mitotically these interneurons are identified via their expression of Isl1 (Liem et al., 1997, Pfaff et al., 1996). Analysis of neurotransmitter phenotype in the juvenile animal indicated that this population is exclusively excitatory (Bui et al., 2013). The first thorough examination of dI3 interneurons was carried out in functionally mature animals (P13-20) in which it was shown that dI3 interneurons are equally distributed among laminae V, VI, and VII (Bui et al., 2013).

These interneurons target both motorneurons and other spinal interneurons located within the ipsilateral side of the spinal cord. Reconstruction of Neurobiotin filled dI3 cells as well as Cre-mediated YFP labelling of Isl1-expressing neurons reveal dI3 terminals in close apposition to the somata and proximal dendrites of motorneurons (Bui et al., 2013). Monosynaptically restricted rabies virus injection into the quadriceps muscle revealed premotor dI3 interneurons located at all segmental levels within the lumbar enlargement, exclusively in the ipsilateral spinal cord (Stepien

et al., 2010, Goetz et al., 2015). Synaptic connections onto spinal interneurons was demonstrated using YFP-labelling of $Isl1^{+}$ cells (Bui et al., 2013). dI3 terminals were found in contact with interneurons throughout the intermediate laminae, including other dI3 cells.

Sensory input to dI3 interneurons was demonstrated using both immuno-histochemistry and electrophysiology. Primary afferent terminals, identified via vGluT1 immunoreactivity, were identified on the vast majority of dI3 interneurons (Bui et al., 2013, Alvarez et al., 2004). Intracellular recording from dI3 interneurons revealed the functional significance of these terminals since approximately 30% of tested dI3 interneurons received clear monosynaptic input following dorsal root stimulation (Bui et al,. 2013). Based on the response to varying stimulus intensities, the authors proposed that dI3 interneurons integrate information from proprioceptive and low-threshold cutaneous afferents. Furthermore, as these cells are monosynaptically connected to motorneurons it was suggested they could mediate excitatory disynaptic reflex pathways. In fact, gastrocnemius motor response to sural nerve stimulation is lost in transgenic mice in which vGluT2 expression is eliminated from Isl1-expressing dI3 cells, providing further evidence that dI3 interneurons mediate short latency, low threshold cutaneous reflexes (Bui et al, 2013).

As removal of the dorsal horn does not abolish locomotor activity (Kiehn &Kjaerulff, 1998), dI3 interneurons cannot be fundamental to locomotor rhythm generation. Silencing of the excitatory dI3 interneuron population does not eliminate the ability to walk in adult animals (Bui et al., 2013). Rather, this loss impairs fine motor activities which require cutaneous afferent feedback, for instance walking on the rungs of a ladder. The most marked behavioural phenotype observed in Isl1 deficient mice is a significant reduction in grip strength, possibly due to reduced sensation in the paws.

Class B Dorsal Interneurons

dI4 Interneurons

Like the *dp3* domain, *dp4* progenitors can be identified via Ascl1 expression, however they can be distinguished from the more dorsal domain by high expression of Pax7. Like all Class B dorsal interneuron, post-mitotic dI4 interneurons express Lbx1. Pax2 and Lhx1/5 are also expressed by dI4 cells, though these are shared with the dI6 population (Gross et al., 2002, Muller et al., 2002). The relatively unique transcription factor Ptf1a is of particular importance in securing dI4 identity and suppressing dI5 cell fate (Glasgow et al., 2005, Pillai et al., 2007). dI4 cells are inhibitory and represent a major contingent of GABAergic interneurons in the deep dorsal horn (Glasgow et al., 2005, Pillai et al., 2007).

dI5 Interneurons

The *dp5* progenitors share Ascl1 and high Pax7 expression with the *dp4* progenitor domain and post-mitotic dI5 cells express Lbx1, similar to dI4 cells (Muller et al., 2002). The dI5 population is primarily identified by its relatively unique expression of Lmx1b and, in a subset of cells, Phox2a (Gross et al., 2002, Muller et al., 2002, Ding et al., 2004). dI5 interneurons constitute an excitatory population (Ding et al., 2004, Pillai et al., 2007). Beginning at E10.75, some dI5 interneurons migrate towards the ventral horn while others migrate dorsally (Muller et al., 2002). By E11.5, clusters of dI5 interneurons reside laterally, above the motor column (Gross et al., 2002). To date, the role of the ventrally situated dI5 interneurons has not been investigated.

dIL_A & dIL_B Late Born Interneurons

The two late born populations migrate into the superficial dorsal horn, where they serve a function in pain and temperature sensation. The dIL_A and dIL_B populations share transcription factor profiles with the dI4 and dI5 populations, respectively, and as such the functions of the early and late born populations can be difficult to distinguish using genetic approaches. Similar to dI4 interneurons, post-mitotic dIL_A cells express Ptf1a, Lbx1, Lhx1/5 and Pax2 (Gross et al., 2002, Glasgow et al., 2005). dIL_A cells project exclusively ipsilaterally and have been proposed to develop into the association interneurons of the substantia gellatinosa (Gross et al., 2002). Soon after their birth they assume a GABAergic phenotype and thus contribute to inhibition in sensory transmission (Helms & Johnson, 2003, Cheng et al., 2004, Glasgow et al., 2005). Like the dI5 cells, dIL_B neurons express Lbx1, Lmx1b, Tlx3, and Brn3a. At E13.5, vGluT2 expression was demonstrated in 98% of Lmx1b-expressing cells found in the superficial dorsal horn (Cheng et al., 2004). Thus dIL_A and dIL_B cells serve opposing functions of providing inhibition and excitation, respectively, within the superficial dorsal horn.

dI6 Interneurons

A major focus of the Gosgnach laboratory and of this thesis is the dI6 interneuron population. The dI6 interneurons have proven difficult to characterize as an exclusive molecular marker that encompasses the entire population has not been discovered. Consequently, conclusions about cellular characteristics have been drawn based on assumed commonalities to interneuron populations with similar transcription factor expression profiles. In the absence of experimental evidence, such speculation must be approached with skepticism. Chapter 4 of this thesis provides an in depth examination of the physical characteristics of the dI6 population within the lumbar

enlargement, so the information hereafter provides a background regarding the developmental origin of these cells and highlights many of the assumptions prevalent in the literature.

The dI6 interneurons derive from progenitors in the ventral-most aspect of the dorsal neural tube, immediately dorsal to the sulcus limitans (Gross et al., 2002, Muller et al., 2002). The dp6 progenitor domain shows high levels of Pax7, co-expressed with Dbx2 (Muller et al., 2002). Like other Class B dorsal interneurons, upon leaving the ventricular zone dI6 cells express Lbx1. Additional transcription factors include Lhx1/5 and Pax2, though these are also expressed by other interneuron populations (Gross et al., 2002, Muller et al., 2002). Isolation of dI6 cells has typically relied on a process of elimination: the dorsal limit is defined by Lmx1b expression, which labels dI5 cells and the ventral boundary is defined by Dbx1 expression, which is restricted to V0 interneurons.

Currently two molecular markers are used to identify dI6 interneurons: Wt1 and DMRT3. The transcription factor Wt1 was first introduced as a marker of dI6 cells in a review paper (Goulding, 2009). Unfortunately, little supporting data is available, hence, it is impossible to evaluate the validity of this claim. It remains unclear what proportion of the total dI6 population is captured by this marker or whether it is exclusive to dI6 cells. Nevertheless, the review is regularly cited as evidence that dI6 cells can be identified by Wt1 expression. Recently, DMRT3 has been proposed as a novel marker for a subpopulation of dI6 cells (Andersson et al., 2012). At E11.5, DMTR3 expressing cells are found adjacent to the ventral-most aspect of the $Pax7^{+}$ progenitor domain and show considerable coexpression of Pax2 and Lbx1. $DMRT3^{+}$ cells do not coincide with Lmx1b or Evx1 immunolabeled cells, indicating they are neither dI5 nor $V0_{V}$ interneurons, leading the authors conclude DMRT3 labels dI6 interneurons. At E14.5, there was partial overlap between the expression of DMRT3

and Wt1, from which the authors propose that each transcription factor labels different, but partially overlapping subpopulations of dI6 cells. It is worth noting that this study could not exclude the possibility that some of the DMRT3 expressing cells belong to the $V0_D$ population which are derived immediately adjacent to dI6 cells and share many transcription factors.

The approach used in this thesis to demarcate dI6 interneurons takes advantage of Cre recombinase expression in a peculiar transgenic mouse. The $TgDbx1^{Cre}$ transgenic mouse line used has been described previously (Dyck et al., 2012). In short, during neural tube development Cre recombinase expression is partially dorsally shifted relative to Dbx1 expression, resulting in its expression in the dorsal V0 population ($V0_D$) and a subset of dI6 interneurons. As β-galactosidase labelling accurately recapitulates Dbx1 protein expression in the $Dbx1^{lacZ}$ transgenic mouse line, it can be used to distinguish genuine p0-derived V0 interneurons from the spuriously labelled dI6 interneurons. Comparison of enhanced fluorescent protein (EFP) expression and β-gal labelling in $TgDbx1^{Cre}$:Rosa26EFP:$Dbx1^{lacZ}$ spinal cords allows for the identification of three populations of interneurons. Interneurons which show β-gal labelling are $V0_V$ cells and those which show both β-gal and EFP labelling are $V0_D$. Cells which lack β-gal labelling and only express EFP are dI6 interneurons. As with DMRT3 and Wt1, it remains unclear what proportion of the total dI6 population is captured, however solitary EFP expression can reliably be used to identify dI6 cells.

Similar to subpopulations of dI5, dI6 interneurons have begun to migrate ventrally at E10.75 and by E12.5 they are well established within the ventral horn (Muller et al., 2002). Their final settling position has not previously been well studied. Previous description of the $Wt1^+$ dI6 cells indicated they settle in lamina VIII postmitotically (Hendricks & Goulding, 2007). dI6 interneurons identified via DMRT3-expression are likewise found in the medial ventral horn, though this was not

thoroughly described (Andersson et al., 2012). A prior report from the Gosgnach laboratory revealed that at least a small contingent of dI6 interneurons are located in lamina VII, immediately dorsal to the central canal (Dyck et al., 2012).

The neurotransmitter utilized by dI6 cells is unknown, though they are speculated to be inhibitory (Lanuza et al., 2004, Goulding et al., 2006, Rabe et al., 2009). Molecular pathways regulating neurotransmitter phenotype within the dorsal spinal cord involve a variety of transcription factors including Pax2, Lbx1, Tlx1 and Tlx3 (Cheng et al., 2004, 2005). Studies show that within the superficial dorsal horn Pax2 expression is associated with a GABAergic phenotype, whereas Tlx1/3 are expressed in glutamatergic cells (Cheng et al., 2004). Likewise, Lbx1 is associated with an inhibitory phenotype in the dorsal horn unless antagonised by Tlx3, which is expressed in the excitatory dI3 and dI5 populations (Cheng et al., 2005). Such studies led to the pervasive assumption that dI6 cells, which express Pax2 and Lbx1, must be inhibitory.

Unfortunately, these studies addressed only the dorsal horn and as a significant number of dI6 interneurons migrate ventrally, they would not have been examined. Differentiation does not proceed in the same manner across the spinal cord so it is possible ventral dI6 cells do not develop along the same path as dorsally located cells despite common transcription factors. Moreover, the studies are limited to early embryonic time points (E11.5-14), which may not accurately represent final maturation of the neurons. In fact, it was noted that *Pax2* expressing cells in deep dorsal laminae no longer express *Gad1* at E15.5 or P0, despite continued co-expression in the superficial dorsal horn (Cheng et al., 2004). Furthermore, ectopic Pax2 expression in the chick embryo does not cause increased Gad1 expression. This demonstrates Pax2 expression may be necessary to maintain an inhibitory nature, but is not sufficient to induce GABAergic differentiation. At P11, DMRT3-expressing interneurons express *Viaat* and are hence inhibitory (Andersson et al., 2012). Again,

as DMRT3 is not expressed in all dI6 interneurons it is unclear whether they are representative of the population as a whole. While it is indeed possible that dI6 cells are exclusively inhibitory, this has not been directly demonstrated and thus further investigation is warranted.

The incorporation of molecular genetics into the investigation of the locomotor CPG sought to divide the spinal cord into a defined number of functionally related populations. While transcription factor expression in the embryo proved pivotal by defining cardinal interneuron populations, subsequent research has demonstrated a spectrum of subpopulations within each. Furthermore, many of the complex functions of the spinal cord involve cells of diverse developmental origin. Although the solutions may not be as simple as originally thought, molecular genetics have significantly refined the possible avenues for exploring spinal neural networks.

1.5 Comparison of genetically and functionally defined spinal interneurons

The incongruous methodologies applied in investigations of the locomotor CPG in mice versus cats has confounded direct comparison between the spinal cord architecture of the two mammals. As the mouse has primarily been studied at early developmental stages, either embryonic or neonatal, it is debatable whether the spinal circuitries can be directly compared to those of the functionally mature mouse, let alone to the cat. Currently, very few analogous interneuron populations described in the cat have been shown to derive from a genetically-defined interneuron population in the mouse.

Renshaw cells are exclusively of V1 origin

Renshaw cells were the first functionally defined interneurons whose developmental origin was discovered. In $Pax6^{-/-}$ mice the V1 interneurons population does not differentiate and Renshaw cells cannot be found (Sapir et al., 2004). In $En1^{-/-}$ mice, the V1 populations develop, and primitive Renshaw cells can be found, however they fail to migrate correctly and their projections to motorneurons are impaired. Thus correct development of the V1 population is critical to the development of Renshaw cells and the pathways mediating recurrent inhibition.

Ia Inhibitory Interneurons arise from V1 and V2b interneurons

While all Renshaw cells develop from $En1^{+}$ interneurons, these cells represent only 10% of the total V1 population (Sapir et al., 2004). Therefore, the ipsilaterally projecting inhibitory V1 population undoubtedly contributes to additional spinal functions. In fact, V1 interneurons were also shown to give rise to 90.2% of the Ia inhibitory interneurons, as defined by their immunoreactivity for parvalbumin with a dense surrounding calbindin plexus (Alvarez et al., 2005). Again, this represents a small proportion of the total V1 population. In wildtype pups, examination of the inhibitory reflex pathway from the quadriceps nerve to posterior biceps/semitendonosus (PB/St) motorneurons reveals hyperpolarizing potentials arriving in motorneurons at disynaptic latencies, a hallmark feature of reciprocal inhibitory reflexes (Wang et al., 2008, Zhang et al., 2014). In contrast, these potentials are lost in $Gata3^{Cre};En1^{Cre};R26^{floxstop\text{-}TeNT}$ transgenic pups, indicating the necessity for neurotransmission from V2b and V1 interneurons. Elimination of synaptic release from either population alone (using $Gata3^{Cre};R26^{floxstop\text{-}TeNT}$ or $En1^{Cre};R26^{floxstop\text{-}TeNT}$ offspring) was insufficient to abolish disynaptic inhibitory potentials in motorneurons, suggesting the dual origin of Ia Inhibitory Interneurons (Zhang et al.,

2014). In addition to defining the embryonic origin of one of the most well studied spinal interneuron types, this study was significant in that it demonstrated for the first time that one functionally-defined population can derive from more than one genetically-defined precursor population.

Presynaptic Inhibition derives from dI4 interneurons

It has been shown that dI4 interneurons supply most, if not all, GABAergic inhibition of sensory afferents, indicating they are fundamentally responsible for presynaptic inhibition (Betley et al., 2009). Although no genetic marker has been identified to distinguish subpopulations of dI4 interneurons, the expression of different proteins by dI4 cells targeting afferents mediating discrete sensory modalities indicates that subpopulations must exist. For instance, dI4 cells contacting cutaneous afferents express GlyT2, encephalin, and neuropeptide Y. None of these are found in dI4 interneurons which inhibit proprioceptive afferent terminals (Betley et al., 2009). This provides an example of the way in which function based approaches can be combined with genetic based approaches for elucidating spinal cord circuitry.

As the available genetic tools advance and investigation of the locomotor CPG in mice progresses towards the adult animal, the identity of the classical functionally-defined interneurons of the cat will undoubtedly be reconciled with their genetically-defined precursors. Two groups have recently developed a decerebrate mouse preparation which would allow the sensorimotor control of locomotion in the adult cat to be directly compared to the adult mouse (Nakanishi & Whelan, 2012, Meehan et al., 2012). Undeniably, examination of genetically-defined interneurons in the adult decerebrate mouse has the potential to harmonize our understanding of the mammalian locomotor CPG across the two dominant experimental models.

1.6 Conceptual models of the locomotor CPG

Throughout the history of the locomotor CPG, diverse conceptual models have been proposed in an attempt to consolidate observed locomotor-related behavioural phenomena with known neural connectivity of the spinal cord. The following section reviews the more prevailing models.

Half-Centre Model

The Half-Centre Model posits that the locomotor rhythm is generated through mutual inhibition between two reciprocally connected half-centres, one promoting extension and the other flexion. Activity in the extensor half-centre directly excites extensor motorneurons while simultaneously inhibiting the flexor half-centre, thereby suppressing flexor motorneuron activity. As activity in the extensor half-centre decreases through a fatigue mechanism, the flexor half-centre is relieved of inhibition and the dominant motor output switches to flexion. Initially proposed by Thomas Graham Brown in the early 20th century (Brown, 1911), this model gained popularity in the 1960s when Lundburg and Jankowska first recorded from spinal neurons which could potentially support this mechanism (Lundburg 1965, Jankowska et al., 1967*a,b*). As previously described (Section 1.3.2.4), stimulation of the FRAs causes excitation of the ipsilateral flexors and contralateral extensors, coupled to inhibition of their respective antagonists. Interneurons located in lamina VII of the feline lumbar spinal cord were identified which were activated by ipsilateral Flexor Reflex Afferent (FRA), contralateral FRA, or both ipsi- and contralateral FRA stimulation. Following administration of L-DOPA and nialamide to spinal cats, brief FRA stimulation could elicit bouts of self-sustained alternating flexor-extensor bursting. Critically, stimulation of contralateral FRAs could abolish bursting activity resulting from ipsilateral FRA stimulation thus demonstrating reciprocal inhibitory pathways. This strong mutual

inhibition provided the first demonstration of connectivity between spinal interneurons which could potentially comprise Graham Brown's half-centre.

Miller & Scott Model

This model was briefly described in Section 1.3.2.6, but is here revisited as an elaboration of the Half-Centre Model. Taking into account the defined spinal pathways between Renshaw cell (RCs), Ia inhibitory interneuron (IaINs) and motorneurons, Miller and Scott (1977) proposed their model in which RCs are responsible for the rundown of the dominant half centre. Activity in extensor motorneurons increases drive to their coupled RC. This causes RCs to inhibit the agonist motorneurons via recurrent inhibition and simultaneously inhibit the IaINs which suppress antagonist motorneurons. This relieves flexor motorneurons of inhibition and favours phase switching to flexion. This model has been refuted as blocking nAChRs with mecamylamine, thereby blocking RC activation by motorneuron collaterals failed to abolish locomotion (McCrea et al., 1980, Pratt & Jordan, 1987). Furthermore, locomotor rhythm persists, albeit slowed, in the absence of V1 interneurons (Gosgnach et al., 2006) which have been shown to be the sole source of RCs (Sapir et al., 2004).

Unit Burst Generator Model

Limbed locomotion is significantly more complex than clumsy alternation between all extensors and all flexors of a limb; some bifunctional muscles, such as the semitendinosus, are active during both stance and swing, some flexor muscles are active before the onset of the primary flexor burst (see Rossignol, 1996) and some muscles switch function depending on the gait. The Unit Burst Generator (UBG) model proposes multiple separate rhythm generators controlling activity at each joint of each limb (Grillner & Zangger, 1974). Activity of all UBGs is integrated to yield comprehensive locomotor output, yet each remains sufficiently independent to allow

deviations away from strict flexor-extensor alternation. The rhythmogenic basis of each UBG remains, however, coupled flexor-extensor half centres driving flexor and extensor motorneurons.

Two-Layer Half-Centre Model

One experimental observation which all previously described models fail to explain is the spontaneous absence of bursts during ongoing fictive locomotor activity which can occur across several synergist muscles (Lafreniere-Roula & McCrea, 2005). These missed bursts, termed deletions, are classified as either resetting or non-resetting based on the timing of the resumed locomotor activity. Resetting deletions are those in which the onset of the returning bursts is either advanced or delayed relative to the pre-deletion activity. If post-deletion activity instead returns at the time predicted had the deletion not occurred, it represents a non-resetting deletion. The authors suggest non-resetting deletions divulge a mechanism by which the timing of locomotor rhythm is maintained, independent of control of motor output. Such a mechanism cannot exist in models in which the rhythm generating circuits directly activate motorneurons and thus the authors proposed the Two-Layer Half-Centre Model (Lafreniere-Roula & McCrea, 2005, McCrea & Rybak, 2008).

In this model distinct rhythm generating (RG) and pattern forming (PF) layers exist; the former generates the locomotor rhythm and activates the latter which, in turn, recruits the appropriate motor pools (McCrea & Rybak, 2008). As in earlier models, the RG layer generates the basic rhythm through flexor and extensor half-centres which reciprocally inhibit one another via inhibitory interneurons. Each half-centre is comprised of a homogeneous pool of mutually connected excitatory interneurons which possess intrinsic cellular properties (most notably a slowly inactivating persistent sodium current [NaPIC]) which support rhythmogenesis. Burst

onset results primarily due to the NaPIC, whereas burst offset results from the reciprocal inhibition between RG half centres. The PF network has a similar cellular connectivity to the RG layer but the constituent neurons have significantly weaker rhythm generating capacity. Rhythmic activity in the PF layer results from 1) excitation from the RG half-centre, as well as 2) inhibition from the same inhibitory interneuron populations which secure alternation between the two RG half-centres. Rhythmically active interneurons of the PF-layer depolarize the appropriate motorneurons, while an additional population of inhibitory interneurons, driven by the PF network, hyperpolarize motorneurons of the antagonist muscles. Thus, neurons of the PF layer secure flexor-extensor motorneuron alternation within a limb, but are only rhythmically active as a result of the phasic input from the RG layer.

Such a network composition can explain both types of experimentally observed deletions. A resetting deletion occurs due to a disturbance in the activity of the RG layer such that timing of switching between active half-centres is affected. This 'error' is transmitted to the PF layer and subsequently down to the motor pools, resulting in advanced or delayed locomotor output. In contrast, a non-resetting deletion occurs due to a disturbance to the PF layer and consequently while the motor output across many synergist muscles may be affected, the timing of the locomotor rhythm is preserved by the unaffected RG layer. When the PF layer recovers, locomotor activity resumes at the appropriate time because the rhythm of the PF layer is under the direction of the RG layer. Interestingly, a similar phenomenon has been observed in the mammalian respiratory CPG (Kam et al., 2013), suggesting that two-layer neural circuits may represent a common mechanism controlling rhythmic motor outputs in higher vertebrates.

While the Two-Layer Half-Centre model has considerable explanatory power, there remain several findings it cannot explain. The initial Two-Layer Model proposed

a symmetry between extensor and flexor elements (McCrea & Rybak, 2008). However, more recent experimental evidence has countered this as non-resetting deletions occurring in the extensor-related L5 ventral root do not necessary correspond to a complementary disruption in activity of the flexor-related L2 ventral root (Zhong et al., 2012). In contrast, deletions on the L2 root are invariably associated with sustained activity of the L5 root. This general pattern is reminiscent of the results of earlier transection experiments. During drug-induced fictive locomotion, partial transection through the L3 segment eliminated rhythmic activity in the L5 ventral root without effecting activity of its ipsilateral L2 root (Kiehn & Kjaerulff, 1996). Both observations suggest a dominating effect from the flexor onto the extensor, rather than balanced reciprocal inhibition between the two. It may therefore be worth revisiting asymmetrical models of the locomotor CPG, such as the Flexor Burst Generator model (Pearson & Duysens, 1976).

While it could be argued that the flexor-extensor asymmetry arises at the pattern forming layer, and thus does not reveal the nature of rhythm generation, several recent studies suggest that mutually inhibitory half-centres may not be the source of the rhythm. Recent optogenetic studies which activated excitatory lumbar interneurons within a limited region demonstrated that nearby flexor or extensor motorneurons become rhythmically active. It is argued this demonstrates independent activation flexor or extensor circuitry without reciprocal connections between the two (Hagglund et al., 2013). Additionally, silencing the output from the V1 and V2b interneuron populations abolishes flexor-extensor alternation but does not eliminate rhythmic locomotor activity (Zhang et al., 2014). This strongly argues against mutual inhibition between flexor-extensor half centres as the primary mechanism of locomotor rhythm generation. Thus, while the suggestion that distinct pattern forming and rhythm generating populations of cells contribute to the locomotor CPG seems valid, it

remains unclear whether the Two-Layer Half-Centre Model adequately explains the origin of the fundamental locomotor rhythm.

1.7 Conclusion

Over a century of research has expanded the initial simple suggestion of a spinally restricted locomotor central pattern generator into an elaborate network of functionally and genetically defined neurons. Research has evolved from broad examination of locomotor activity at the network level towards detailed investigation of individual CPG interneurons. The recent incorporation of molecular genetics to identify neuronal populations builds upon an extensive foundation obtained from careful examination of the control of locomotion in the cat. All of this research provides valuable information about the constituent CPG interneurons, the nature of their interconnectivity, and the manner in which their combined activity yields the remarkably resilient and elegant locomotor output.

The experiments presented in the following thesis were designed to broaden our understanding of the cellular architecture of the mammalian locomotor CPG. Chapter 1 addresses the distribution and morphology of putative pattern forming and rhythm generating interneurons identified solely based on their behaviour during locomotion. Chapter 2 adopts a molecular genetic approach to distinguish $V0_V$ and $V0_D$ interneurons and examine the anatomical and functional diversity between the two subpopulations. Finally, Chapter 3 examines one of the most poorly understood populations located in the postnatal ventral spinal cord, the dI6 cells. A combination of electrophysiological and immunohistochemical experiments provide insight into the location, connectivity, and locomotor-related activity of this elusive population. This

work contributes to the general understanding of the composition of the locomotor central pattern generator as well as provides a detailed characterization of three of its genetically-defined constituent populations.

Chapter 2 - Regional distribution of rhythm generating and pattern forming components of the mammalian locomotor CPG.

Griener A, Dyck J, Gosgnach S. (2013) Regional distribution of putative rhythm-generating and pattern-forming components of the mammalian locomotor CPG. Neurosci. 250: 644-50.

2.1 Abstract

The ventromedial spinal cord of mammals contains a neural network known as the locomotor central pattern generator (CPG) which underlies the basic generation and coordination of muscle activity during walking. To understand how this neural network operates, it is necessary to identify, characterize, and map connectivity amongst its constituent cells. Recently, a series of studies have analyzed the activity pattern of interneurons that are rhythmically active during locomotion and suggested that they belong to one of two functional levels; one responsible for rhythm generation and the other for pattern formation. Here we use electrophysiological techniques to identify locomotor-related interneurons in the lumbar spinal cord of the neonatal mouse. By analyzing their activity during spontaneous deletions that occur during fictive locomotion we are able to distinguish between those likely to belong to the rhythm generating and pattern forming levels, and determine the regional distribution of each. Anatomical tracing techniques are also employed to investigate the morphological characteristics of cells belonging to each level. Results demonstrate that putative rhythm generating cells are medially located and extend locally projecting axons, while those with activity consistent with pattern formation are located more laterally and send axonal projections to the lateral edge of the spinal cord, in the direction of the motoneuron pools. Results of this study provide insight into the detailed anatomical organization of the locomotor CPG.

2.2 Introduction

A neural circuit, commonly referred to as the locomotor central pattern generator (CPG) is embedded within the thoraco-lumbar spinal cord of mammals and is responsible for generating the basic alternating motoneuron activity necessary for locomotion (see Kiehn 2006 for review). With appropriate tuning via inputs from higher centers and the periphery, this circuit is able to provide a wide range of output to hindlimb motoneurons resulting in task specific locomotor behavior (McCrea 2001; Rossignol et al. 2006).

Early studies employing electrophysiological techniques to investigate this neural network were successful in identifying cells that were rhythmically active during locomotion, however the inability to identify neurons belonging to functionally homogeneous populations has limited the conclusions that could be drawn regarding the overall architecture of the locomotor CPG. In the past decade the genetic dissection of the mammalian spinal cord has led to the identification of several populations of molecularly-defined interneurons that are components of the locomotor CPG. Genetic silencing techniques combined with electrophysiological studies have enabled the specific function of several of these populations to be determined (see Goulding 2009 for review). Despite this work, the cells responsible for generating the locomotor rhythm have yet to be identified.

In parallel with the work described above, several conceptual models of the locomotor CPG have been proposed (Gurfinkel and Shik 1973; Miller and Scott 1977; Grillner 1975; McCrea and Rybak 2008; see Guertin 2009 for review) in an attempt to provide insight into the network structure of this neural circuit. One that has recently received considerable attention is the two-level model of the locomotor CPG (Rybak et al. 2006a,b) in which interneurons that are rhythmically active during locomotion are separated into two functional levels. Cells at the rhythm generating (RG) level function

as a clock and set the frequency of network oscillation as well as phase duration. Cells at the pattern forming (PF) level receive input from RG cells, project to hindlimb motoneurons and control their burst amplitude and duration (see McCrea and Rybak 2007; 2008 for review). In addition to providing a framework to test hypotheses regarding the structure and function of the locomotor CPG, a recent study has demonstrated that this model provides a means of identifying neurons involved in rhythm generation and pattern formation based on their behavior during spontaneous omissions of fictive locomotor activity in which the phase of the rhythm does not change following resumption of locomotion (i.e. a non-resetting deletion) (Zhong et al. 2012). Components of the RG level are expected to maintain oscillatory activity during non-resetting deletions, consistent with their function of controlling oscillation frequency and phase duration. Cells belonging to the PF level, on the other hand, are expected to cease rhythmic oscillation (McCrea and Rybak 2008; Zhong et al. 2012).

In order to provide insight into the functional organization of the locomotor CPG we incorporate this analysis approach to identify, in the neonatal mouse spinal cord, candidate cells involved in locomotor rhythm generation and pattern formation, determine the regional distribution of each, and compare their morphological characteristics. Results demonstrate that cells with an activity pattern consistent with rhythm generators are clustered in the medial regions of the lumbar spinal cord and extend short, locally projecting axons. Cells with an activity pattern consistent with pattern formers are distributed more laterally and send long processes to the lateral aspect of the spinal cord in the direction of the motor pools.

2.3 Experimental Procedures

Animals. All procedures were in accordance with the Canadian Council on Animal Care (CCAC) and approved by the Animal Welfare Committee at the University of

Alberta. In total, experiments were performed on 38 neonatal (0-3 days of age; i.e. P0-P3) mice. Offspring from CD1 (wildtype), $Dbx1^{Cre}$:$Rosa26^{EFP}$ and/or $Dbx1^{LacZ}$ mice were used for all experiments. The majority of animals used did not express reporter protein (i.e. Cre^- or EFP^- offspring) and thus the specific genetic population to which they belonged could not be determined.

In-vitro preparation. Mice were quickly decapitated, eviscerated and the spinal cord was dissected out in a bath containing oxygenated, ice-cold dissecting artificial cerebrospinal fluid (d-aCSF) with a low Ca^{2+} and high Mg^{2+} concentration. This solution was comprised of (in mM) 111 NaCl, 3.08 KCl, 11 glucose, 25 $NaHCO_3$, 1.18 KH_2PO_4, 3.7 $MgSO_4$, 0.25 $CaCl_2$, (pH of 7.4, osmolarity 280-300 mOsm). Since the majority of interneurons that comprise the locomotor CPG are located in the intermediate nucleus of the lumbar spinal cord we focussed our investigation on lamina VII and X. The preparation used for targeting interneurons located in the inner laminae of the spinal cord for whole cell recording while leaving the locomotor CPG functionally intact has been described in detail (Dyck & Gosgnach, 2009). Briefly, the spinal cord was transferred to a vibratome chamber containing oxygenated d-aCSF and pinned, dorsal side up, to a strip of agarose. The vibratome was then used to shave away sections of the dorsal aspect of the lumbar spinal cord until the dorsal extent of the central canal was visible with a dissecting microscope. Removal of tissue ventral to this point negatively impacted our ability to generate fictive locomotion (Dyck & Gosgnach, 2009). Following sectioning, the spinal cord was situated dorsal side up on a coverslip in a plexi-glass recording chamber and held in place via nylon threads stretched over a platinum wire flattened into a horseshoe shape.

Electrophysiological Recording. The preparation was constantly perfused with room temperature, oxygenated recording artificial cerebrospinal fluid (r-aCSF) which was identical to the dissecting solution except for the following (in mM): 1.25 $MgSO_4$,

2.52 $CaCl_2$. In all experiments fictive locomotor activity was induced by bath application of 10-15μM 5-hydroxytryptamine creatine sulfate complex (5-HT) and 5-15 μM N-Methyl-D-Aspartate (NMDA) (both from Sigma-Aldrich) and monitored via electroneurogram (ENG) activity recorded from bipolar suction electrodes (A-M Systems Inc.) positioned on the flexor-related (second or third lumbar i.e. L2 or L3) and/or extensor-related (fifth lumbar i.e. L5) ventral roots. In most cases recordings were made from only one of the aforementioned ventral roots due to the limited working distance under the objective lens of the microscope. ENG signals were amplified (20,000x) and band pass filtered (100Hz-1kHz) with custom made equipment (R&R Designs). All ENG and whole cell data was digitized (Digidata 1440A) and recorded using pClamp software on a PC.

For whole cell recordings, patch electrodes (tip resistance: 4–7 MΩ) were pulled from borosilicate glass and filled with internal solution containing (in mM): K-gluconate, 138; Hepes, 10; $CaCl_2$, 0.0001; GTP-Li, 0.3; ATP-Mg, 5 (pH adjusted to 7.2, osmolarity 290-305 mOsm). For morphological analysis Neurobiotin (0.2%, Vector Labs) was included in the intracellular solution. A micromanipulator (MPC-385, Sutter Instruments) was used to position the electrode over the cut region of the spinal cord and lower it into the tissue. An infrared differential interference contrast (IR-DIC) filter was used to target cells located along the extent of the cut region of the spinal cord for recording. Cells located 20-60 μm from the cut surface of the lumbar spinal cord tended to be healthy and accessible with the recording electrode. The position of the target cell along the mediolateral axis was measured using the micromanipulator coordinates (midpoint of the central canal was used as a reference point for all measurements). Since spinal cords from animals of different ages differ in size, the relative mediolateral position of each cell was calculated by dividing its distance from the central canal by the mean "half-width" (measured from the lateral edge of the

spinal cord to the midpoint of the central canal) of a spinal cords of an age-matched mice. The relative position value was used for all analysis.

Using a whole cell recording amplifier (Multiclamp 700B) in voltage clamp mode, a 10 mV square pulse (50 Hz) was used to monitor tip resistance as the electrode was advanced towards a cell of interest. Once a giga-ohm seal with a cell was formed, the command voltage was set to -60 mV and gentle suction was applied to break through the membrane to obtain a whole cell recording. Series resistance (R_S) was determined in voltage-clamp mode using the compensation features on the Multiclamp commander software and monitored throughout the course of each recording. Initial values of R_S were typically 10-20 MΩ. Recordings where R_S exceed 30 MΩ were excluded from analysis. In some instances, a small amount of negative bias current (10-25 pA) was required to hyperpolarize the cell to prevent spontaneous firing of action potentials. To allow an assessment of their activity pattern during pharmacologically induced fictive locomotion, cells were typically held for 20-25 minutes. This also provided sufficient time for their neurites to be filled with the anatomical tracer Neurobiotin.

Anatomical Reconstruction. Following electrophysiological recording, entire spinal cords containing Neurobiotin-filled cells were fixed overnight in 4% paraformaldehyde/PBS at 4°C, prepared for immunohistochemistry, and incubated overnight in Cy3-conjugated Streptavidin. After washes, spinal cords were placed on a slide, dorsal side down so that the cut surface could be inspected with the objective lens of an inverted spinning disk confocal microscope (Olympus IX81). Z-stack images comprised of 1 µm thick optical sections were captured using Volocity software. Thickness of the Z-stack was set so that all projections were followed until they terminated, or were unable to be deciphered with the microscope. Reconstructions of cells were made using the Simple Neurite Tracer (Longair et al. 2011) plugin in ImageJ. Axons were distinguished from dendrites by analyzing their shape (dendrites taper as

they leave the soma while axons maintain a constant radius- Jan et al. 2010). When analyzing axonal length of cells with multiple axon branches the longest branch was measured. All figures were assembled with Corel Draw and Adobe Photoshop.

Data Analysis and Statistics. All means are reported ± standard deviation (SD). The Rayleigh test for directionality (Drew & Doucet, 1991) was used to identify neurons that were related to fictive locomotor activity. Only those cells in which the P value <0.01 were deemed to be related to ENG activity and included in the data set. Rhythmically active cells were considered to belong to the RG or PF level (referred to as putative RG (i.e. PRG) or putative PF (i.e. PPF) cells from this point forward) based on their behavior during non-resetting deletions of ENG activity on the ipsilateral side of the spinal cord during fictive locomotion (McCrea & Rybak, 2008, Zhong et al., 2012). Non-resetting deletions, defined as spontaneous omissions of rhythmic motoneuron bursting after which activity reappears at a time interval equal to an integer multiple of the pre-deletion cycle period (Lafreniere-Roula & McCrea, 2005), were identified by determining the average cycle period of the 5 ENG bursts immediately preceding the spontaneous deletion, and comparing it to the cycle period in which the deletion occurred. The t-statistic was calculated and a significance level of $p<0.05$ was used to determine whether the cycle period following the deletion met the criteria (see Lafreniere-Roula & McCrea, 2005; Zhong et al., 2012 for details and equations).

2.4 Results

In total, whole cell recordings were made from 75 rhythmically active interneurons in the intermediate nucleus of the neonatal mouse spinal cord between the L1 and L5 segments during pharmacologically induced fictive locomotion. Rhythmic

ENG activity recorded from the ipsilateral L2, L3 or L5 ventral roots was used to monitor fictive locomotion since these have been shown to be comprised of primarily flexor (L2, L3) or extensor (L5) motor axons. All cells analyzed exhibited rhythmic activity that was related to either the active or inactive phase of fictive locomotion in the ipsilateral ventral root belonging to the same spinal segment in which they were located (i.e. the local ventral root- Figure 1A).

Since the goal of this study was to compare properties of cells belonging to the RG and PF levels of the locomotor CPG in the lumbar spinal cord, the first step involved differentiating between cells belonging to each level. This has previously been accomplished by analyzing their activity during spontaneous, non-resetting deletions that occur in motoneurons located on the ipsilateral side of the spinal cord (Zhong et al., 2012). It has been proposed that cells belonging to the RG level maintain oscillatory activity during these deletions, while components of the PF level cease rhythmic oscillation (McCrea & Rybak, 2008, Zhong et al., 2012).

In total, at least one ipsilateral non-resetting deletion was observed during fictive locomotion while recording from 42 of the 75 rhythmically active interneurons (mean number of deletions per cell in the 42 cells was 3.2 ± 2.7). The number of cells with a behavior consistent with those belonging to the RG (i.e. putative RG or PRG cells) and PF (i.e. putative PF or PPF cells) level was identical with 21 neurons maintaining their rhythmic oscillation (Figure 1B) and 21 neurons showing no oscillation during the deletion (Figure 1C). A comparison of their membrane resistances indicated that the size of PRG (mean Rm= 832 ± 474 MΩ) and PPF (mean Rm= 821 ± 395 MΩ) cells did not differ significantly ($p=0.25$, *t*-test).

The specific location of each cell along the mediolateral plane was determined by using the micromanipulator coordinates during whole cell recording to measure the distance from the soma to the midpoint of the central canal. To correct for size differences between spinal cords of various ages, the relative position of each cell was

calculated and used for all analysis. The relative mediolateral position of all PRG and PPF cells is mapped on the schematic in Figure 2A which ranges from 0 (the midline) to 1.0 (the lateral edge). PRG and PPF neurons were recorded on either side of the spinal cord however for the sake of comparison, all PPF cells have been placed on the left side of the schematic (black circles) and PRG cells have been placed to the right (open circles). Statistical analysis indicates that the mean mediaolateral position was significantly greater for PPF cells compared to PRG cells (Figure 2B, $Mean_{PPF}$=0.41 ± 0.14, $Mean_{PRG}$=0.25 ± 0.11 , $p<0.0001$, *t*-test). Use of the relative location value enabled us to determine the number of PPF and PRG cells located in each of four equal quadrants. A substantially greater proportion of PRG cells (15/21) were located in the most medial quadrant (i.e. quadrant 1) of the spinal cord (Figure 2A, 2C) when compared to the PPF cells (5/21) which were distributed among quadrants 1, 2, and 3.

In many cases the inclusion of Neurobiotin in the recording pipette allowed the soma and neurites of rhythmically active interneurons to be passively filled during whole cell recording. A morphological analysis of PRG and PPF cells was performed post hoc (Figure 3). As expected, based on the similarity of their membrane resistance values, the soma diameter (measured across the long axis) of PRG and PPF cells did not differ significantly ($Mean_{PPF}$=18.2 ± 3.9 μm, $Mean_{PRG}$=17.9 ± 2.2 μm, p=0.31, t-test) nor did the number of dendritic branches observed ($Mean_{PPF}$=3.6 ± 2.1, $Mean_{PRG}$=4.8 ± 2.4, p=0.30, t-test).

There were however, clear differences in axonal length and the direction of axonal projection between PRG and PPF cells. Axons (processes ending with a dot in Figure 3C) of PPF cells were significantly longer than those extending from PRG cells ($Mean_{PPF}$=178.1 ± 73.9 μm, $Mean_{PRG}$=62.6 ± 35.8 μm, p=0.002, t-test). Seven of eight PPF cells (based on their activity during non-resetting deletions) extended a long process laterally, towards the motor pools in lamina IX (Figure 3B, black somas in Figure 3C). PRG cells, on the other hand, did not appear to preferentially extend an

axon in any one direction and five of the seven filled cells extended axons that appeared to terminate nearby (Figure 3A, white somas Figure 3C).

2.5 Discussion

The concept of a two-level locomotor CPG comprised of separate cell populations responsible for rhythm generation and pattern formation was initially proposed several decades ago (Orsal et al. 1990). Subsequent support for this arrangement came from investigations studying motoneuron activity in response to sensory stimulation during walking (Kriellaars et al. 1994; Guertin et al. 1995; Perreault et al. 1995; Stecina et al. 2005), as well as the analysis of spontaneous deletions of motoneuron activity during locomotion (Lafreniere-Roula and McCrea 2005; Zhong et al. 2012). Here we make whole cell recordings from rhythmically active interneurons during fictive locomotion in the neonatal mouse, use the organizational principles of the two-level model to identify cells that exhibit activity patterns of neurons responsible for rhythm generation and pattern formation, and map the specific location of each within the spinal cord. While it is likely that some rhythmically active cells included in the dataset were downstream of the CPG and not necessarily components of the RG or PF layer (hence the putative RG and PF designations), results demonstrate that the majority PRG cells are clustered medially with 15/21 located in the most medial quadrant of the lumbar spinal cord. The proportion of PRG cells located in this region is even greater (13/15) if analysis is limited to the rostral segments (L1-L3) which have been shown to be the primary source of rhythmogenesis during locomotion (Kjaerullf and Kiehn 1996; Cowley and Schmidt 1997; Kremer and Lev-Tov 1997; Bonnot and Morin 1998; Christie and Whelan 2005). In contrast only 3 of the 16 PPF cells located in the L1-L3 segments are located in the most medial quadrant of the spinal cord. While the observation that the lateral segments of the lumbar spinal cord, when isolated, exhibit minimal rhythm generating capacity (Kjaerullf & Kiehn,

1996) has led to the assumption that the rhythm generating core of the locomotor CPG is located in the medial region of the spinal cord, the incorporation of this new analysis approach developed by Zhong et al. (2012) allows us to identify interneurons likely to be involved in locomotor rhythm generation and determine their specific distribution within the lumbar spinal cord. It is worth noting that our experimental preparation dictated that all neurons analyzed were located within approximately 60 μm (Dyck & Gosgnach, 2009) of the dorsal edge of the central canal, and it is possible that the distribution of PRG and PPF cells may differ in more ventral regions of the spinal cord. However our observation that sectioning to the ventral extent of the central canal typically results in the inability to pharmacologically evoke fictive locomotion suggests that the majority of rhythm generating cells are located in the region studied.

The proposed network structure of the two-level model of the locomotor CPG suggests that cells belonging to the RG and PF layers have distinct axonal projection patterns (Rybak et al., 2006*a*, McCrea & Rybak, 2008). Cells involved in rhythm generation have been proposed to synapse onto one another as well as members of the PF layer (McCrea & Rybak 2008; see also Brownstone & Wilson, 2008). Cells involved in pattern formation, on the other hand, have been suggested to synapse primarily onto Ia inhibitory interneurons and motoneurons with a subset making contact with other members of the PF layer (McCrea & Rybak, 2008; see also Brownstone & Bui, 2010). In addition to these targets it is possible that cells belonging to either layer may project to propriospinal neurons in order to coordinate motoneurons that control postural muscles, relay neurons that project to the brainstem/cerebellum/cortex to provide information on the ongoing locomotor task (Fedirchuk et al., 2013, Shakya Shrestha et al., 2012), and the intermediolateral nucleus which contains autonomic motoneurons that regulate the sympathetic nervous system.

The results of our anatomical tracing experiments support the assertion that neurons belonging to the RG and PF levels have unique morphologies that are particularly suited to their proposed functions. While Z-stack images in the semi-intact spinal cord preparation were collected in an attempt to identify and follow all neurites to their termination, a number of cells were not included in our analysis since their axons were unable to be identified. This included neurons that projected axons dorsally (dorsal spinal cord was removed to access intermediate nucleus) or a substantial distance ventrally (maximum depth of field with confocal microscope was approximately 100 μm from the surface). Despite this "cell loss" there were clear differences in the axonal projection of PRG and PPF cells. Seven of the eight PPF cells which ceased firing during an ipsilateral non-resetting deletion extended a long neurite laterally, towards the region of the spinal cord in which motoneurons and Ia inhibitory interneurons (and the intermediolateral nucleus) are located, while only one PRG cell projected an axon in this direction. In contrast five of seven PRG cells extended significantly shorter axons medially or caudally. Based on our data indicating that PRG cells are clustered in the medial regions of the lumbar spinal cord this projection pattern is compatible with the premise that cells involved in rhythm generation synapse with functionally homogeneous cells in order to perpetuate the locomotor rhythm (Roberts & Tunstall, 1990, Rowat & Selverston, 1997, Brownstone & Wilson 2008).

Conclusion

An extensive list of characteristic properties have been attributed to interneurons responsible for locomotor rhythm generation (reviewed in Kiehn 2006; Brownstone and Wilson 2008; Brocard et al. 2010). Unfortunately, the fact that none of these properties are unique to rhythm generating cells has hindered their

identification and characterization. The work presented here takes advantage of computational modeling which predicts that rhythm generating cells will exhibit a signature firing pattern during non-resetting deletions. This enables us to identify interneurons likely to be involved in rhythm generation, determine their location in the spinal cord, and investigate their morphological characteristics. This work provides insight into the network structure of the locomotor CPG and sets the stage for future experiments incorporating a similar approach to identify populations of genetically defined interneurons that are involved in rhythm generation. Based on the location of PRG cells identified in the present study and the distribution of genetically-defined interneuronal populations we predict that, in addition to the involvement of the V2a cells (Zhong et al. 2012), members of the Hb9 and dI6 population also play a role in the generation of the locomotor rhythm.

2.6 References

Bonnot A, Morin D. (1998) Hemisegmental localisation of rhythmic networks in the lumbosacral spinal cord of neonate mouse. Brain Res. 793:136-148.

Brocard F, Tazerart S, Vinay L. (2010) Do pacemakers drive the central pattern generator for locomotion in mammals? Neuroscientist. 16:139-155.

Brownstone RM, Bui TV. (2010) Spinal interneurons providing input to the final common path during locomotion. Prog Brain Res. 187:81-95.

Brownstone R, Wilson J. (2008) Strategies for delineating spinal locomotor rhythm-generating networks and the possible role of Hb9 interneurones in rhythmogenesis. Brain Res Rev. 57:64-76.

Christie KJ, Whelan PJ. (2005) Monoaminergic establishment of rostrocaudal gradients of rhythmicity in the neonatal mouse spinal cord. J Neurophysiol. 94:1554-1564.

Cowley KC, Schmidt BJ. (1997) Regional distribution of the locomotor pattern-generating network in the neonatal rat spinal cord. J Neurophysiol. 77, 247–259.

Drew T, Doucet S. (1991) Application of circular statistics to the study of neuronal discharge during locomotion. J Neurosci Methods. 38:171-181.

Dyck J, Gosgnach, S (2009) Whole cell recordings from visualized neurons in the inner laminae of the functionally intact spinal cord. J Neurophys. 102:590-597.

Dyck J, Lanuza GM, Gosgnach S. (2012) Functional characterization of dI6 interneurons in the neonatal mouse spinal cord. J Neurophysiol. 107:3256-3266

Goulding M. (2009) Circuits controlling vertebrate locomotion: moving in a new direction. Nat Rev Neurosci. 10:507-518.

Grillner S, (1975) Locomotion in vertebrates: central mechanisms and reflex interaction. Physiol Rev. 55, 247–304.

Guertin PA. (2009) The mammalian central pattern generator for locomotion. Brain Res Rev. 62:45-56.

Guertin P, Angel MJ, Perreault MC, McCrea DA. (1995) Ankle extensor group I afferents excite extensors throughout the hindlimb during fictive locomotion in the cat. J Physiol. 487:197-209.

Gurfinkel VS, Shik ML. (1973) The control of posture and locomotion. In: Gydikov F, Tankov F, Kosarov F. (Eds.), Motor control. Plenum Press, New York, pp. 217–234.

Jan YN, Jan LY. (2010) Branching out: mechanisms of dendritic arborization. Nat. Rev. Neurosci. 11:316-328.

Kiehn O. (2006) Locomotor circuits in the mammalian spinal cord. Ann Rev Neurosci. 29:279-306.

Kjaerulff O, Kiehn O. (1996) Distribution of networks generating and coordinating locomotor activity in the neonatal rat spinal cord in vitro: a lesion study. J Neurosci. 16:5777–94.

Kremer E, Lev-Tov A. (1997) Localization of the spinal network associated with generation of hindlimb locomotion in the neonatal rat and organization of its transverse coupling system. J Neurophysiol. 77, 1155–70.

Kriellaars DJ, Brownstone RM, Noga BR, Jordan LM. (1994) Mechanical entrainment of fictive locomotion in the decerebrate cat. J Neurophysiol. 71:2074-86.

Lafreniere-Roula, M, McCrea, DA. (2005) Deletions of rhythmic motoneuron activity during fictive locomotion and scratch provide clues to the organization of the mammalian central pattern generator. J. Neurophysiol. 94:1120–32.

Lanuza GM, Gosgnach S, Pierani A, Jessell TM, Goulding M. (2004) Genetic identification of spinal interneurons that coordinate left-right locomotor activity necessary for walking movements. Neuron. 42:375–86.

Longair MH, Baker DA, Armstrong JD. (2011) Simple Neurite Tracer: open source software for reconstruction, visualization and analysis of neuronal processes. Bioinformatics. 27:2453-54.

McCrea DA. (2001) Spinal circuitry of sensorimotor control of locomotion. J Physiol. 533:41-50.

McCrea DA, Rybak IA. (2007) Modeling the mammalian locomotor CPG: insights from mistakes and perturbations. Prog Brain Res. 2007;165:235-53

McCrea DA, Rybak IA. (2008) Organization of mammalian locomotor rhythm and pattern generation. Brain Res Rev. 57:134-146.

Miller S, Scott PD. (1977) The spinal locomotor generator. Exp Brain Res. 30:387-403.

Orsal D, Cabelguen JM, Perret C. (1990). Interlimb coordination during fictive locomotion in the thalamic cat. Exp Brain Res. 82:536-546.

Perreault MC, Angel MJ, Guertin P, McCrea DA. (1995) Effects of stimulation of hindlimb flexor group II afferents during fictive locomotion in the cat. J Physiol. 487:211-220.

Roberts A, Tunstall MJ. (1990) Mutual Re-excitation with Post-Inhibitory Rebound: A Simulation Study on the Mechanisms for Locomotor Rhythm Generation in the Spinal Cord of Xenopus Embryos. Eur J Neurosci. 2:11-23.

Rossignol S, Dubuc R, Gossard JP. (2006) Dynamic sensorimotor interactions in locomotion. Physiol Rev. 86:89-154.

Rowat PF, Selverston AI. (1997) Synchronous bursting can arise from mutual excitation, even when individual cells are not endogenous bursters. J Comput Neurosci. 4:129-39.

Rybak I, Shevtsova N, Lafreniere-Roula M, McCrea D. (2006*a*) Modeling spinal circuitry involved in locomotor pattern generation: insights from deletions during fictive locomotion. J Physiol. 577:617-639.

Rybak IA, Stecina K, Shevtsova NA, McCrea DA. (2006*b*) Modelling spinal circuitry involved in locomotor pattern generation: insights from the effects of afferent stimulation. J Physiol. 577:641-658.

Schmid B, Schindelin J, Cardona A, Longair M, Heisenberg M. (2010) A high-level 3D visualization API for Java and ImageJ, BMC. Bioinformatics 11: 274.

Stecina K, Quevedo J, McCrea DA. (2005) Parallel reflex pathways from flexor muscle afferents evoking resetting and flexion enhancement during fictive locomotion and scratch in the cat. J Physiol. 569:275-90.

Zhong G, Shevtsova NA, Rybak IA, Harris-Warrick RM. (2012) Neuronal activity in the isolated mouse spinal cord during spontaneous deletions in fictive locomotion: insights into locomotor central pattern generator organization. J Physiol. 590:4735-59.

2.7 Figures

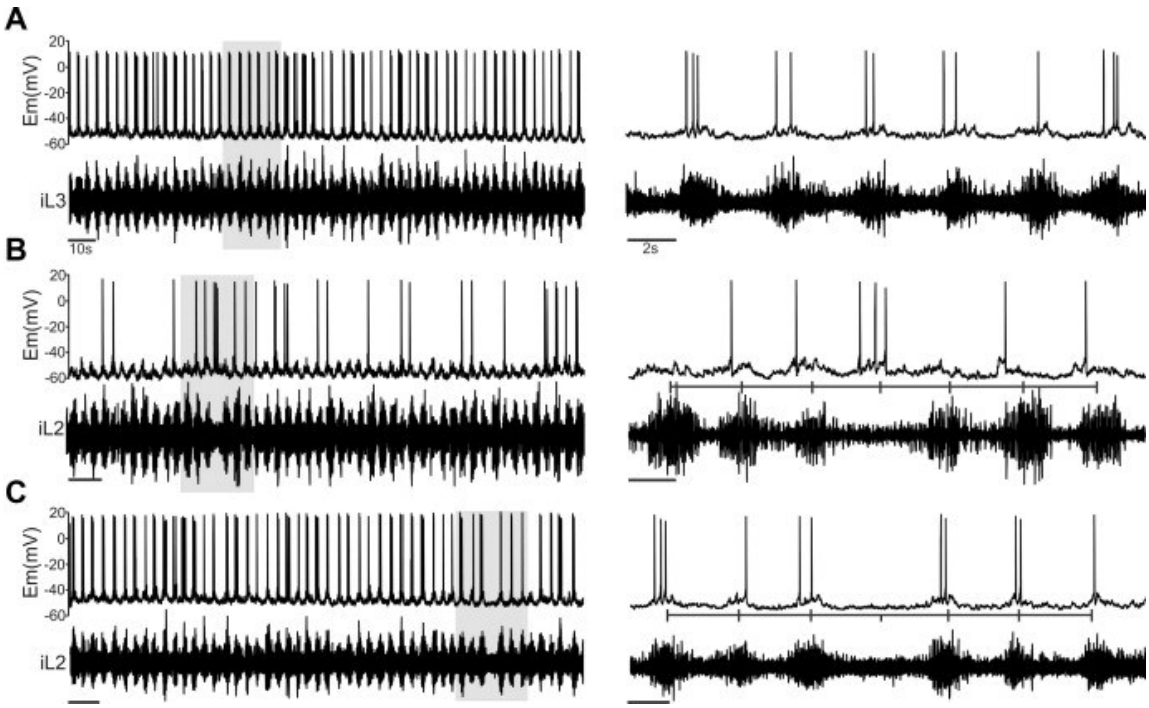

Figure 1. *Activity of RG and PF cells during ipsilateral non-resetting deletions of fictive locomotion.* Panels A-C illustrate typical recordings of fictive locomotion recorded in a lamina VII interneuron (upper trace of each panel) and the local ventral root (lower trace of each panel). Panels to the right (scale bar indicates 2s) are magnifications of the grey shaded region in the left panel (scale bar indicates 10s). A. Typical whole cell recording of a lamina VII interneuron located in the L3 segment and ENG activity in the ipsilateral L3 ventral root during pharmacologically induced fictive locomotion evoked by application of 5 μM NMDA and 10 μM 5-HT. B. A cell recorded in the L2 segment is rhythmically active in phase with the local ventral root. This cell continues firing during a non-resetting deletion recorded in the ipsilateral L2 ventral root indicating that it is PRG cell. C. During a non-resetting deletion recorded in the L2 ventral root rhythmic activity in a lamina VII interneuron located in the same segment stops and resumes following the deletion indicating that it belongs to the PPF level.

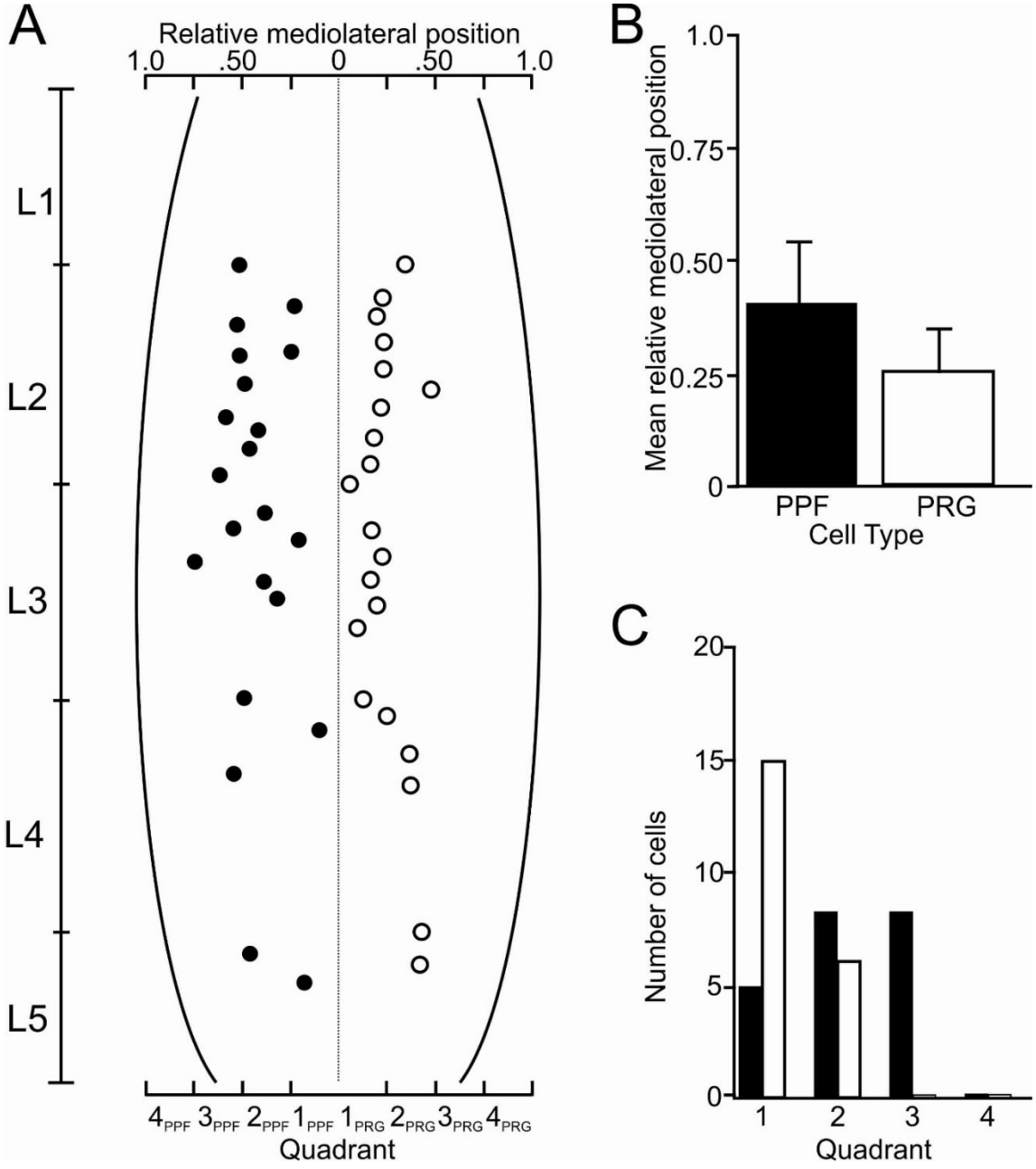

Figure 2. *Regional distribution of PPF and PRG cells*. A. Schematic of neonatal mouse lumbar spinal cord indicating the segmental,relative mediolateral position, and corresponding quadrant of all PPF cells (black circles to the left of the midline) and PRG cells (white circles to the right of the midline) B. Bar graph illustrates that PRG cells

(white bar) tend to be located in a more medial position than PPF cells (black bar). **C.** Bar graph representing the number of PRG (white bar) and PPF (black bar) cells located within each quadrant of the mediolateral plane of the spinal cord. The majority of PRG cells are located within quadrant 1. PPF cells are distributed across quadrants 1, 2, and 3.

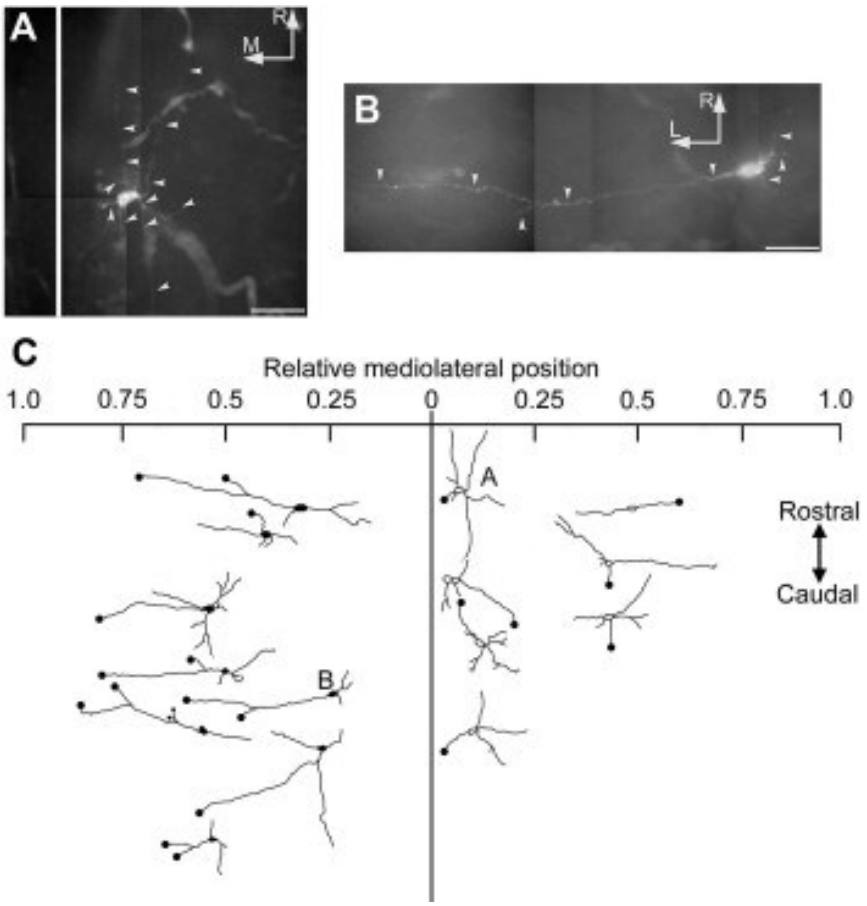

Figure 3. *Morphological characteristics of PPF and PRG cells*. A-B. Anatomical reconstructions of PRG (A) and PPF (B) cells filled with Neurobiotin after whole cell recording and imaged in the semi-intact spinal cord. Scale bars represent 50μm. Neurites projecting from the soma are indicated by white arrowheads. C. Schematic of neonatal mouse lumbar spinal cord displaying the relative mediolateral position and morphology of PPF (black somas to the left of the midline) and PRG (white somas to the right) cells that were filled and reconstructed. Cells illustrated in panels A and B are identified. Axons are indicated by neurites terminating with black dot.

Chapter 3 – Probing diversity within subpopulations of locomotor-related V0 interneurons.

Griener A, Zhang W, Kao H, Wagner C, Gosgnach S. (2015) Probing diversity within subpopulations of locomotor-related V0 interneurons. Dev Neurobiol. 75:1189-1203.

3.1 Abstract

The V0 interneuronal population is derived from Dbx1 expressing progenitors. Initial studies on these interneurons in the mouse spinal cord demonstrated that they project commissural axons and are involved in coordinating left-right alternation during locomotion. Subsequent work has indicated that the V0 population can be divided into genetically-distinct ventral ($V0_V$) and dorsal ($V0_D$) subpopulations, and experimental evidence suggests that each is responsible for left-right alternation at different locomotor speeds. In this study we perform a series of experiments to probe the location and connectivity of these subpopulations in neonatal mice and demonstrate that they are more diverse than previously predicted. While the distribution of either subpopulation remains consistent along the extent of the lumbar spinal cord, a cluster of $V0_D$ cells lateral to the central canal receive substantial input from primary afferents. Retrograde tracing and activity dependent labeling experiments demonstrate that a group of V0 interneurons located in this same region preferentially project axons towards contralateral motoneurons via an oligosynaptic pathway, and are active during fictive locomotion. Our results suggest that this subset of V0 interneurons may be primarily responsible for coordination of left-right alternation during locomotion. Furthermore these experiments indicate that while genetic identity is one determinant of the function of a neuron during locomotion, the specific position in which the cell is located may also play a key role.

3.2 Introduction

The basic pattern of left-right and flexor-extensor alternation characteristic of locomotion is generated by a neural network referred to as the locomotor central pattern generator (CPG) which is located in the mammalian spinal cord and functional just before birth. While traditional anatomical and electrophysiological experiments have elucidated many of the basic mechanistic tenets of the locomotor CPG (Kiehn 2006; Jankowska 2008), recent work incorporating a molecular approach has been successful in identifying several genetically-defined populations of interneurons that comprise this circuit (Goulding, 2009).

Although parent cell populations can be identified by expression of a unique complement of transcription factors at early embryonic time points, some level of heterogeneity nonetheless exists within each genetically-defined population that settles in the ventral spinal cord (Moran Rivard et al. 2001; Gosgnach et al. 2006; Crone et al. 2009; Dyck et al. 2012; Borowska et al. 2013). Some of these populations (V0, V2 cells) have been subdivided into genetically distinct subpopulations based on transcription factor expression downstream of their parent marker (Kiehn 2011).

One of the first genetically-defined populations to have its function during locomotion elucidated were the V0 cells. Initial experiments indicated that this population differentiates from a discrete progenitor domain which expresses the homeodomain transcription factor Dbx1 (Pierani et al. 2001) and can be divided into a ventral subpopulation which transiently express Evx1 (i.e. $V0_V$ interneurons) and a dorsal subpopulation ($V0_D$ interneurons) that do not express Evx1 (Pierani et al. 2001; Moran- Rivard et al., 2001). V0 interneurons settle in the ventromedial region of the postnatal mouse spinal cord, project primarily commissural axons, and are required for appropriate coordination of left-right alternation during locomotion (Lanuza et al. 2004). More recent work demonstrates that functional diversity exists between $V0_V$ and $V0_D$ subpopulations with the dorsal cells believed to be responsible for left-right

alternation at slow locomotor speeds while the ventral cells serve the same function during fast stepping (Talpalar et al. 2013).

In order to provide insight into the organization of the locomotor CPG, and further investigate the diversity between the subpopulations of V0 interneurons we examine the regional distribution and connectivity of each. We also use c-fos labeling to identify specific regions of the spinal cord which contain V0 cells that are active during various frequencies of fictive locomotion. Results indicate that the majority of each subpopulation is clustered in the region surrounding the central canal and a small subset of $V0_D$ cells are heavily innervated by primary afferent fibers. Furthermore, activity-dependent labeling was seen in a small subset of V0 cells, located lateral to the central canal, at all locomotor frequencies. Based on this data, as well as the tendency for V0 cells in this region to project towards contralateral motoneurons, we postulate that this regionally distinct subset of V0 interneurons plays a major role in the control of left-right alternation during locomotion.

3.3 Materials and Methods

Animals. All procedures were in accordance with the Canadian Council on Animal Care (CCAC) and approved by the Animal Welfare Committee at the University of Alberta. $TgDbx1^{Cre}$ and $Dbx1^{LacZ}$ mouse strains were generously provided by the Goulding laboratory (Salk Institute, La Jolla, CA) and the generation of each has been described previously (Pierani et al. 2001; Dyck et al. 2012). Reporter strains ($ROSA26^{EYFP}$, $ROSA26^{tdTomato}$) were acquired from Jackson Laboratories and are collectively referred to as $R26^{EFP}$ indicating mice were used that expressed either the tdTomato, or EYFP, reporter protein. We have previously demonstrated that crossing these reporter strains with $TgDbx1^{Cre};Dbx1^{LacZ}$ mice results in a portion of offspring carrying the $TgDbx1^{Cre};R26^{EFP};Dbx1^{LacZ}$ genotype. In this mouse strain EFP+ cells

belong to the dI6 population, EFP+/B-gal+ cells arise from Pax7 progenitors and belong to the $V0_D$ population while EFP-/B-gal+ cells co-express Evx1 at early embryonic stages and thus belong to the $V0_V$ population (Dyck et al. 2012). In total, experiments were performed on 40 male and female neonatal (0-4 days of age) $TgDbx1^{Cre};R26^{EFP};Dbx1^{LacZ}$ mice.

Immunohistochemistry. Mice used exclusively for immunohistochemistry were transcardially perfused with 0.01M PBS followed by 4% paraformaldehyde in 0.1M phosphate buffer. Spinal cords were dissected out and prepared for antibody staining using one of two protocols. Tissue to be cut on a cryostat was cryoprotected, embedded in OCT compound and 20 µm thick transverse sections were collected. Tissue to be cut on the microtome was dehydrated, cleaned in xylene, embedded in paraffin and 6 µm thick transverse sections were collected. $V0_V$ and $V0_D$ cells were identified with antibodies to EGFP (kind gift from Eusera - goat, 1:5000,) and β-gal (chicken, 1:700, Aves). tdTomato+ cells could be visualized without an antibody. Antibodies were also used to detect excitatory primary afferent terminals (VGlut1, guinea pig, 1:2500, Millipore), glycinergic cell bodies (Glycine, rat, 1:1000, Immunosolutions), cells firing action potentials during a locomotor task (c-fos, rabbit, 1:400, Santa Cruz), and microtubules (MAP2, mouse, 1:200, Sigma).

For cryostat sections all primary antibodies were applied directly to tissue overnight, followed by incubation with species-specific secondary antibodies conjugated with Cy2, Cy3, Cy5, or DyLight 405 (Jackson Immunoresearch). Slides containing paraffin-embedded sections were de-waxed, rehydrated with graded alcohols, and washed in phosphate buffer solution (PBS) before antigen retrieval with 10 mM sodium citrate buffer. Slides were then washed and incubated with primary antibodies overnight at room temperature under continuous agitation. The following

day, slides were incubated with the appropriate secondary antibodies (see above). All slides were coverslipped with Fluorsave reagent (Calbiochem) and examined with a Zeiss Axioplan microscope using a LSM 510 NLO laser configured to a computer running Zen software. Acquired images were exported in TIFF format, and figure preparation was performed in Adobe Photoshop and Corel Draw.

In order to investigate regional distribution of V0 cells the spinal cord was divided into 6 equal vertical regions using the lateral edges of the spinal cord and the midpoint of the central canal as landmarks (the left and right side were divided into 3 regions of equal width). Four equal horizontal divisions were made using the dorsal lip of the central canal, the dorsal and ventral extents of the spinal cord as landmarks (see Figure 1E). A script was written in Matlab which divided each image up into the aforementioned regions and identified the X and Y coordinates of each labeled cell with respect to a point of origin (the midpoint of the central canal). All plots of cell position and topography were generated by this script. All means are reported ± standard deviation (SD). Student's t-tests and one-way ANOVAs were used to determine whether means were significantly different. A p-value <0.05 was used as a threshold to indicate statistical significance.

Retrograde tracing. Injections of a strain of pseudorabies virus which expresses GFP in all cells that it infects (PRV-152, see Smith et al. 2000) into hindlimb muscles of $TgDbx1^{Cre};R26^{tdTomato};Dbx1^{LacZ}$ mice were performed according to Kerman et al. (2003). Briefly, 1-2 µl of Bartha PRV-152 viral stock (6.68×10^8 infectious units per µl) was pressure injected into either a flexor (tibialis anterior- TA) or an extensor (gastrocenemius- GC) muscle at P1 using glass micropipettes connected to a picospritzer. Animals were euthanized 36 or 48 hours after injection as a detailed analysis of PRV-152 transport has demonstrated that these are the times at which last order interneurons (30-40 hours) and neurons that are disynaptically connected to

motoneurons (40-50 hours) are infected (Jovanovic et al. 2010; Coulon et al. 2011). Spinal cords were dissected out in ice cold PBS before fixation in 4% paraformaldehyde-PBS at 4°C. Cryostat sections from the lumbar spinal cord were stained with antibodies to GFP and β-gal (tdTomato+ cells could be seen without an antibody) to identify trans-synaptically labeled $V0_V$ and $V0_D$ interneurons that make monosynaptic or disynaptic connections onto motoneurons. All spinal cords included in the data set had a similar labeling pattern and density to previous work after 36 or 48 hours (Jovanovic et al. 2010; Coulon et al. 2011).

Fictive locomotion/c-fos labeling. In order to identify cells that were active during locomotor behavior we probed for expression of the immediate early gene c-fos in V0 cells located in the lumbar spinal cord following a sustained bout of fictive locomotion. Early postnatal (P0-P1) $TgDbx1^{Cre};R26^{EFP};Dbx1^{LacZ}$ mice were decapitated, eviscerated and spinal cords were dissected out in ice-cold Ringers solution (Kjaerulff and Kiehn, 1996). Isolated spinal cords were pinned, ventral side up, in a recording chamber constantly perfused with oxygenated Ringer's solution composed of 111 mM NaCl, 3.08 mM KCl, 11 mM glucose, 25 mM $NaHCO_3$, 1.18 mM KH_2PO_4, 1.25 mM $MgSO_4$, 2.52 mM $CaCl_2$. All recordings were made at room temperature (20°C). Two, three or four of the second and fifth lumbar ventral roots on the right and left (i.e., rL2, lL2, rL5, lL5) were placed in suction electrodes to monitor fictive locomotor activity. Electroneurogram (ENG) recordings were amplified, bandpass filtered (100 Hz–1 kHz), digitized, collected, and stored on a PC using Axoscope software (Axon Instruments). Rhythmic locomotor activity was induced by adding N-methyl-D-aspartic acid (NMDA, 1-10 μM) and 5-hydroxytryptamine (5-HT, 5–30 μM) to the perfusing Ringer's solution. Step cycle period (defined as the interval between onset of burst n and burst n+1) was calculated by averaging 20 consecutive values from a single ventral root during stable fictive locomotor activity. Frequency of locomotion was calculated by taking the

reciprocal of the step cycle period. For frequency vs. time plots the frequency of every second pair of bursts in the L2 ventral root was calculated and plotted at the time of onset. After 1 hour of stable fictive locomotor activity, spinal cords were immersed in ice-cold 4% paraformaldehyde-PBS, prepared for immunohistochemistry (as described above), and stained with antibodies to EFP, β-gal and c-fos. In control experiments, spinal cords were placed in a recording chamber for the same amount of time however NMDA and 5-HT application was omitted.

3.4 Results

Regional distribution of $V0_V$ and $V0_D$ cells in the lumbar spinal cord.

Interneuronal components of the locomotor CPG have been shown to be distributed in the ventromedial region of the lower thoracic and lumbar spinal segments with the greatest number located in the rostral lumbar cord. In order to assess the regional distribution of the $V0_D$ and $V0_V$ subpopulations in the rostral-caudal and medial-lateral planes, the lumbar region of the spinal cord was isolated from eight P0 TgDbx1^{Cre};R26^{EFP};Dbx1^{LacZ} mice and prepared for immunohistochemistry. For each animal the total number of V0 cells belonging to the $V0_V$ (β-gal+, EFP-) and $V0_D$ (β-gal+, EFP+) subpopulations were counted in two sections of the spinal cord taken from each of the L1-L5 segments (Figure 1A). The specific location of each $V0_V$ and $V0_D$ cell, were plotted on a schematic using a custom written Matlab script which used the middle of the central canal as a reference point and identified the X and Y coordinates of each labeled cell (Figure 1B). While there was a slight increase in the total number of V0 cells from L1-L4, this followed the increase in mean area of the spinal cord along these segments (Table 1) and was not statistically significant when normalized for the size of the spinal segment in which they were located ($p=0.53$ one way ANOVA). A similar trend was observed for each of the $V0_V$ and $V0_D$ subpopulations (Figure 1B, 1C, Table

1) with a non significant increase in number from L1-L4 (p_{V0V}=0.11, p_{V0D}=0.18, one way ANOVA). At all segmental levels, however, the total number of $V0_V$ cells was greater than the number of $V0_D$ cells (for all segmental levels $p<0.01$ t-test, Figure 1C, Table 1).

In order to examine the detailed regional distribution of V0 cells within each lumbar segment, sections from the same eight spinal cords were divided into 24 regions (Figure 1E) and the number of V0 cells within each region was identified. V0 cells were clustered in the ventromedial regions along the extent of the lumbar spinal cord with 94.7% of all V0 cells located in regions 14-17, 20-23. Cells located in regions 13, 14, 17 and 18 that were β-gal+ and had small, oblong nuclei were not included in the counts as these cells have been shown to be NeuN- and glia cells (Lanuza et al. 2004). Topographical maps of cell density were generated with pooled data from all spinal cords analyzed and indicated that the regions immediately surrounding the central canal (regions 15, 16) contained the highest density of $V0_V$ and $V0_D$ cells at all segmental levels investigated (Figure 1D).

Taken together, this data indicates that $V0_V$ cells may predominate $V0_D$ cells postnatally, both subpopulations are evenly distributed in the rostral-caudal plane, and are most densely clustered in the region immediately surrounding the central canal in each of the segments studied.

$V0_D$ cells use the neurotransmitter glycine.

Initial investigation of V0 cells demonstrated that they are a mixed population of inhibitory and excitatory interneurons based on expression of the markers vesicular inhibitory amino acid transporter (VIAAT) and vesicular glutamate transporter 2 (Vglut2) (Lanuza et al. 2004). A recent report of the functional diversity of $V0_V$ and $V0_D$ subpopulations investigated the neurotransmitter phenotype of each

subpopulation and demonstrated that $V0_V$ cells are almost entirely excitatory. $V0_D$ cells, on the other hand, are not excitatory and approximately half are GABAergic (Talpalar et al. 2013). Since glycine is one of the primary inhibitory neurotransmitters used in the spinal cord (Sibilla and Ballerini 2009) we used an antibody that has been shown to effectively mark glycinergic spinal interneurons (Coulon et al. 2011) to determine the proportion of $V0_D$ cells that use this neurotransmitter.

In each of the 10 spinal cords examined the vast majority of $V0_D$ cells were immunopositive for the glycine antibody while, consistent with previous reports (Talpalar et al. 2013), few glycinergic $V0_V$ cells were observed. This is illustrated in Figure 2A in which only one (arrow with asterix) of 15 glycinergic V0 cells is tdTomato-, and thus a $V0_V$ cell. The remainder (white arrowheads) belong to the $V0_D$ subpopulation. In total, 13.1% of $V0_V$ cells and 78.2% of $V0_D$ cells were immunopositive for the glycinergic marker in the rostral segments while 10.6% $V0_V$ cells and 70.6% of $V0_D$ cells were glycine positive at caudal levels (Figure 2B). The clear tendency for $V0_D$ cells to be glycinergic combined with the demonstration that more than half of this subpopulation is GABAergic (Talpalar et al., 2013) suggests that many $V0_D$ cells may co-release GABA and glycine.

$V0_D$ cells in the lumbar spinal cord receive primary afferent input.

Identifying neurons which receive primary afferent contacts can provide insight into their function during locomotion. Sensory afferents have been shown to contribute substantially to motoneuron output during a locomotor task, and also play a critical role in regulating the timing of locomotor outputs (McCrea 2001). Vesicular glutamate transporter 1 (Vglut1) is one of three proteins responsible for transporting glutamate into synaptic terminals and has been shown to be preferentially expressed in primary afferent terminals, while excitatory interneurons express Vglut2 (Oliveira et al. 2003). In order to determine whether either subpopulation of V0 cells receives primary

afferent input we inspected sections from 5 P0 TgDbx1^{Cre};R26^{EFP};Dbx1^{LacZ} mice for VGlut1+ terminals in close proximity to $V0_V$ and $V0_D$ soma or proximal processes at rostral and caudal lumbar levels.

In the most ventro-medial regions of the spinal cords examined (previously defined as areas 21/22) there was sparse VGlut1 labeling surrounding both $V0_V$ and $V0_D$ cells ($V0_V$ cell marked by yellow arrowhead in Figure 3A1, 3A2). The most dense VGlut1 labeling in the intermediate nucleus was seen just lateral to the central canal (i.e. areas 15/16), the area in which the greatest population of V0 cells reside (white box in Figure 3A1, 3A2, 3B1, 3B2, boxed region is magnified in 3A3, 3B3). While VGlut1 labeling in this region has been shown previously at all segmental levels (Mirnics and Koerber 1995), the manner in which terminals surrounded a cluster of $V0_D$ cells (indicated by white arrows in all panels of Figure 3) was quite striking. In 6 μm thick sections examined at both rostral and caudal levels there were typically 3-9 $V0_D$ cells located in areas 15/16 that were surrounded by VGlut1+ terminals. Given that the area surrounding the cluster of $V0_D$ cells is likely to contain dendrites from these cells, this finding is suggestive of synaptic connectivity between these cells and primary afferents. While terminals were seen surrounding $V0_V$ cells in this region (yellow arrows in all panels of Figure 3) it was not nearly as consistent or dense. Just lateral to this (areas 14/17) there was an area receiving VGlut1+ terminals (white ($V0_D$) and yellow ($V0_V$) arrowheads in Figure 3B1, 3B2), however they were not seen to preferentially surround either V0 subpopulation.

Both Vo_V and Vo_D cells receive serotonergic input.

Serotonin (5-HT) has been shown to be involved in the initiation of locomotion, modulation of the ongoing rhythm, and control of reflex pathways in mammals (see Schmidt and Jordan 2000). While V0 cells are thought the be part of the locomotor CPG, innervation of these cells by serotonergic fibers has yet to be demonstrated. To

determine whether V0 cells receive serotonergic input and, if so, whether this is preferential to either the dorsal or ventral subpopulation, spinal cords from six P2-P4 TgDbx1^{Cre};R26^{EFP};Dbx1^{LacZ} mice were prepared for microtome sectioning and tissue stained with antibodies to β-gal, EFP and 5-HT. Slightly older animals were used for these experiments as it has been demonstrated that the mature pattern of serotonergic innervation of the lumbar spinal cord occurs at approximately P3 in rodents (Rajaofetra et al. 1989).

Clear swellings along serotonergic fibers, presumed to be varicosities (Pearson et al. 2000), were seen in the ventral half of the spinal cord at all lumbar segments examined with extensive labeling surrounding presumptive motoneurons in the most ventrolateral region and more sparse labeling throughout the intermediate nucleus (Figure 4A1, 4B1). Presumptive serotonergic varicosities were located in close proximity to $V0_D$ cell soma (and presumably nearby dendrites) throughout the ventromedial laminae in both rostral and caudal segments (white arrows Figure 4A1, 4A2, 4B1, 4B2). Serotonergic contacts onto $V0_V$ cells were not immediately apparent however this was largely due to the fact that the β-gal marker is specific to the nucleus thus contacts onto the soma and proximal dendrites, while in many cases likely (yellow arrows Figure 4A1, 4A2, 4B1, 4B2), were unable to be confirmed. Two additional spinal cords were processed and stained with an antibody for the microtubule marker MAP-2 (in addition to β-gal, EFP and 5-HT) to enable the cytoplasm of $V0_V$ cells to be identified. Images of this tissue (Figure 4C) provide evidence of serotonergic varicosities on both $V0_V$ (yellow arrows) and $V0_D$ (white arrows) cell bodies in all four regions suggesting that both subpopulations of V0 interneurons can be modulated by 5-HT regardless of their specific position in the spinal cord.

Vo cells contact contralateral motoneurons via an oligosynaptic pathway.

Consistent with their role in coordinating left-right alternation during locomotion, previous work has used the retrograde trans-synaptic tracer PRV-152 to suggest that the V0 population makes monosynaptic contacts onto contralateral motoneurons in the lumbar spinal cord (Lanuza et al. 2004). More recent work studying the transport time of retrograde trans-synaptic viral tracers (Jovanovic et al. 2010; Coulon et al. 2011) raises the possibility that these connections may have been disynaptic (i.e. one interneuron interposed between the V0 cell and contralateral motoneuron). Here we investigate the connectivity pattern of both the ventral and dorsal subpopulation of V0 cells to probe for differences in their connectivity to contralateral motoneurons. To this end, 1-2 µl of the transynaptic, retrograde tracer PRV-152 was injected into the gastrocenimius (GC) muscle of P0-P1 TgDbx1^{Cre};R26^{tdTomato};Dbx1^{LacZ} mice. To probe for monosynaptic connectivity between V0 subpopulations and contralateral motoneurons two spinal cords were prepared for immunohistochemistry 36 hours after injection as this has been shown to be sufficient time for the tracer to infect all cells which make monosynaptic contacts onto GC motoneurons in the P1 mouse (Coulon et al. 2011). At this time point the laminar distribution of PRV+ cells in both spinal cords was similar to both of the previous studies (Jovanovic et al. 2010; Coulon et al. 2011) which carried out a detailed analysis of the time course of PRV labeling following GC injection, making us confident that labeling was restricted to last order interneurons. While ipsilateral motoneurons and interneurons labelled with GFP were observed at this time point (Figure 5A, 5B), few GFP-labelled interneurons (white arrows Figure 5B, typically 0-3 per 20 µm section), and no GFP-labelled V0 cells, were seen on the contralateral side of the spinal cord indicating that few, if any, V0 cells make monosynaptic contacts onto contralateral motoneurons. A small population of V0 cells ipsilateral to the injection were observed to have taken up the virus at this time point and likely belong to the Pitx2+ subpopulation which have been shown to provide monosynaptic, excitatory input to ipsilateral motoneurons (Zagoraiou et al. 2009).

An additional 6 spinal cords were harvested 48 hours after PRV-152 injection, a time at which cells making disynaptic contact onto motoneurons are labeled with the virus (Coulon et al. 2011). An abundance of ipsilateral labeling with GFP was observed at this time point as was a modest region in the ventromedial aspect of the contralateral side of the spinal cord (Figure 5C). PRV-152 infected V0 cells could be found in all lumbar segments examined (Figure 5E, 5F) and in all of our previously defined areas of interest (14-17, 20-23) with a statistically significant proportion of these located in areas 15/16 ($p=0.02$, one way ANOVA). The most striking finding was that while both subpopulations could be found to take up the tracer there was a clear tendency for $V0_V$ cells, as opposed to $V0_D$ cells, to be labelled at this time point (Figure 5E, 5F). In total 87% of all V0 cells that expressed the tracer 48 hours after injection of the GC muscle belonged to the ventral subpopulation and, at all segments investigated, significantly more $V0_V$ cells were labeled ($p<0.002$, t-test for each of L1-L5).Based on these results we were curious to determine whether $V0_V$ and $V0_D$ cells preferentially project towards extensor and flexor motoneurons respectively. The tibialis anterior (TA, ankle flexor) muscle of 3 additional $TgDbx1^{Cre};R26^{tdTomato};Dbx1^{LacZ}$ mice was injected with PRV-152. The same pattern of GFP expression as described above was observed when these spinal cords were processed 48 hours after injection (Figure 5D, 5E, 5F). The greatest number of PRV-infected V0 cells were located in the segment which houses the TA motoneurons (L5), the majority of cells were located in areas 15/16 ($p=0.04$, one way ANOVA) and significantly more $V0_V$ cells projected to the TA motoneurons in all segments except for L3 ($p<0.03$, t-test for L1, L2, L4, L5 segments, $p=0.08$ t-test for L3 segment).

V0 cells lateral to the central canal are active during fictive locomotion.

Based on left-right coordination defects that have been observed in the absence of either the $V0_V$ or $V0_D$ cell populations, it has been postulated that these cells play

distinct functions during locomotion with the ventral subpopulation active and responsible for coordinating contralateral alternation at fast locomotor speeds while the dorsal subpopulation is active and carries out this role during slow walking (Talpalar et al. 2013). Unfortunately the lack of a mouse line that enables either subpopulation to be targeted for recording in live tissue has precluded a direct investigation of the activity of either subpopulation of V0 cells over a range of locomotor speeds. In order to identify specific regions of the spinal cord that house V0 cells that participate in fictive locomotion we induced this behavior in $TgDbx1^{Cre};R26^{EFP};Dbx1^{LacZ}$ mice and examined expression of the immediate early gene c-fos, a marker of active cells that has been shown to be expressed in neurons that participate in locomotion (Jasmin et al., 1994; Carr et al., 1995; Dai et al. 2009), after 1 hour of stable rhythmic activity.

Locomotor activity was induced in 9 spinal cords which were subsequently processed for c-fos expression. There was a clear difference in the number of c-fos+ cells observed in spinal cords in which fictive locomotion was evoked (Figure 6A, 6B) when compared to control cords (n=4, Figure 6C). c-fos expression was observed in both the dorsal and ventral subpopulations, however when data from all spinal cords was pooled, significantly more $V0_V$ cells were c-fos+ following fictive locomotion at both rostral ($\bar{x}_{V0V}$=7.6 ± 2.3 c-fos+ cells per 20 μm section, $\bar{x}_{V0D}$= 1.8 ± 1.0 cells p=0.004 t-test) and caudal ($\bar{x}_{V0V}$=7.4 ± 1.4 cells, $\bar{x}_{V0D}$=2.1 ± 1.1 cells, p=0.009 t-test) segments. Active V0 cells were present in all of our previously defined areas of interest (14-17, 20-23) (Figure 6D) with a statistically significant number located in areas 15/16 ($p<0.01$ ANOVA), and 77% of the total number of c-fos+ V0 cells were located above the ventral lip of the central canal in areas 15/16 (Figure 6A, 6B). Locomotor frequencies obtained ranged from 0.18 - 0.48 Hz. Surprisingly, at both the lowest (Figure 6A) and highest (Figure 6B) locomotor frequencies c-fos expression was much more common in $V0_V$ cells as opposed to $V0_D$ cells, and significantly more $V0_V$ cells were c-fos+ at all locomotor frequencies ($p<0.03$ t-test for all frequencies, see Figure

6E). When interpreting these results it is important to keep in mind that c-fos is unlikely to be a comprehensive marker of cells active during locomotion (Barajon et al. 1992; Carr et al, 1995), and simply provides a readout of active cells, rather than identifying those that are rhythmically active (see Discussion). Taken together however this data does indicate that V0 cells immediately lateral to the central canal may play an instrumental role during mammalian locomotion, regardless of the frequency of the rhythm.

3.5 Discussion

Topographic organization of $V0_V$ and $V0_D$ interneurons.

V0 cells were the first of the parent genetically defined interneuronal populations to have their function identified during locomotion (Lanuza et al. 2004). While it has recently been shown that functional diversity exists between $V0_V$ and $V0_D$ cells (Talpalar et al. 2013) many properties of these interneuronal subtypes have yet to be elucidated. Although the specific location of the ventral and dorsal V0 subpopulations has been demonstrated in the embryonic CNS (Francius et al. 2013), the present study is the first to carry out a full investigation of the regional distribution of $V0_V$ and $V0_D$ cells in the postnatal spinal cord, a time point after neuronal migration is complete. Here we demonstrate that the distribution of either population is consistent throughout the L1-L5 segments with the majority of each located in areas 15/16. Our observation that there are a greater number of $V0_V$ (58%) compared to $V0_D$ cells (42%) postnatally differs from analyses of either subpopulation in the mouse embryo which indicated either an equivalent number of each at E12 (Francius et al. 2013), or a predominance of $V0_D$ cells at E15.5 (Talpalar et al. 2013). While it is possible that labeling of $V0_D$ cells in our mouse strain is incomplete, previous work (Dyck et al. 2012) suggests this is not the case as β-gal+/EFP- cells in the $TgDbx1^{Cre};R26^{EFP};Dbx1^{LacZ}$ mouse co-localize

only with Evx1-expressing cells (i.e. $V0_V$ population), while β-gal+/EFP+ cells co-localize with virtually all Dbx1+ cells that do not express Evx1 but do express Pax7 (i.e. $V0_D$ population). The validity of our transgenic model for differentiating between the subpopulations is further strengthened by the neurotransmitter data in this study which demonstrates that few β-gal+/EFP- (i.e. $V0_V$ cells), but the majority of β-gal+/EFP+ cells (i.e. $V0_D$ cells), are inhibitory, consistent with a previous report (Talpalar et al. 2013). The conflicting reports of the proportion of V0 cells belonging to either subpopulation at embryonic and postnatal time points is surprising, however it has been shown that the number of ventrally located interneurons is drastically reduced by apoptosis between E14 and P4 in mouse (Prasad et al. 2008), a period during which synapse elimination also occurs (Hua and Smith 2004). Interestingly, the V0 population in particular experiences an enormous amount of apoptosis with the number of cells belonging to this population at E14 reduced by 40% by E15.5 and by more than 80% by P0 (Prasad et al. 2008). This may result in a shift of the relative number of $V0_V$ and $V0_D$ interneurons at different developmental time points. The rate of V0 cell apoptosis levels off after P0, however it is possible that the precise number and proportion of $V0_D$ and $V0_V$ cells in the mature spinal cord differs from this, as well as previous reports, due to selective cell death during maturation.

Serotonergic and primary afferent contacts onto $V0_V$ and $V0_D$ interneurons.

The specific location of V0 subpopulations in the lumbar spinal cord becomes particularly interesting when we look at sources of input to $V0_V$ and $V0_D$ cells. Our data raises the possibility that regionally restricted subsets of each subpopulation may play a specific function during locomotion. We focussed our study on serotonergic, and primary afferent, fibers as these have both been shown to be involved in the modulation of locomotor activity. While serotonergic varicosities were seen in close apposition to both subpopulations of V0 cells (suggestive of synaptic contact onto the

soma or dendrites), they did not preferentially contact either subtype, nor were they prolific in any particular area of the lumbar cord suggesting that either population is able to be modulated via serotonergic input. Since serotonin has a wide range of modulatory effects (Schmidt and Jordan, 2000) it is difficult to draw conclusions regarding its specific effects on the V0 population without performing whole cell recordings from $V0_V$ and $V0_D$ cells and applying 5-HT directly.

In contrast to this finding, there was a prominent source of primary afferent input surrounding a small cluster of $V0_D$ soma located adjacent to the central canal at all levels of the spinal cord examined. If we combine this with our observation, as well as that of others (Talpalar et al. 2013), that $V0_D$ cells are primarily inhibitory, it suggests that a subset of inhibitory $V0_D$ cells immediately lateral to the central canal may be excited by primary afferents and involved in sensory processing. While testing this hypothesis directly must await a preparation which enables the activity in subpopulations of $V0_D$ cells to be investigated during overground locomotion in the intact mouse, a preparation in which sensory input is present, our activity dependent labeling experiments, which indicate that relatively few $V0_D$ cells are c-fos+ following fictive locomotion, a behavior devoid of sensory feedback, provides preliminary support for this hypothesis.

Axonal projection pattern of V0 interneurons and their activity during fictive locomotion.

Commissural interneurons that make short latency contacts onto motoneurons have been shown to be relatively rare compared to those that project ipsilaterally (Stepien et al. 2010; Jovanovic et al. 2010; Coulon et al. 2011). Consistent with previous reports on the V0 population as a whole (Lanuza et al. 2004), experiments incorporating the retrograde, trans-synaptic tracer PRV-152 indicate that these cells project axons towards contralateral motoneurons. Importantly, while we did note a scant number of $V0_V$ cells ipsilateral to the injection site that expressed the tracer after

36 hours (presumably members of the Pitx2+ V0 subpopulation), the fact that no contralaterally located V0 cells expressed GFP until >40h after hindlimb muscle injection provides strong evidence that synaptic contacts between these cells and motoneurons are oligosynaptic with the shortest pathway between the two cell types being disynaptic, rather than monosynaptic, as was previously predicted (Lanuza et al. 2004). While all labeled interneurons that make short latency contacts onto motoneurons are not necessarily part of the locomotor CPG, our data demonstrates that a significant majority of the V0 cells identified to make disynaptic contacts onto the contralateral GC and TA motor pools belong to the $V0_V$ subpopulation, indicating that these cells make shorter latency contact onto contralateral motoneurons compared to the $V0_D$ subpopulation. Furthermore 32% of the V0 interneurons that made disynaptic contact onto contralateral motoneurons were located dorsal to the ventral lip of the central canal, in the region which houses the majority of V0 cells which express c-fos after fictive locomotion. Although the activity of the specific V0 interneurons that made disynaptic contact with commissural interneurons could not be assessed during locomotion in the present study, and there are inherent issues with using c-fos expression as a means to identify cells that are active during locomotion (see below), taken together these results suggest that the region just lateral to the central canal may contain a substantial proportion of locomotor-related V0 cells.

While the total number of commissural, last order interneurons labeled in this study were primarily located in lamina VIII, consistent with previous reports (Quinlan and Kiehn 2007; Stepien et al. 2010; Jovanovic et al. 2010; Coulon et al. 2011), the number of cells is more modest than some observations (Stepien et al. 2010) raising the possibility that not all pre-motor V0 interneurons were labeled in our experiments. While this is a possibility, we ascribe the variation to analysis of different motor pools between studies, since the density and pattern of labeling that we observe 36 (and 48)

hours after application of the tracer to the GC muscle is consistent with other experiments in which this muscle was targeted (Coulon et al. 2011).

c-fos expression has previously been used to provide a readout of neurons involved in locomotor activity (Jasmin et al., 1994; Carr et al., 1995; Lanuza et al. 2004; Dai et al. 2009; Brownstone and Wilson 2009; Bretzner and Brownstone 2013). In the present study fictive locomotion evoked ranged from 0.18-0.48 Hz, frequencies that range from slow to moderately fast based on previous work. Taken alone, the observation of preferential expression of c-fos in $V0_V$, rather than $V0_D$, cells at all locomotor frequencies, points towards the ventral subpopulation being primarily responsible for left-right coordination regardless of the speed of locomotion. These results appear to contradict the report of a locomotor speed dependent recruitment of V0 subpopulations (Talpalar et al. 2013). We did however observe that a modest number of $V0_D$ cells, which express c-fos after fictive locomotion, are located immediately lateral to the central canal. One explanation could be that $V0_D$ cells play a minor role in left-right coordination and are able to partially compensate for the absence of the $V0_V$ subpopulation. This would result in weakened left-right alternation in the absence of the $V0_D$ cells and much greater deficits in the absence of the $V0_V$ subpopulation, precisely the locomotor phenotypes observed (Talpalar et al. 2013). The maintained coordination at low speeds in the absence of $V0_V$ cells can be accounted for by $V0_D$ cells compensating when the demands are limited, but unable to cope as the workload increases at higher speeds resulting in the lack of coordination observed.

Several caveats to this explanation must be considered based on the data generated in our study. First, as mentioned previously, c-fos does not enable us to distinguish between tonically-active and rhythmically-active cells thus the involvement of c-fos+ V0 cells in locomotor activity is unclear. Second, it is likely that all locomotor-related V0 cells do not express c-fos. Pooled data from all segments studied gives us a mean of 7.6 active $V0_V$ and 1.9 active $V0_D$ cells per 20 µm section, numbers

consistent with a previous study which incorporated c-fos labeling to investigate the activity of the entire V0 population during locomotion (Lanuza et al. 2004). While the proportion of V0 cells that are rhythmically-active and involved in coordination of locomotor outputs has not been determined, the number of c-fos+ V0 cells seems surprisingly low given that they have been shown to be primarily responsible for coordination of left-right alternation. Third, c-fos has been shown to be directly linked to the firing of action potentials rather than simply depolarization (Douglas et al. 1988; Herrera and Robertson 1996). It is possible that, when activated during locomotion, $V0_V$ cells simply fire action potentials at a greater frequency compared to $V0_D$ cells, a intrinsic property that would be consistent with their proposed role of coordinating left-right alternation at faster locomotor speeds, resulting in preferential c-fos expression in $V0_V$ cells. Finally, it is important to keep in mind that all sensory input is absent in the in vitro fictive locomotor preparation and many more cells would be expected to be active in the intact mouse. This point is particularly compelling given our observation of sensory terminals in close proximity to $V0_D$ cells.

Summary

The data collected in this study indicates that V0 cells located immediately lateral to the central canal are active during fictive locomotion and many make disynaptic, rather than monosynaptic, contact with contralateral motoneurons. While it is difficult to draw conclusions from c-fos labeling alone, the fact that these characteristics were preferentially observed in $V0_V$ cells make this regionally-restricted subset of the ventral subpopulation excellent candidates to be involved in regulating left-right alternation. Since this subset has been shown to be primarily glutamatergic (Talpalar et al. 2013), our data suggests that $V0_V$ cells involved in coordinating left-right alternation during locomotion activate contralateral local circuit inhibitory interneurons which, in turn, inhibit motoneurons, a network structure that has been proposed previously (Butt and

Kiehn 2003; Quinlan and Kiehn 2007; Talpalar et al. 2013). While relatively few $V0_D$ cells were observed to express c-fos during fictive locomotion, a subset of these, also situated just lateral to the central canal, receive primary afferent input and lead us to hypothesize that, in addition to a role in left-right coordination they may also be involved in modulating the locomotor rhythm in response to sensory stimuli. The results of our retrograde tracing experiments lead us to suggest that this subpopulation of V0 cells influence the activity of contralateral motoneurons via a polysynaptic pathway.

Ultimately, confirmation of the specific roles of $V0_V$ and $V0_D$ interneurons during locomotion must await a preparation in which the activity in each subpopulation can be assessed at various locomotor speeds. Taken together the results of this study indicate that the V0 cells are a much more diverse population than was initially proposed. Moreover the data presented here suggests that while genetic identity is one determinant of the function of a neuron during locomotion, the specific position in which the cell is located may also play a key role.

3.6 References

Barajon I, Gossard JP, Hultborn H. (1992) Induction of fos expression by activity in the spinal rhythm generator for scratching. Brain Res. 588:168-72.

Borowska J, Jones CT, Zhang H, Blacklaws J, Goulding M, Zhang Y. (2013) Functional subpopulations of V3 interneurons in the mature mouse spinal cord. J Neurosci. 33:18553-65.

Bouvier J, Thoby-Brisson M, Renier N, Dubreuil V, Ericson J, Champagnat J, Pierani A, Chédotal A, Fortin G. (2010) Hindbrain interneurons and axon guidance signaling critical for breathing. Nat Neurosci. 13: 1066–74.

Bretzner F, Brownstone RM. (2013) Lhx3-Chx10 reticulospinal neurons in locomotor circuits. J Neurosci. 33:14681-92.

Brownstone R, Wilson J. (2008) Strategies for delineating spinal locomotor rhythm-generating networks and the possible role of Hb9 interneurones in rhythmogenesis. Brain Res Rev. 57: 64–76.

Butt SJ, Kiehn O. (2003) Functional identification of interneurons responsible for left-right coordination of hindlimbs in mammals. Neuron 38: 953-963.

Carr, P.A., Huang, A., Noga, B.R., and Jordan, L.M. (1995) Cytochemical characteristics of cat spinal neurons activated during fictive locomotion. Brain Res Bull. 37: 213–218.

Coulon P, Bras H, Vinay L. (2011). Characterization of last-order premotor interneurons by transneuronal tracing with rabies virus in the neonatal mouse spinal cord. J Comp Neurol. 519:3470-87.

Crone SA, Zhong G, Harris-Warrick R, Sharma K. (2009) In mice lacking V2a interneurons, gait depends on speed of locomotion. J Neurosci. 29:7098-109.

Douglas RM, Dragunow M, Robertson HA. (1988) High-frequency discharge of dentate granule cells, but not long-term potentiation, induced c-fos protein. Mol Brain Res 4:259-262.

Dai Y, Carlin KP, Li Z, McMahon DG, Brownstone RM, Jordan LM. (2009) Electrophysiological and pharmacological properties of locomotor activity-related neurons in cfos-EGFP mice. J Neurophysiol. 102:3365-83.

Dyck J. Lanuza GM, Gosgnach S. (2012) Functional characterization of dI6 interneurons in the neonatal mouse spinal cord. J Neurophysiol. 107:3256-66.

Francius C, Harris A, Rucchin V, Hendricks TJ, Stam FJ, Barber M, Kurek D, Grosveld FG, Pierani A, Goulding M, Clotman F. (2013) Identification of multiple subsets of ventral interneurons and differential distribution along the rostrocaudal axis of the developing spinal cord. PLoS One. 8:e70325.

Gosgnach S, Lanuza GM, Butt SJ, Saueressig H, Zhang Y, Velasquez T, Riethmacher D, Callaway EM, Kiehn O, Goulding M. (2006) V1 spinal neurons regulate the speed of vertebrate locomotor outputs. Nature 440:215-219.

Goulding, M. (2009) Circuits controlling vertebrate locomotion: moving in a new direction. Nat Rev Neurosci. 10:507-18.

Herrera DG, Robertson HA. (1996) Activation of c-fos in the brain. Prog. In Neurobiology. 50: 83-107.

Hua JY, Smith SJ. (2004) Neural activity and the dynamics of central nervous system development. Nat Neurosci. 7:327-32.

Jankowska E. (2008) Spinal interneuronal networks in the cat: elementary components. Brain Res Rev. 57: 46-55.

Jasmin L, Gogas, KR, Ahlgren SC, Levine JD, and Basbaum AI. (1994) Walking evokes a distinctive pattern of Fos-like immunoreactivity in the caudal brainstem and spinal cord of the rat. Neuroscience 58, 275–286.

Jovanovic K, Pastor AM, O'Donovan MJ. (2010) The use of PRV-Bartha to define premotor inputs to lumbar motoneurons in the neonatal spinal cord of the mouse. PLoS One. 5:e11743.

Kerman IA, Enquist LW, Watson SJ, Yates BJ. (2003) Brainstem substrates of sympatho-motor circuitry identified using trans-synaptic tracing with pseudorabies virus recombinants. J. Neurosci. 23: 4657-66.

Kiehn, O. (2006) Locomotor circuits in the mammalian spinal cord. Ann Rev Neurosci. 29:279-306.

Kiehn O. (2011) Development and functional organization of spinal locomotor circuits. Curr Opin Neurobiol. 21:100-109.

Kjaerulff O, Kiehn O. (1996) Distribution of networks generating and coordinating locomotor activity in the neonatal rat spinal cord in vitro: a lesion study. J Neurosci. 16:5777–94.

Lanuza GM, Gosgnach S, Pierani A, Jessell TM, Goulding M. (2004) Genetic identification of spinal interneurons that coordinate left-right locomotor activity necessary for walking movements. Neuron 42:375–86.

McCrea DA. (2001) Spinal circuitry of sensorimotor control of locomotion. J Physiol. 533:41-50.

Mirnics K, Koerber HR. (1995) Prenatal development of rat primary afferent fibers: II. Central projections. J Comp Neurol. 355:601-14.

Moran-Rivard, L, Kagawa, T, Saueressig, H, Gross, MK, Burrill, J, Goulding, M. (2001) Evx1 is a postmitotic determinant of V0 interneuron identity in the spinal cord. Neuron 29:385-99.

Oliveira AL, Hydling F, Olsson E, Shi T, Edwards RH, Fujiyama F, Kaneko T, Hökfelt T, Cullheim S, Meister B. (2003) Cellular localization of three vesicular glutamate

transporter mRNAs and proteins in rat spinal cord and dorsal root ganglia. Synapse. 50:117-29.

Pearson JC, Sedivec MJ, Dewey DE, Fyffe RE. (2000) Light microscopic observations on the relationships between 5-hydroxytryptamine-immunoreactive axons and dorsal spinocerebellar tract cells in Clarke's column in the cat. Exp Brain Res 130: 320–27.

Pierani A, Moran-Rivard L, Sunshine MJ, Littman DR, Goulding M, Jessell TM. (2001) Control of interneuron fate in the developing spinal cord by the progenitor homeodomain protein Dbx1. Neuron 29:367–84.

Prasad T, Wang X, Gray PA, Weiner JA. (2008) A differential developmental pattern of spinal interneuron apoptosis during synaptogenesis: insights from genetic analyses of the protocadherin-gamma gene cluster. Development. 135:4153-64.

Quinlan KA, Kiehn O. (2007) Segmental, synaptic actions of commissural interneurons in the mouse spinal cord. J Neurosci 27:6521-30.

Rajaofetra N, Sandillon F, Geffard M, Privat A. (1989) Pre- and post-natal ontogeny of serotonergic projections to the rat spinal cord. J Neurosci Res. 22:305-21

Sibilla S, Ballerini L. (2009) GABAergic and glycinergic interneuron expression during spinal cord development: dynamic interplay between inhibition and excitation in the control of ventral network outputs. Prog Neurobiol. 89:46-60.

Smith, BN, Banfield BW, Smeraski CA, Wilcox CL, Dudek FE, Enquist LW, Pickard GE. (2000) Pseudorabies virus expressing enhanced green fluorescent protein: A tool for in vitro electrophysiological analysis of transsynaptically labeled neurons in identified central nervous system circuits. Proc Natl Acad Sci USA. 97:9264-69.

Stepien AE, Tripodi M, Arber S. (2010) Monosynaptic rabies virus reveals premotor network organization and synaptic specificity of cholinergic partition cells. Neuron. 68:456-72.

Talpalar AE, Bouvier J, Borgius L, Fortin G, Pierani A, Kiehn O. (2013) Dual-mode operation of neuronal networks involved in left-right alternation. Nature. 500:85-88.

Zagoraiou L, Akay T, Martin JF, Brownstone RM, Jessell TM, Miles GB. (2009) A cluster of cholinergic premotor interneurons modulates mouse locomotor activity. Neuron. 64:645-62.

Table 3.1. Distribution of all V0 interneurons as well as ventral and dorsal subpopulations in the mouse lumbar spinal cord.

		Spinal Cord Segment				
		L1	L2	L3	L4	L5
Cell Type	n	$\bar{x}$ cells± SD	$\bar{x}$ cells± SD	$\bar{x}$ cells± SD	$\bar{x}$ cells± SD	$\bar{x}$ cells± SD
V0	8	103.9± 7.7	113.0± 11.2	124.6± 10.2	134.6± 8.3	124.5± 13.4
$V0_D$	8	45.6± 4.5	49.6± 7.2	56.4± 5.4	61.4± 4.9	55.4± 7.1
$V0_V$	8	58.3± 4.9	63.4± 7.2	68.4± 6.0	73.2± 7.3	69.2± 7.5
area (mm^2)	8	0.838±0.08	0.894±0.11	0.973±0.09	1.06±0.11	0.985±0.10

3.7 Figures

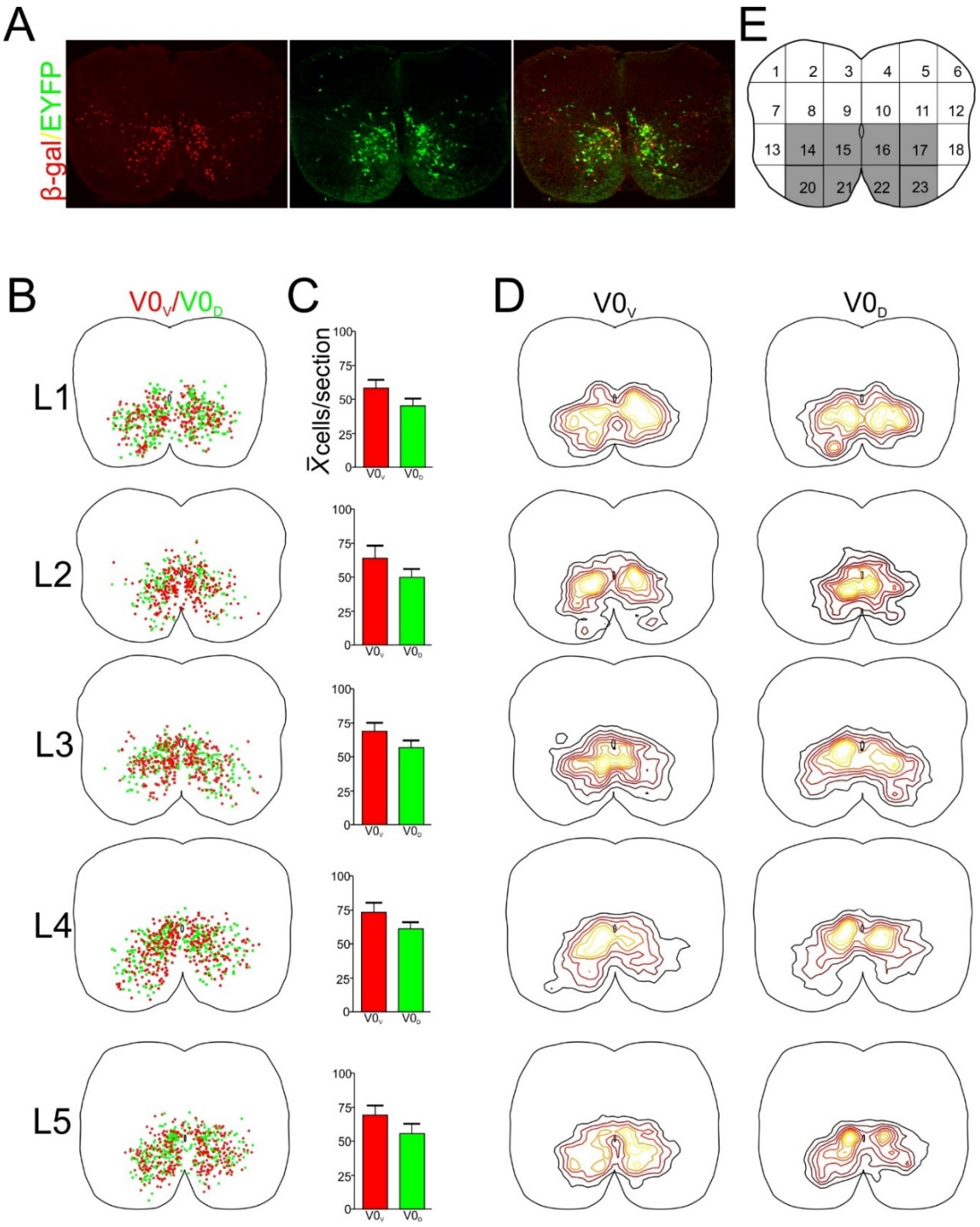

Figure 1. *Distribution of V0 subpopulations in the lumbar spinal cord*. A. 20 μm section cut from a P0 TgDbx1^{Cre};R26^{EYFP};Dbx1^{LacZ} mouse spinal cord labeled for β-gal (red) and

EYFP (green). In merged image $V0_V$ cells appear red (β-gal only) and $V0_D$ cells appear yellow (β-gal+, EYFP+). B. Schematics of sections from the L1-L5 spinal cord with the location of each $V0_V$ (red) and $V0_D$ (green) cell plotted with respect to the central canal. C. Plot of mean number of $V0_V$ (red bar) and $V0_D$ (green bar) cells per section +SD for each segment. D. Topographical maps illustrating the distribution of $V0_V$ (left panels) and $V0_D$ cells (right panels) at each lumbar segment investigated. Black rings indicate lowest density of cells. Yellow lines indicate highest density. E. Schematic of the L2 segment of the spinal cord indicating the manner in which the spinal cord was divided into 24 regions in order to analyze the regional distribution of the V0 subpopulations.

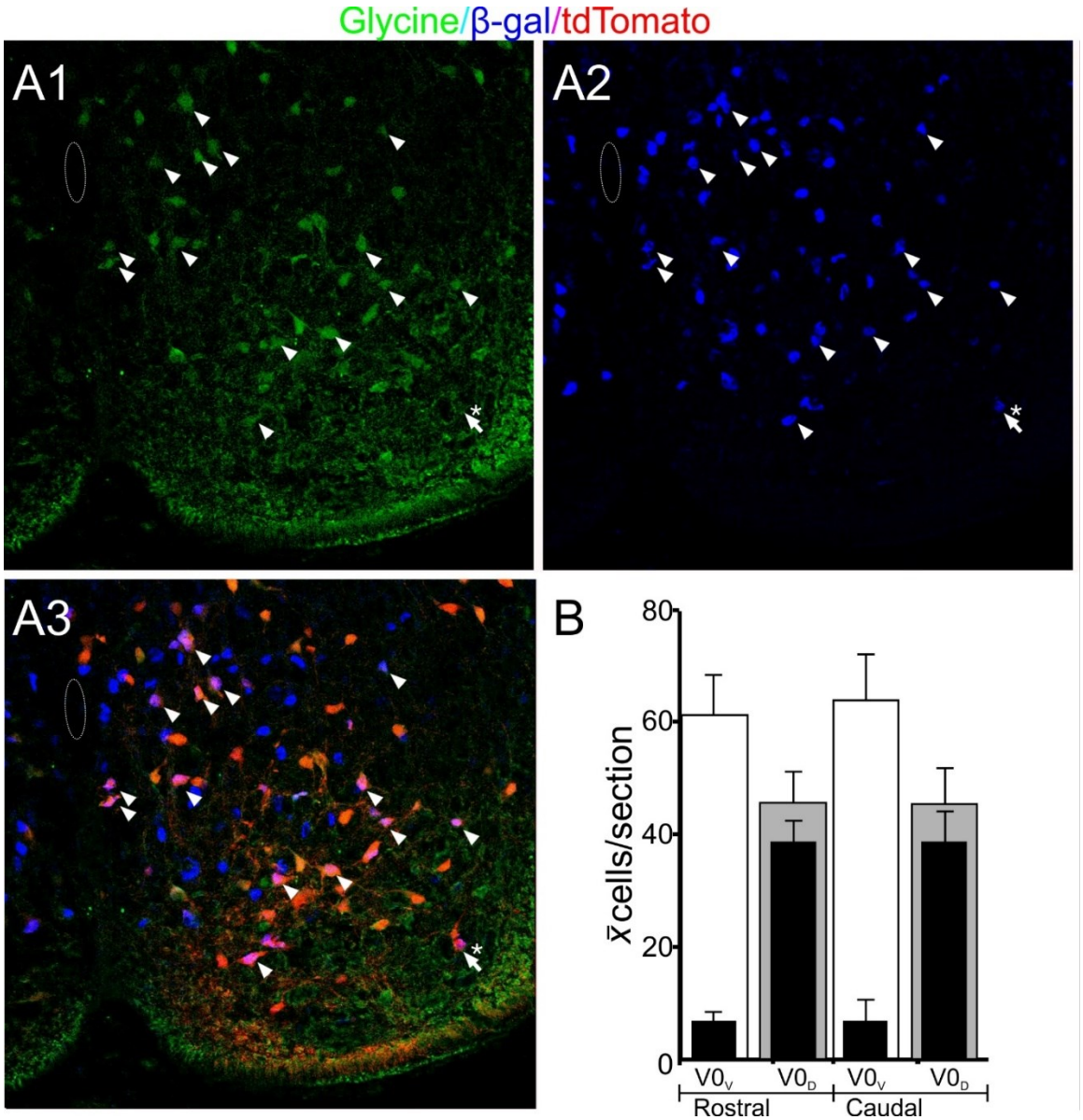

Figure 2. *V0D cells are glycinergic*. A1-A3. Image of the ventral horn of a 20 µm section cut from a P0 TgDbx1^{Cre};R26^{tdTomato}; Dbx1^{LacZ} mouse spinal cord labeled for glycine (green, panel A1) β-gal (blue, panel A2). tdTomato cells (red, panel A3) can be seen without an antibody. In merged image (A3) V0V cells appear blue (β-gal only) and V0D cells appear purple (β-gal+, tdTomato+). White arrowheads indicate all glycinergic V0 cells. One V0D cell in this image (white arrow with asterix) is not glycinergic. B. Plot of the mean number of total V0V (white bars), total V0D (light grey bars) per spinal cord

section at rostral (L1, L2) and caudal (L4, L5) segmental levels. Superimposed black bars indicate number of glycinergic cells belonging to each population. Means are plotted + SD.

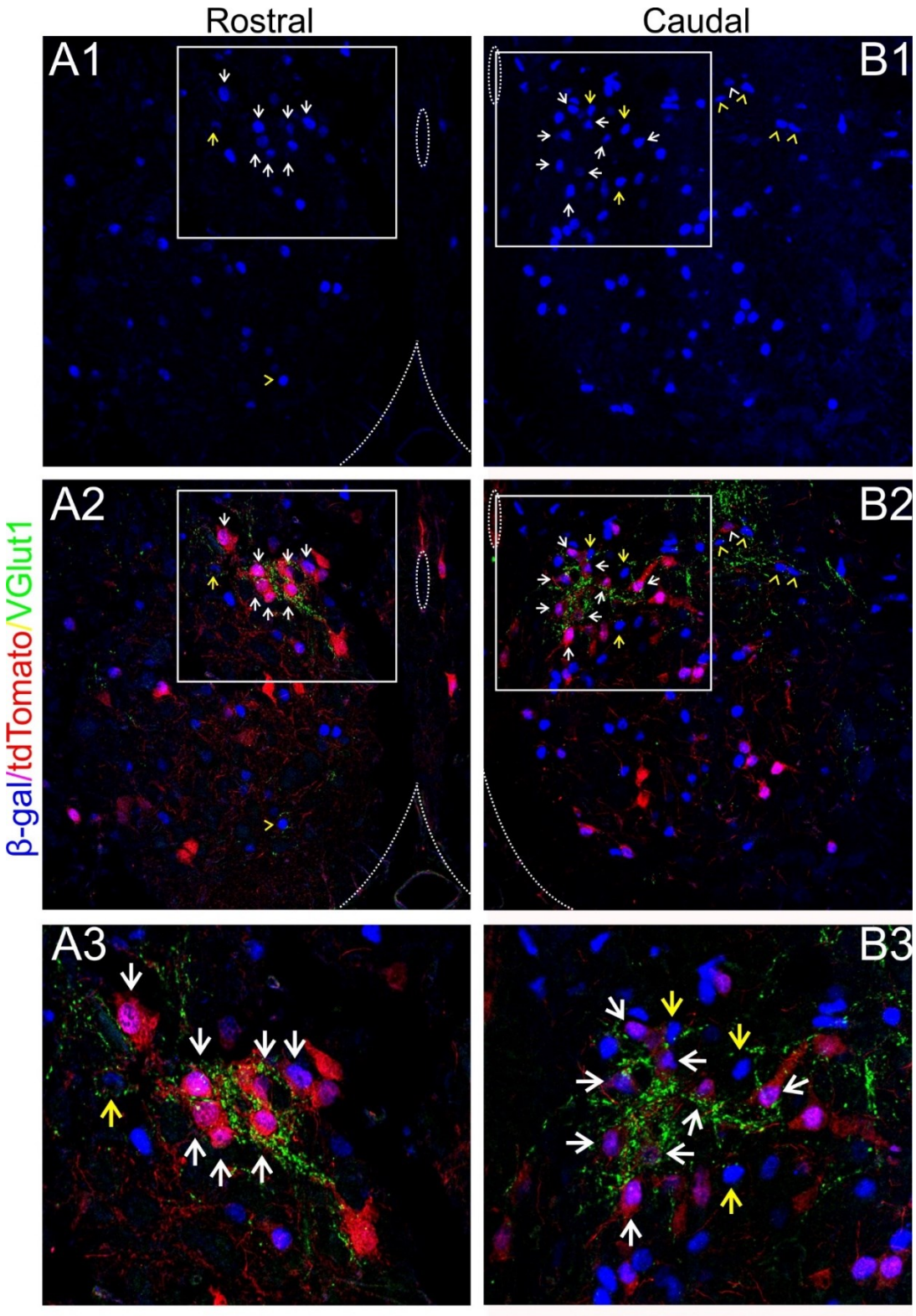

Figure 3. *V0$_D$ cells receive primary afferent input*. Image of the ventral horn of a 6 µm thick section cut from a P0 TgDbx1^{Cre};R26^{tdTomato}; Dbx1^{LacZ} mouse spinal cord at rostral

(A) and caudal (B) levels labeled for VGlut1 (green) and β-gal (blue). tdTomato cells (red) can be seen without an antibody. All V0 cells (blue cells) can be seen in panel A1, B1. In merged panels (A2, B2) $V0_V$ cells appear blue (β-gal only) and $V0_D$ cells appear purple ($\beta\text{-gal}^+$, tdTomato^+). Greatest density of VGlut1 staining occurs in the region surrounded by the white box, lateral to the central canal. Extensive terminations can be seen surrounding $V0_D$ cells (white arrows) and relatively few terminals are seen surrounding $V0_V$ cells (yellow arrows). Boxed regions are magnified in panels A3, B3. A substantial number of VGlut1 labeling is seen lateral to the boxed region nearby $V0_V$ (yellow arrowheads) and $V0_D$ cells (white arrowheads).

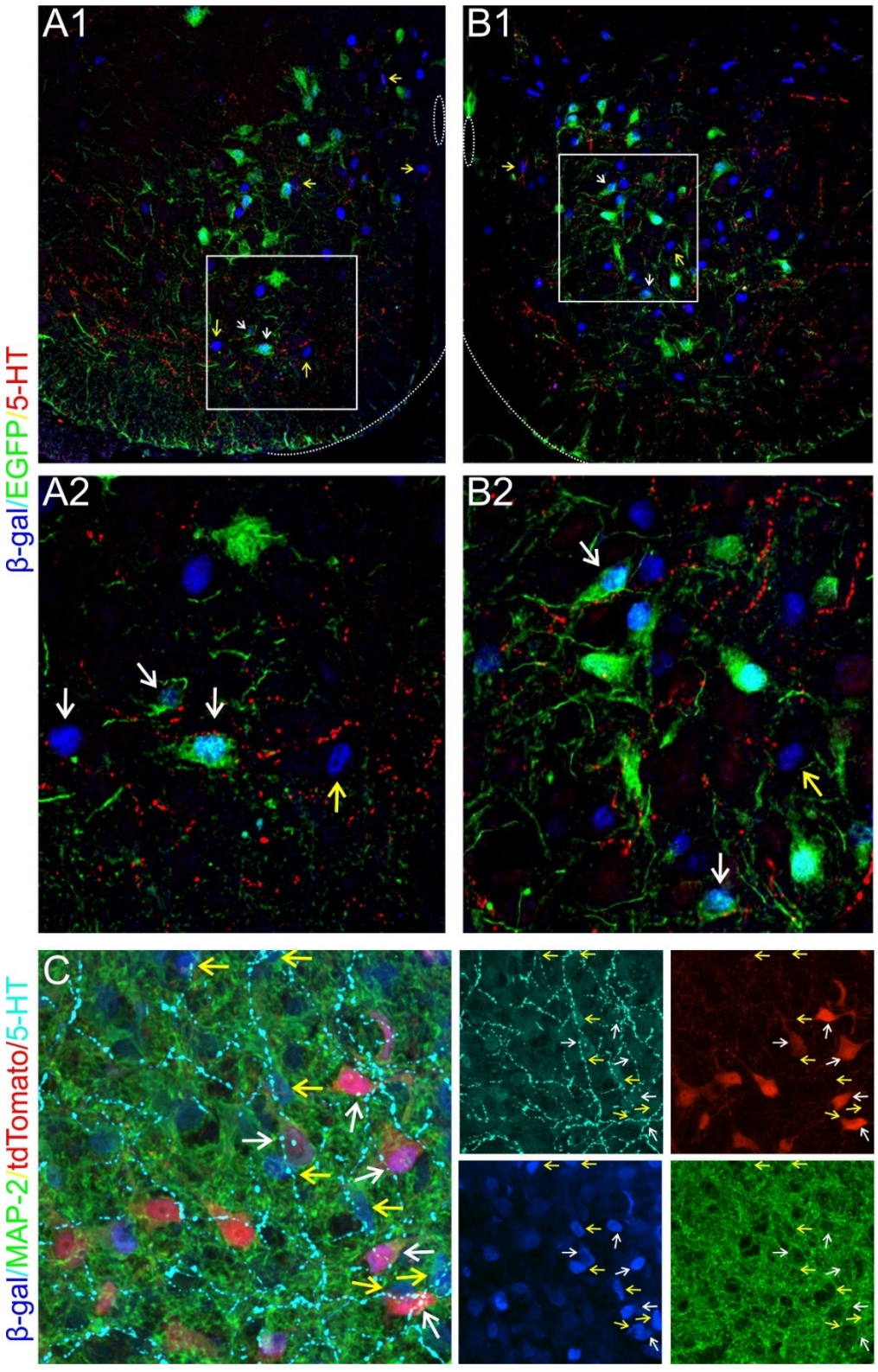

Figure 4. *Serononergic innervation of V0$_V$ and V0$_D$ cells*. A.1, B.1. Images of 6 μm thick section cut from a TgDbx1^{Cre};R26^{EYFP}; Dbx1^{LacZ} mouse spinal cord stained with

antibodies to EFGP (green), β-gal (blue) and 5-HT (red) at rostral (A) and caudal (B) levels. Presumptive serotonergic varicosities can be seen in close proximity to blue $V0_V$ (cells receiving varicosities indicated by yellow arrow) and cyan $V0_D$ (cells receiving varicosities indicated by white arrow) cells. A2, B2 Enlargements of boxed regions in panels A.1 and B.1. C. Section cut from TgDbx1Cre;R26tdTomato; Dbx1LacZ mouse spinal cord stained with an antibody to MAP2 (green) as well as β-gal (blue) and 5-HT (cyan), tdTomato+ cells (red) can be seen without an antibody. Merged image illustrates clear 5-HT varicosities present on both $V0_V$ (blue cells indicated by yellow arrows) and $V0_D$ (purple cells indicated by white arrows) cells. To the right of the panel the image is split into four channels for confirmation of labeling.

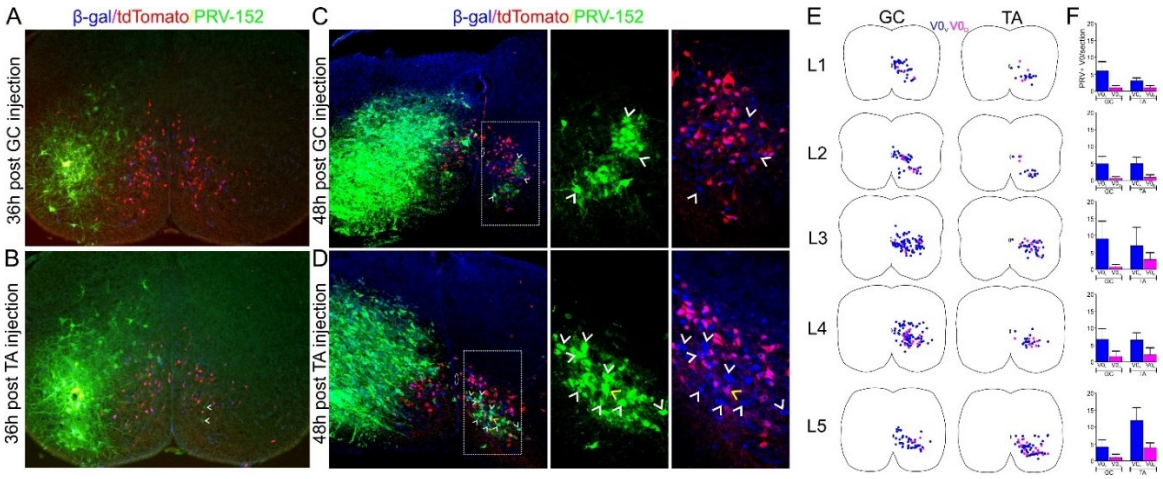

Figure 5. *V0 cells project axons towards contralateral motoneurons*. A, B. Images of sections cut from a TgDbx1^{Cre};R26^{tdTomato}; Dbx1^{LacZ} mouse spinal cord that was fixed 36 hours after PRV-152 injection into the GC muscle. V0$_V$ cells appear blue (β-gal only) and V0$_D$ cells appear purple (β-gal$^+$, tdTomato$^+$). Cells which have taken up the PRV appear green. PRV-152$^+$ cells are abundant on the left half of the cord (ipsilateral to the injection), two contralateral cells are weakly labeled (white arrowheads, panel B). C, D Same experimental paradigm as panels A, B with section from spinal cord fixed 48 hours after PRV-152 injection into the GC (C) and TA (D) muscle. V0 cells that are synaptically connected to contralateral motoneurons are located within the dashed box and indicated by the white (V0$_V$) and yellow (V0$_D$) arrowheads. Boxed region is magnified and split into channels on the right. E. Schematics of sections from the L1-L5 spinal cord with the location of each PRV$^+$ V0$_V$ (blue) and V0$_D$ (purple) cell observed 48h after GC and TA injection plotted with respect to the central canal. F. Plot of mean number of PRV$^+$ V0$_V$ (blue bar) and PRV+ V0$_D$ (purple bar) cells per section +SD.

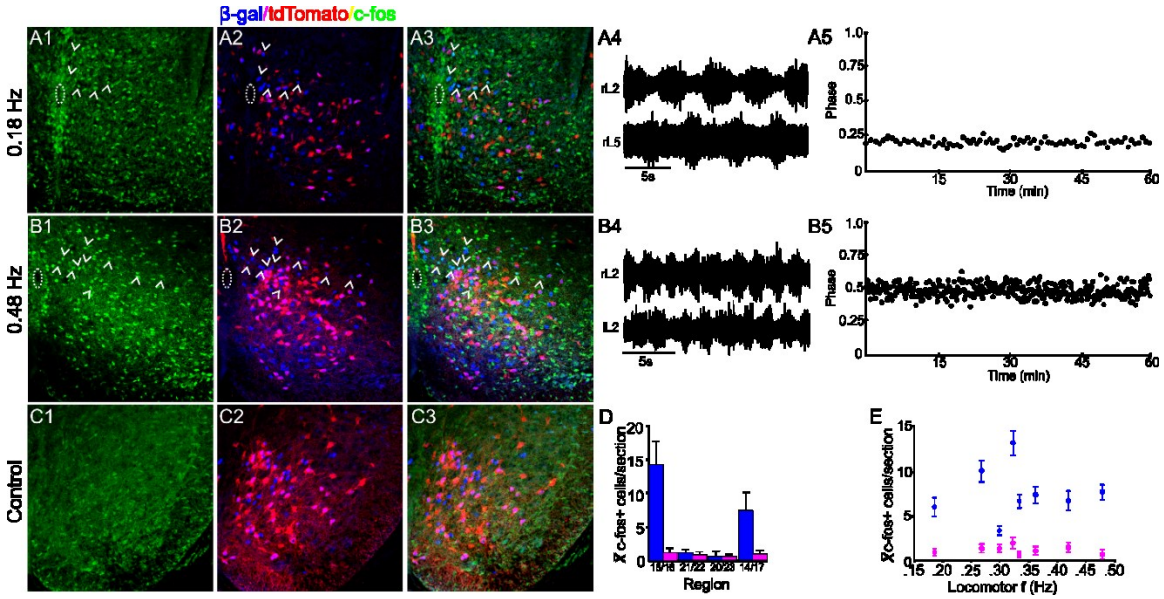

Figure 6. *V0 cells lateral to the central canal are active at all fictive locomotor frequencies*. A, B. Images of ventromedial region of spinal cord from L2 segment following a 1h bout of fictive locomotion at 0.18 Hz (A) and 0.48 Hz (B). A1, B1 Cells active during fictive locomotion are labeled with c-fos (green). A2, B2 B-gal (blue) and tdTomato (red) labeling allows $V0_V$ (blue) and $V0_D$ (purple) cells to be identified. Active $V0_V$ cells (white arrowheads) can be seen in merged image (A3, B3). No c-fos+ $V0_D$ cells were observed in these sections. A4, B4 ENG recordings illustrating fictive locomotor activity evoked and recorded via suction electrodes placed on the left (l) and right (r) L2 and L5 ventral roots. A5, B5 plots of locomotor frequency vs time for spinal cords represented in panels A and B. C1-C3. Images illustrating reduced c-fos labeling (green, C1) as well as $V0_V$ (blue) and $V0_D$ (purple) cells (C2) in a control experiment in which fictive locomotion is not induced. No c-fos+ V0 cells are visible in the merged panel (C3) D. Plot of mean number of $V0_V$ (blue bar) and $V0_D$ (purple bar) cells per section ±SD in each of the regions of interest. E. Plot indicating mean number of $V0_V$ (blue) and $V0_D$ (purple) cells per section ±SD that were observed to be c-fos+ at each fictive locomotor frequencies obtained.

Chapter 4 – Anatomical and electrophysiological characterization of dI6 interneurons in the neonatal mouse spinal cord.

Anna Griener, Wei Zhang, Henry Kao, Simon Gosgnach

4.1 Abstract

The locomotor central pattern generator is a network of neurons located in the ventromedial aspect of the lumbar spinal cord that is responsible for generating and coordinating locomotor activity. The dI6 interneurons remain one of the most poorly understood cell populations to settle in the ventral spinal cord, as the lack of an adequate molecular marker has prevented their thorough characterization. They have long been speculated to be inhibitory commissural premotor interneurons, however evidence in support of this is sparse. In the current study, we took advantage of the unique TgDbx1^{Cre}; ROSA26^{EFP}; Dbx1^{LacZ} transgenic mouse model which has previously been shown to identify dI6 interneurons. We describe the post-natal distribution of dI6 cells throughout the spinal cord and examine their synaptic partners within the lumbar enlargement. We show dI6 interneurons are abundant in laminae VII and VIII along the entire spinal cord and describe a novel dorsally situated subpopulation in rostral levels. Retrograde dextran tracing experiments confirm the overwhelming majority of dI6 cells are commissural however, monosynaptic and disynaptic contacts were observed on both ipsilaterally and contralaterally located motorneuron. During drug-induced fictive locomotion using the semi-intact spinal cord preparation, electrophysiological recordings from rhythmically active dI6 interneurons revealed two functionally distinct subpopulations. Putative rhythm generating (pRG) dI6 interneurons continued to oscillate during spontaneous non-resetting deletions, whereas rhythmic activity failed in putative pattern forming (pPF) dI6 cells. Comparison of the location of each cell type indicated pRG dI6 interneurons were evenly distributed throughout all regions in which dI6 cells were found. In contrast, pPF dI6 cells were predominantly located laterally. This study provides the first thorough characterization of the dI6 population and provides evidence of their involvement in diverse aspects of locomotor control.

4.2 Introduction

A neural network referred to as the locomotor central pattern generator (CPG) is situated in the ventro-medial aspect of the mammalian lumbar spinal cord and generates the basic pattern of left-right, flexor-extensor alternation which regulates hindlimb activity during locomotion. Recently, an experimental approach incorporating molecular genetics, electrophysiology, and anatomical tracing has been successful in describing the cellular properties and specific locomotor functions of a number of genetically-defined interneuronal populations located within this region of the spinal cord (i.e. Rexed laminae VII/VIII; Goulding, 2009).

The dI6 population is one such genetically-defined interneuronal population located in the ventro-medial aspect of the postnatal spinal cord that has not been thoroughly investigated. During embryonic development, dI6 cells originate from progenitors immediately dorsal to the p0 domain and, along with all other Class B dorsal populations, express the transcription factor Lbx1 (Gross et al., 2002). While some dI6 cells express the transcription factors Wt1 and/or DMRT3 postmitotically, the lack of a unique molecular marker for the entire population has hindered their characterization. Preliminary studies have indicated that dI6 cells are a mixed population of inhibitory and commissurally projecting interneurons (Hendricks & Goulding, 2007, Rabe et al., 2009). The DMRT3-expressing dI6 subpopulation, studied independently, are primarily inhibitory and commissurally projecting (Andersson et al., 2012). While the activity of these cells during locomotion has not been investigated analysis of locomotor activity in transgenic mice lacking the DMRT3 subpopulation led to the suggestion that these cells are responsible for generating diverse gaits and maintaining general locomotor stability in some quadrupeds (Andersson et al., 2012).

A previous study from our laboratory demonstrated that the $TgDbx1^{Cre};ROSA26^{EFP};Dbx1^{LacZ}$ transgenic mouse can demarcate dI6 interneurons, in addition to distinguishing $V0_D$ from $V0_V$ cells (Dyck et al., 2012). Intracellular

recordings showed that approximately 50% of the dI6 interneurons situated immediately dorsal to the central canal are rhythmically active during fictive locomotor behavior and have intrinsic electrophysiological properties suggestive of involvement in either locomotor rhythm generation or pattern formation (Dyck et al., 2012).

It was recently proposed that, in lieu of intrinsic membrane properties, the behavior of a cell during spontaneous non-resetting deletions in motor output can be used to decipher its specific locomotor function (McCrea & Rybak, 2008). A non-resetting deletion is a spontaneous omission of ventral root bursting after which rhythmic activity resumes at the time predicted based on the locomotor cycle period immediately preceding the deletion. Cells which maintain rhythmic activity during non-resetting deletions in ventral root activity are proposed to be involved in rhythm generation, whereas those which fall silent are purportedly involved in pattern formation. Such an approach has been applied to investigate the general organizational principles of unidentified rhythmically active CPG interneurons, as well as members of the genetically-defined V2a population (Zhong et al., 2012, Griener et al., 2013).

In the current study, we performed anatomical and electrophysiological characterization of dI6 interneurons labelled in the TgDbx1^{Cre};ROSA26^{EFP};Dbx1^{LacZ} transgenic mouse model in order to characterize this population of interneurons and provide further insight into their involvement in the production of locomotor activity. Our results describe the distribution of dI6 interneurons in the postnatal spinal cord and characterize their synaptic partners within the lumbar enlargement. Analysis of activity during non-resetting deletions revealed that rhythmically active dI6 interneurons exhibit behaviour consistent with involvement in either rhythm generation or pattern formation, with those cells involved in pattern formation located more laterally.

4.3 Materials and Methods

Animals. All procedures were performed in accordance with the Canadian Council on Animal Welfare and approved by the Animal Welfare Committee at the University of Alberta. Transgenic TgDbx1^{Cre} and Dbx1^{LacZ} mouse strains were generously provided by the Goulding laboratory (Salk Institute, La Jolla, CA) and the generation of each strain has been described previously (Pierani et al. 2001, Dyck et al. 2012). TgDbx1^{Cre} mice were crossed with reporter lines (ROSA26^{EYFP} and ROSA26^{tdTomato}: Jackson Laboratories), collectively called R26^{EFP}. Adult TgDbx1^{Cre};R26^{EFP} offspring were subsequently crossed with Dbx1^{LacZ} mice to generate TgDbx1^{Cre};R26^{EFP};Dbx1^{LacZ} pups used for immunohistochemistry or TgDbx1^{Cre};R26^{EFP} pups used for electrophysiology. TgDbx1^{Cre};R26^{EFP};Dbx1^{LacZ} mice have been shown to express EFP reporter in dI6 and V0$_D$ cells and β-gal reporter in V0$_D$ and V0$_V$ cells, thereby allowing dI6 interneurons to be differentiated from V0 interneurons (Dyck et al. 2012, Griener et al. 2015).

Immunohistochemistry. Spinal cords were dissected from neonatal (postnatal day 0-3: P0-P3) mice following anaesthetization via submersion in ice and transcardial perfusion with 4% paraformaldehyde (PFA) in 0.1 *M* phosphate buffer solution (PBS). Tissue sections were cut using either a cryostat or microtome. Following overnight fixation (4°C, 4% PFA in 0.1 *M* PBS), the lumbar enlargement was cryoprotected, embedded in OCT compound, and 20 µm thick transverse sections were cut on a cryostat. Alternately, spinal cord tissue was dehydrated, cleaned in xylene, and embedded in paraffin before 6 µm thick sections were cut using a microtome. Antibodies to EGFP (generous gift from Eusera – goat, 1:5000) and β-gal (chicken, 1:700, Aves) were used to distinguish dI6 cells from V0$_D$ cells. No antibody was required to visualize tdTomato. Antibodies were also used to detect glycinergic cell bodies (glycine; rat, 1:1000, Immunosolutions), primary afferent terminals (vGluT1;

guinea pig, 1:2500, Millipore), and serotonergic terminals (5-HT; rabbit, 1:2500, Immunostar).

For cryostat sections, tissue was incubated with primary antibodies overnight (4^{o}C), followed by incubation with species-specific secondary antibodies conjugated to Cy2, Cy3, or Cy5 (Jackson Immunoresearch). For microtome sections, sections were dewaxed, rehydrated with graded alcohols, and washed with PBS prior to antigen retrieval with 10 m*M* sodium citrate buffer. Sections were washed and incubated with primary antibodies overnight (room temperature) under continuous agitation, followed by incubation with species-specific secondary antibodies conjugated to Cy2, Cy3, or Cy5 (Jackson Immunoresearch). All slides were coverslipped with Fluorosave reagent (Calbiochem). Images were collected using either a Zeiss Axioplan microscope using LSM 510 NLO laser configured to a computer running Zen software or a Leica DM 5500 running Metamorph software. All images were exported to TIFF format and figure preparation was performed in Adobe Photoshop and Corel Draw. Cell distribution was analyzed using a custom written Matlab script (Henry Kao) which assigned X,Y coordinates to each cell relative to the origin set at the midpoint of the central canal.

Dextran labelling. TgDbx1^{Cre};R26^{EFP};Dbx1^{LacZ} pups were anaesthetized via submersion in ice before transcardial perfusion with ice-cold oxygenated dissecting artificial cerebrospinal fluid (d-aCSF), containing (in mM) 111 NaCl, 3.08 KCl, 11 glucose, 25 $NaHCO_3$, 1.18 KH_2PO_4, 3.7 $MgSO_4$ and 0.25 $CaCl_2$ (pH 7.4). Spinal cords were dissected out into d-aCSF. In a darkened room, a dissecting pin (0.02mm stainless steel insect pins, Austerlitz) coated with tetramethylrhodamine dextran (TMRD, Invitrogen) or dextran conjugated to Alexa Flour 488 (Invitrogen) were inserted unilaterally into the ventral spinal cord at either the L2 or L4 segment. Dye insertion was repeated 3-4 times per spinal cord, proceeding from the midline towards the lateral edge. TMRD was used exclusively in TgDbx1^{Cre};R26^{EYFP};Dbx1^{LacZ} tissue and

Dextran conjugated to Alexa Flour 488 was used exclusively in TgDbx1^{Cre};R26^{tdTomato};Dbx1^{LacZ} tissue. The spinal cords were incubated in the dark for 24 h in room temperature (20^{o}C) oxygenated recording-aCSF (r-aCSF), which was identical to d-aCSF except for (in mM) 1.25 $MgSO_4$ and 2.52 $CaCl_2$. The tissue was then transferred to 4% PFA in 0.1 *M* PBS, fixed overnight (4^{o}C) and processed for immunohistochemistry using antibodies to β-gal and/or EGFP.

Retrograde trans-synaptic labelling. In P1 TgDbx1^{Cre};ROSA26^{tdTomato};Dbx1^{LacZ} mice, hindlimb flexor (tibialis anterior [TA] or extensor gastrocnemius [GC]) muscles were injected with a strain of pseudorabies virus which expresses GFP in all infected cells (PRV-152, see Smith et al., 2000) according to a protocol described in Kerman et al., (2003). Briefly, 1-2 µL of PRV-152 viral stock (6.68 x 108 infectious units per µL) was pressure injected into the hindlimb muscle using glass micropipettes connected to a picospritzer. Animals were euthanized 38 or 48 h after injection as these are the times at which virus-labelled interneurons are monosynaptically (30-40 h) or disynaptically (40-50 h) connected to motorneurons (Jovanovic et al., 2010). Spinal cords were dissected out and processed for immunohistochemistry as described above. The pattern and density of viral labelling in all spinal cords included in the data set were similar to those previously reported for 36 or 48 h (Jovanovic et al., 2010). Some of the spinal cords collected at 48 h post infection were analyzed for GFP expression in $V0_V$ and $V0_D$ cells and the data were presented previously (Griener et al., 2015).

Electrophysiology. Neonatal TgDbx1^{Cre};R26^{EFP} pups (P0-P3) were anaesthetized on ice, transcardially perfused with oxygenated (d-aCSF), decapitated and eviscerated. Spinal cords were dissected out into ice-cold oxygenated d-aCSF. The *in vitro* preparation used for performing electrophysiological recordings from dI6 interneurons in the functionally intact locomotor CPG has been described previously (Dyck &

Gosgnach 2009). Briefly, the isolated spinal cord was transferred to the cutting chamber of a Leica VT1200 vibratome containing ice-cold oxygenated d-aCSF and pinned, dorsal aspect up, to an agarose block. Horizontal sections (100 μm) were serially removed until the central canal was visible, as it has been previously shown that the nearly all EFP^+ cells located above the central canal are dI6 interneurons (Dyck et al. 2012). Immediately following sectioning, the spinal cord was transferred to the recording chamber of a Zeiss Axioplan microscope. The spinal cord was continually perfused with room-temperature (20°C) oxygenated r-aCSF.

Fictive locomotion was induced via bath application of N-methyl-D-aspartate (NMDA, 5-10μM) and 5-hydroxytryptamine creatine sulfate complex (5-HT, 10-15 μM; both from Sigma-Aldrich). Drug-induced fictive locomotor activity was monitored via electroneurogram (ENG) recording using bipolar suction electrodes (A-M Systems Inc., Carlsborg, WA) positioned on the flexor-related second or third lumbar (L2 or L3) and/or extensor-related fifth lumbar (L5) ventral roots. ENG signals were amplified (×20,000) and band-pass filtered (100 Hz – 1 kHz) with custom made equipment (R&R Designs, Winnipeg, MB). All ENG and whole-cell data were digitized (Digidata 1440A, Molecular Devices, Sunnydale, CA) and recorded using pClamp software (Axon Instruments) on a PC.

For whole-cell recording, patch electrodes (tip resistance: 3-7 MΩ) were pulled from borosilicate glass (Harvard Instruments) and filled with intracellular solution containing (in mM) 138 K-gluconate, 10 HEPES, 0.0001 $CaCl_2$, 0.3 GTP-Li, and 5 ATP-Mg (pH adjusted to 7.2). For morphological analysis Neurobiotin (0.2% Vector Labs, Burlington, ON) and/or Lucifer Yellow (probably 0.1%, Invitrogen) were included in the intracellular solution. An infrared differential interference contrast (IR-DIC) filter was used to target for recording cells located along the extent of the cut surface of the dorsal horn-removed lumbar spinal cord. Cells located 20-60μm below the cut surface

were healthy and accessible for recording. A micromanipulator (MPC-3885, Sutter Instruments, Novato, CA) was used to position the electrode over the cut region of the spinal cord and lower it into the tissue.

Anatomical reconstruction. During electrophysiological recording, cells were held for 20-25 minutes to allow Neurobiotin and/or Lucifer yellow to fill the neurites. After removal of the intracellular electrode, the spinal cord was perfused with room temperature r-aCSF for a minimum of 30 minutes to allow the cell membrane to recover prior to transfer to 4% PFA in 0.1 *M* PBS. Spinal cords were fixed overnight (4^{o}C), washed with 0.1% PBS-Tween, and incubated with Cy3-conjugated Streptavidin (1:300, Jackson Immunoresearch). Spinal cords were then treated to a methylsalicylate clearing protocol. After optical clearing spinal cords were placed, dorsal side down on a slide and the cut surface was inspected with the objective lens of an inverted spinning disk confocal microscope (Olympus IX81, Olympus Canada, Richmond Hill, ON, Canada). Z-stack images capturing all discernible projections were obtained using Volocity software. Individual optical sections were 1-µm thick to enable maximal identification of filled neurites. The Simple Neurite Tracer plugin (Longair et al., 2011) in ImageJ was used to reconstruct the cells. Axons were identified as those projections which maintained a constant radius, whereas projections which tapered as they left the soma were identified as dendrites (Jan & Jan, 2010). All figures were assembled in Adobe Photoshop and Corel Draw.

Data and Statistical analysis. The relationship between rhythmic cellular activity and fictive locomotor-related ventral root activity was assessed using circular statistics (Zar, 1974). The latency between the onset of cellular activity and the onset of ENG activity was divided by the ventral root cycle period to provide the phase value. Phase values around 0 indicate activity between the cell and the ventral root that is in phase and phase values around 0.5 indicate activity that is out of phase. To calculate

r values, phase values were calculated for each burst over a 5 minute data collection period and analyzed as described previously (Butt et al., 2002*b*, Kiehn & Kjaerulff, 1996). Rayleigh's test for directionality was performed to identify neurons with the *p* value <0.01 that were deemed to be related to fictive locomotor activity (Drew & Doucet, 1991). Cells were classified as putatively rhythm generating (RG) or pattern forming (PF) depending on their activity during non-resetting deletions in ENG recordings from the local ventral root (i.e., the ventral root originating in the ipsilateral hemisegment in which the recorded cell was located) Comparison of the cycle period in which the deletion occurred to the average cycle period of the 5 ENG bursts immediately preceding the spontaneous deletion was used to classify deletions. The calculated *t*-statistic and significance level of $p<0.05$ were used to determine whether a deletion was non-resetting (see Lafreniere-Roula & McCrea, 2005, Zhong et al., 2012 for details and equations).

Micromanipulator coordinates were used to measure the distance of each recorded cell from the midpoint of the central canal, as described previously (Griener et al., 2013). To correct for size differences between spinal cords from animals of different ages, the relative medio-lateral position of each cell was calculated by dividing its distance from the central canal by the mean width of an age-matched hemicord. Evaluation of the medio-lateral distribution of recorded cells was performed using a Wilcoxon-Rank Sum test.

4.4 Results

The distribution of dI6 interneurons identified in $TgDbx1^{Cre};R26^{EFP};Dbx1^{LacZ}$ transgenic mice is not uniform along the rostro-caudal extent of the spinal cord.

In the mouse, the core elements of the locomotor CPG are located in the ventro-medial aspect of the low thoracic and lumbar segments (Kiehn & Kjaerulff, 1998).

While dI6 interneurons differentiate from progenitors immediately dorsal to the sulcus limitans, post-mitotically they migrate ventrally to settle within the ventral horn (Gross et al., 2002, Muller et al., 2002). To fully describe the settling position of dI6 interneurons in the postnatal spinal cord, transverse spinal cord sections were prepared from P0-P2 TgDbx1^{Cre};R26^{EFP};Dbx1^{LacZ} mice and processed for immunohistochemistry. Three distinct interneuron populations can be identified using TgDbx1^{Cre};R26^{EFP};Dbx1^{LacZ} transgenic mice: V0$_V$, V0$_D$, and dI6 (Dyck et al., 2012, Griener et al., 2015). In neonatal pups, EFP reporter protein is expressed in all progeny of Cre-expressing cells, namely the dI6 and V0$_D$ populations. B-gal expression recapitulates Dbx1 expression and therefore labels the entire V0 population (Pierani et al., 2001). Comparison of reporter expression allows the dI6 cells (i.e., EFP$^+$/ β-gal$^-$) to be differentiated from the V0$_D$ (i.e., EFP$^+$/ β-gal $^+$) and V0$_V$ (i.e., EFP$^-$/ β-gal $^+$) interneurons.

All dI6 interneurons (i.e., EFP$^+$/ β-gal $^-$) were counted in two sections from representative cervical, thoracic, and sacral segments (*n*=2, Figure 1A). The laminar distribution of dI6 cells was assessed by comparison to a published atlas of the P4 mouse spinal cord (Sengul et al., 2012). As the primary focus of this paper is investigating locomotor related dI6 cells, a more thorough analysis of their distribution was conducted in the lumbar enlargement, with cell counts carried out in two sections from each of the T12-L5 segments (*n*=5 T12, L4; *n*=6 L1-L3, L5). Using custom written Matlab script (Henry Kao), the location of each dI6 interneuron was converted into X, Y coordinates relative to the origin set at the midpoint of the central canal. Topographical maps of cell density for each of the T12 – L5 segments were generated and presented on a spinal cord schematic (Figure 1B).

At all spinal levels almost all dI6 cells were located in the ventro-medial spinal cord, within an area corresponding to laminae VII and VIII (Figure 1). In the cervical,

thoracic, and upper lumbar segments an additional cluster of dI6 interneurons was found dorsally, in an area corresponding to the lateral aspect of lamina V. In all sections analyzed a small number of dI6 cells was scattered throughout the dorsal horn, however the prominent cluster in lamina V was only observed rostrally. To compensate for size differences across different segmental levels and thereby allow comparison of the relative distribution of dI6 interneurons along the rostro-caudal extent of the spinal cord, cell count values were divided by the surface area of the transverse sections to provide a measure of the density of dI6 cells (Table 1). Analysis indicated there are significantly more dI6 cells in the cervical and thoracic segments than in the lumbar or sacral segments ($p<0.01$, one-way ANOVA, *post hoc* Tukey). Closer analysis within the lumbar enlargement indicated that there was no difference between the relative distributions of dI6 cells in any of the T12 to L4 segments. The L5 segment showed a greater density of dI6 cells in comparison to the remainder of the lumbar enlargement ($p<0.05$, one-way ANOVA).

Overall, these results indicate that the majority of dI6 cells are evenly distributed along the length of the lumbar enlargement within laminae VII and VIII, in an area which has been shown to house the locomotor CPG. A previously undescribed dorsal cluster of dI6 cells was also discovered in the dorsal horn, in an area corresponding to lamina V. Based solely on their location this suggests that in addition to their role in locomotion, dI6 interneurons may serve a role in sensory processing, particularly in the forelimbs.

dI6 interneurons receive primary afferent and serotonergic input.

During overground locomotion, sensory feedback provides the CPG network with necessary information regarding ongoing movement of the limb within the environment. Describing the spinal pathways involved in processing this information requires the identification of first-order interneurons which receive monosynaptic input from sensory afferents. Within the spinal cord primary afferent terminals can be identified by their expression of the vesicular glutamate transporter 1 (vGluT1) protein (Oliveira et al., 2003). Thus, to determine whether dI6 interneurons receive primary afferent input, immunohistochemistry was performed on rostral and caudal lumbar sections of P0 TgDbx1^{Cre};R26^{EFP};Dbx1^{LacZ} mice using antibodies to vGluT1.

As the focus of this paper is the involvement of dI6 cells within the locomotor CPG, examination for primary afferent input was limited to the ventral spinal cord. Analysis of the ventral aspect of transverse sections from 5 spinal cords showed the highest density of vGluT1 labelling lateral to the central canal, spanning the full medio-lateral extent of the grey matter. Additional vGluT1^{+} (immunopositive) punctae were seen ventrally and laterally, presumably within the motor nuclei. Inspection of ventrally located dI6 interneurons revealed vGluT1^{+} terminals in close proximity to dI6 interneurons in all segments analysed (white arrowheads in Figure 2A). Comparison of sections from upper lumbar (L1-L2) and lower lumbar (L4-L5) segments revealed no observable difference in density of vGluT1^{+} punctae or number of contacted dI6 cells along the rostro-caudal extent of the lumbar enlargement. Consistent with the general distribution of primary afferent terminals, vGluT1^{+} terminals were predominantly found on the dI6 cells located immediately lateral to the central canal. Occasionally, dI6 interneurons immediately surrounded by vGlut1^{+} punctae were observed ventrally and laterally near the motorneurons. In contrast to the pronounced innervation of V0$_{D}$ interneurons described previously (Griener et al., 2015), the relatively sparse innervation of dI6 cells by primary afferents observed here suggests

that while dI6 cells may receive sensory input, the primary function of the ventrally located cells is not processing sensory information.

Early studies exploring the pharmacological activation of the locomotor CPG in the *in vitro* isolated rodent spinal cord demonstrated that 5-HT, either alone or in combination with glutamate receptor agonists is sufficient to elicit locomotor activity (Cazalets et al., 1992, Cowley & Schmidt, 1994, 1997). Serotonergic input onto ventrally situated dI6 cells in the lumbar spinal cord was examined via immunohistochemistry using antibodies to 5-HT in transverse sections of P2-P4 TgDbx1^{Cre}; R26^{EFP}; Dbx1^{LacZ} pups. Analysis of tissue from 5 spinal cords revealed presumed serotonergic varicosities (identified as swellings along the 5-HT^{+} fibres) distributed throughout the ventral spinal cord. In all sections analyzed, 5-HT^{+} varicosities were found in close proximity to medially-situated dI6 interneurons (Figure 2B). These cells were predominantly located in a region consistent with lamina VIII (Sengul et al., 2012). Comparison between rostral and caudal segments revealed no difference in serotonergic innervation of dI6 interneurons in the upper lumbar versus lower lumbar spinal cord.

The dI6 interneurons project primarily contralaterally.

Commissural interneurons in the lumbar enlargement are responsible for coordinating locomotor activity between the left and right sides of the body (Butt et al., 2002*a*). Previous reports indicate that some dI6 interneurons are commissural (Lanuza et al., 2004, Hendricks & Goulding, 2007, Rabe et al., 2009, Andersson et al., 2012). However, it remains unclear if the methods used to identify the dI6 population included exclusively dI6 interneurons (Rabe et al., 2009), or captured all dI6 interneurons (Hendricks & Goulding, 2007, Andersson et al., 2012) since ipsilaterally projecting cells have been identified (Andersson et al. 2012). Furthermore, prior

investigation has been limited to the embryo (Rabe et al., 2009, Andersson et al., 2012), and may thus only reflect the organization of the immature spinal cord. Consequently, the axonal projection pattern of dI6 interneurons in the postnatal animal required further inquiry.

To examine the postnatal projection pattern of dI6 interneurons within the lumbar enlargement, fluorescent dextran tracers were injected unilaterally into isolated P0 TgDbx1^{Cre};R26^{EFP};Dbx1^{LacZ} spinal cords. Across all 8 spinal cords examined, the majority of retrogradely labeled dI6 interneurons were observed contralateral to the injection site, indicating the dI6 population is predominantly commissural (Figure 3, 84±9.4% contralateral cells, $p<0.0001$, *t*-test). This pattern was consistent following tracer injection into either the L2 (Figure 3B, 80±9.9% contralateral cells, $n=4$, $p<0.0001$, *t*-test) or the L4 segment (Figure 3C, 88±8.2% contralateral cells, $n=4$, $p<0.0001$, *t*-test). Both ipsilaterally and contralaterally located dextran labelled cells were found at distances as great as 2400μm away from the injection site, the farthest distance examined, suggesting that dI6 cells extend long axons throughout the lumbar enlargement.

Overall, injection into L4 yielded a greater number of retrogradely labelled dI6 cells than injection into L2 ($p<0.05$, *t*-test). Limiting analysis to ipsilaterally located dI6 cells revealed no difference between the number of filled cells following injection at either site ($p=0.38$, *t*-test). In contrast, significantly more contralaterally located dI6 cells were observed following injection into the L4 segment ($p<0.05$, *t*-test). These findings suggest that within the lumbar enlargement, dI6 commissural interneurons (CINs) possess predominantly descending projections. Consistent with this, only 28.1% of the backfilled dI6 CINs were found more than one segment caudal to the L2 injection site (Figure 3Bi).

dI6 interneurons form mono- and disynaptic connections bilaterally onto motorneurons.

During drug-induced fictive locomotion in the neonatal rodent spinal cord, motorneurons receive rhythmic excitatory and inhibitory synaptic drives (Hochman & Schmidt, 1998, Endo & Kiehn, 2008). The interneurons that provide these drives are referred to as last-order interneurons of the locomotor CPG. Recent reports utilizing monosynaptically restricted retrograde trans-synaptic viral tracers have revealed the location of premotor interneurons within the lumbar spinal cord and have in some cases defined the genetically-defined population from which they derive (Coulon et al., 2010, Stepien et al., 2010). Previous studies of the DMRT3-expressing dI6 cells demonstrated that some proportion of this subpopulation act as last-order interneurons that project their axons to either ipsilaterally or contralaterally located hindlimb motorneurons (Andersson et al., 2012).

In an attempt to more broadly define the pattern of connections between the dI6 population as a whole and motorneurons, 1-2 µL of the retrograde trans-synaptic tracer PRV-152 was injected into the gastrocnemius (GC, ankle extensor) or tibialis anterior (TA, ankle flexor) of P0 TgDbx1^{Cre};ROSA26^{tdTomato};Dbx1^{LacZ} mice. Animals were euthanized at 38 h or 48 h post injection as previous work has demonstrated that these are the respective incubation periods to label interneurons with mono- or disynaptic connections to motorneurons, respectively (Jovanovic et al., 2010). Only spinal cords with virus labelling pattern consistent with those previously described were included for analysis (see Jovanovic et al., 2010, Griener et al., 2015). By 38 h post-injection into either the TA or GC muscle, the majority of GFP$^+$ interneurons were located in the ventral and intermediate spinal cord ipsilateral to the injected limb (Figure 4B and 4F). Relatively few GFP$^+$ interneurons were located in the contralateral spinal cord, in an area corresponding to lamina VIII. Some virus-labelled cells were located in all lumbar segments analyzed. By 48 h post-injection, in addition to dense GFP-labelling in the

ipsilateral spinal cord, substantially more virus-filled cells were observed contralateral to the injections site (Figure 4D and 4H).

Three spinal cords were collected 38 h after PRV-152 injection into the TA muscle. Examination of transverse sections from across the lumbar enlargement indicated that PRV labelled dI6 cells ($GFP^+/tdTomato^+/\beta\text{-}gal^-$) were unequally distributed between segments (p=0.001, one-way ANOVA). The majority (82.8%) of virus-labelled dI6 cells were located within the L4 and L5 segments, suggesting premotor dI6 interneurons are located in close proximity to their target motorneurons. Consistent with prior investigation of the $DMRT3^+$ dI6 cells (Andersson et al., 2012), the PRV^+ dI6 interneurons we observed were located bilaterally, albeit asymmetrically. Following TA injection, 75.9% of the GFP^+ dI6 cells were located within the spinal hemicord ipsilateral to the virus-injected limb (22/29), with considerably fewer contralateral cells (7/29). Analysis of the L4-L5 segments which contain most of the virus filled dI6 cells indicated significantly more PRV^+ dI6 cells are located ipsilaterally ($p<0.005$, *t*-test). Our findings suggest ankle flexor-related premotor dI6 interneurons are located within a few segments of their target motorneuron, predominantly, but not exclusively within the ipsilateral spinal cord.

An additional 3 spinal cords were collected 48 h after PRV-152 injection into the TA muscle and examined for disynaptic connections between dI6 interneurons and flexor motorneurons. PRV^+ dI6 interneurons were located in all lumbar levels examined, with no significant difference between segments (p=0.34, one-way ANOVA). In contrast to results from 38 h post-injection, equal numbers of GFP^+ dI6 interneurons were situated on either side of the midline (21/42 ipsilateral, 21/42 contralateral). The most striking difference between the two time points is the number of GFP^+ dI6 cells in the rostral lumbar segments. At 38 h, only one virus-infected dI6 cell was found in the L1 and L2 segments. By 48 h, the number of virus-infected rostral

dI6 cells had increased significantly (p=0.01, *t*-test), constituting approximately half of all GFP^+ dI6 cells (20/42). Interestingly, there was no difference between the number of GFP^+ dI6 cells located on either side of the rostral lumbar segments (p=0.46, *t*-test). This leads us to conclude that rostrally located dI6 interneurons make monosynaptic contacts on last-order, premotor interneurons located in either side of the spinal cord of caudal lumbar segments.

Two spinal cords collected 38 h after GC injection met the inclusion criteria stated above. Comparable to results following TA injection, the distribution of GFP^+ dI6 cells was unequal across the lumbar enlargements (p<0.001, one-way ANOVA). The L4 and L5 segments contained 76% of the virus infected dI6 cells. In contrast to ankle flexor injection, roughly equal proportions of GFP^+ dI6 cells were located on either side of the spinal cord (11/25 ipsilateral, 14/25 contralateral). There was no statistical difference between the number of ipsilateral *versus* contralateral GFP^+ dI6 cells at any level examined. These results suggest that dI6 interneurons that synapse directly on ankle extensor motorneurons are bilaterally distributed within neighbouring segments.

To examine disynaptic input from dI6 cells onto extensor motorneurons, 5 spinal cords were collected 48 h after PRV-152 injection into the GC muscle. PRV-152 infected dI6 cells were found in all lumbar segments analyzed with no statistically significant difference in the number of GFP^+ dI6 cells between L1 – L5 (p=0.64, one-way ANOVA). Overall there was a non-significant tendency towards a higher proportion of the virus-labelled cells located within the contralateral spinal cord (16/50 ipsilateral, 34/50 contralateral, p=0.059, *t*-test). Significantly more PRV^+ dI6 interneurons were found in the L1 and L2 segments at 48 h than at 38 h (p<0.05, *t*-test). These virus-labelled cells were equally distributed across the midline (p=0.63, *t*-test). We thus

conclude that the manner of disynaptic connectivity from rostrally located dI6 interneurons to ankle motorneurons is similar between extensors and flexors.

A minority of dI6 interneurons are glycinergic.

A preliminary report has suggested that dI6 interneurons are inhibitory (Hendricks & Goulding, 2007). Recently, it was shown that DMRT3-expressing interneurons express the inhibitory marker v*iaat* but not the excitatory marker *vglut2* in the P11 mouse spinal cord, supporting an inhibitory phenotype of this specific subpopulation of dI6 cells (Andersson et al., 2012). As both glycine and GABA are transported into vesicles by VIAAT (Burger et al., 1991), these results do not conclusively define the neurotransmitter phenotype of the dI6 cells. Commissural interneurons in the ventral lumbar spinal cord, which we now conclude must include dI6 interneurons, utilize glutamate, glycine, GABA, or both glycine and GABA (Restrepo et al., 2009).

Therefore, to determine the precise neurotransmitter utilized by dI6 interneurons, spinal cord sections from the lumbar enlargement of 5 neonatal TgDbx1^{Cre};R26^{EFP};Dbx1^{LacZ} pups were incubated with an antibody which effectively labels glycinergic spinal interneurons (Coulon et al., 2011, Griener et al., 2015). Analysis revealed that only 19.5 ± 7.6% of ventrally located EFP^{+}/β-gal^{-} interneurons are immunopositive for glycine (Figure 5). Further analysis is required to determine whether dI6 cells are exclusively inhibitory but predominantly utilize GABA, or whether there is in fact, an excitatory subpopulation.

Locomotor activity of dI6 interneurons.

In the current study, during NMDA (5-10 μM) and 5-HT (10-15 μM) induced fictive locomotion, whole cell recordings were taken from 86 rhythmically active dI6 interneurons located in the intermediate nucleus of the lumbar enlargement. As

previous work has demonstrated that approximately 90% of all EFP^{+} interneurons located dorsal to the central canal lack β-gal expression and are therefore dI6 interneurons (Dyck et al., 2012), data were collected from isolated spinal cords of neonatal (P0-P3) $TgDbx1^{Cre};R26^{EFP};Dbx1^{LacZ}$ and $TgDbx1^{Cre};R26^{EFP}$ mice. Fictive locomotor activity was monitored via suction electrodes placed on the flexor related (i.e., L2 or L3) and/or extensor related (i.e., L5) ventral roots. Rhythmic activity of dI6 cells was compared to the phase of fictive locomotion recorded from the local ventral root (i.e., the ventral root originating from the hemisegment in which the neuron resided).

Deletions, defined as spontaneous omissions in ongoing locomotor activity, are classified as either resetting or non-resetting. The timing of the resumed locomotor activity is shifted (advanced or delayed) pursuant to a resetting deletion. In contrast, following a non-resetting deletion rhythmic activity resumes at the predicted time had the deletion not occurred. In order to explain the origin of non-resetting deletions, it has been suggested that the locomotor CPG consists of rhythm generating (RG) and pattern forming (PF) levels (Lafreniere-Roula & McCrea, 2005, McCrea & Rybak, 2008). In the isolated mouse spinal cord, analyzing cellular activity during non-resetting deletions that occur in the ipsilateral ventral root can distinguish between constituents of the RG and PF levels (Zhong et al., 2012, Griener et al., 2013). Neurons that continue to oscillate during a non-resetting deletion are considered to be members of the RG layer, while those that fall silent are thought to belong to the PF layer.

Of the 86 rhythmically active dI6 cells, non-resetting deletions in ipsilateral ENG activity occurred during recording from 28 neurons. The number of putative RG cells (Figure 6A), which continued to oscillate during a non-resetting deletion, was approximately equal to the number of putative PF cells (Figure 6B), which ceased rhythmic activity (13/28 pRG, 15/28 pPF). A non-resetting deletion was also observed

while recording from one additional dI6 cell located contralaterally to the recorded ventral root. While it displayed firing behaviour suggestive of pPF nature, it was excluded from analysis as it has been shown that deletions do not necessarily occur bilaterally and thus the role of this cell is difficult to interpret (Zhong et al., 2012). Initial analysis indicated that rhythmically active dI6 interneurons with firing activity consistent with pPF cells were significantly larger than putative pRG dI6 cells (mean R_{mPF} = 644 ± 276 MΩ, mean R_{mRG} = 978 ± 467 MΩ, $p<0.05$, *t*-test). In response to an applied slow voltage ramp, persistent inward currents (PICs) were recorded from both pPF and pRG dI6 interneurons (Figure 6 F.i. & G.i.). Furthermore, each population contained many dI6 cells which did not display a PIC (Figure F.ii. & G.ii.). Thus the two subpopulations of dI6 interneurons cannot be distinguished based solely on their PIC.

To examine the distribution of pRG and pPF populations, the relative mediolateral position of each cell was determined, as described previously (Griener et al., 2013). The position of each cell, measured using micropositioner coordinates during electrophysiological recording and normalized to the half-width of the spinal cord, is presented in the schematic in Figure 6C. Although putative RG and PF cells were recorded on both the left and right sides of the spinal cord, all pRG dI6 cells are presented on the left and all pPF on the right. Analysis revealed that pRG and pPF dI6 interneurons are differentially distributed along the mediolateral plane ($U<0.01$, one tailed Wilcoxon Rank-Sum test). Among the total dI6 population accessible for intracellular recording (i.e., those in lamina VII dorsal to the central canal), pPF dI6 cells were more frequently found laterally, whereas pRG dI6 cells showed no discernible distribution pattern.

All 86 rhythmically active dI6 cells showed a preferred phase of firing, with a bias towards cellular activity occurring in phase with activity of the local ventral root.

Of the rhythmically active dI6 cells located ipsilateral to the recorded ventral root, 63% (43/68) fired in phase and 37% (25/68) fired out of phase with ENG activity. An additional 18 rhythmically active dI6 cells found contralateral to the recorded ventral root were classified as firing either in phase (10/18) or out of phase (8/18) after their activity was normalized to the ipsilateral ventral root.

The preferred phase of firing was determined for all 28 dI6 cells classified as putatively RG or PF as described previously (Butt et al., 2002*b*). The pRG dI6 cells were equally likely to fire during the active or inactive phases of fictive locomotion (6/13 in phase, 7/13 out of phase, Figure 6D). Conversely, the majority of pPF dI6 cells were active in phase with locomotor ENG bursting in the local ventral root (12/15 in phase, 3/15 out of phase, Figure 6E). The *r* values, a measure of the strength of the correlation between the cell and the ventral root, were significantly higher for the pPF cells, indicating their rhythmic activity was much more closely related to motor output ($p<0.001$, *t*-test).

Anatomical Reconstruction.

Post hoc anatomical reconstruction was performed on electrophysiologically characterized dI6 cells in order to determine whether there is a relationship between the proposed function of a cell and its morphology. To that end, Neurobiotin and/or Lucifer yellow were included in the intracellular electrode solution during recording and Cy3-conjugated Streptavidin was used to visualize the filled cells in optically cleared spinal cords. Eight reconstructions were obtained from dI6 cells classified as pRG or pPF based on their behaviour during non-resetting deletions. Representative morphological reconstructions are presented in Figure 7. The segmental and mediolateral position of the soma along with all discernable processes are presented in the schematic in Figure 7.C. While pRF and pPF dI6 cells were recorded on either

side of the midline, for the purpose of clarity all pRG dI6 cells are represented on the left and all pPF dI6 cells on the right. A total of 3 reconstructions were obtained for pRG dI6 cells, all of which are located laterally. Five pPF reconstructions were obtained. Examination of the number of neurites leaving the cell body and trajectory of the identified axon revealed no discernible difference between the morphologies of the two subpopulations of dI6 cells. Generally, all reconstructed dI6 cells projected long axons along the medio-lateral axis of the spinal cord. These axons were more often, though not exclusively directed towards the lateral edge. The small number of recovered cells and the sampling bias towards laterally located cells prevents a definitive comparison between the two functionally defined populations. It appears that the location of a cell along the medio-lateral axis may be a better predictor of morphology than its proposed function.

4.5 Discussion

The dI6 population was first introduced as the early-born, Lbx1-expressing interneurons which arise immediately dorsal to the sulcus limitans (Gross et al., 2002). Since their initial identification, the absence of an exclusive molecular marker which encompasses the entire population has precluded their thorough characterization. Exiguous evidence offered the zinc finger gene Wt1 as a marker for dI6 cells (Hendricks & Goulding, 2007). The Wt1-expressing cells are inhibitory commissural interneurons born at the dorsal-ventral boundary between E11-12 that migrate ventro-medially to settle in lamina VIII. Recently, genetic screening of atypically gaited horses has implicated the DMRT3 gene in locomotion (Andersson et al., 2012). Investigation in the developing mouse spinal cord revealed DMRT3 expression in a subset of dI6 interneurons (Andersson et al., 2012). While the DMRT3^{+} interneurons are inhibitory, analysis in the embryo and neonate showed they project to both ipsi- and contralaterally located targets. This divergence from the dogmatic view of dI6 cells as

strictly commissural suggests there is a greater degree of heterogeneity within this population than was previously appreciated and thus a more thorough characterization is warranted.

Prior research from our laboratory utilized the TgDbx1^{Cre};R26^{EFP};Dbx1^{LacZ} mouse model to target dI6 interneurons in the postnatal animal for electrophysiological recording (Dyck et al., 2012). These experiments demonstrated that during drug-induced fictive locomotion a significant proportion dI6 cells are rhythmically active. It was proposed that rhythmically active dI6 cells could be divided into two distinct groups based on their intrinsic membrane properties and their relationship to locomotor-related ventral root output. One group, called loosely coupled (LC), displayed riluzole-sensitive persistent inward currents (PICs) and showed firing behaviour that while clearly rhythmic, deviated somewhat from ventral root ENG bursting. The second group, termed tightly coupled (TC), fired action potentials almost exclusively within their preferred locomotor phase and showed strictly linear membrane properties in response to an applied voltage ramp. Based on these differences, it was proposed that LC and TC dI6 cells served distinct functions in the locomotor CPG.

In the two-layer half-centre model, two main functions of the locomotor CPG are executed by distinct populations of spinal interneurons; cells of the rhythm generating (RG) layer induce the basic locomotor rhythm and bring about rhythmic activity in cells of the pattern forming (PF) layer which, in turn, are responsible for recruiting the individual motor pools at the correct time and to the appropriate degree (McCrea & Rybak, 2008). Based on their firing behaviour and electrophysiological properties, it was hypothesized that the LC and TC dI6 interneurons belonged to the rhythm generating and pattern forming layers, respectively (Dyck et al., 2012). The current studies were undertaken with two aims; 1) to provide a thorough characterization of the dI6 population using the TgDbx1^{Cre};R26^{EFP};Dbx1^{LacZ} mouse

model, and 2) to evaluate whether the physical characteristics of the dI6 cells support their involvement in either rhythm generation and/or pattern formation.

Distribution of dI6 interneurons.

For the first time we describe the distribution of the dI6 interneurons in the postnatal spinal cord, a time point at which cell migration is complete. We demonstrate that the majority of the dI6 interneurons along the rostro-caudal extent of the spinal cord are located ventrally in laminae VII and VIII. We also describe a novel population of dorsally situated dI6 interneurons which have not been described in previous studies examining DMRT3 or Wt1 expressing dI6 cells (Andersson et al., 2012, Hendricks & Goulding, 2007). The existence of this dorsal dI6 cluster indicates that the TgDbx1^{Cre};ROSA26^{EFP};Dbx1^{LacZ} mouse provides a superior model for investigating this elusive population as it captures dI6 cells which cannot be identified using other currently available molecular markers.

Our analysis of the relative distribution of dI6 interneurons along the length of the spinal cord revealed a greater density of dI6 cells in the cervical and thoracic segments than in the lumbar and sacral segments. This difference is likely attributed to the significant number of dI6 cells in dorsally located clusters which are only observed in more rostral segments. The location of these clusters in the lateral part of lamina V is suggestive of an involvement in pain processing. Further investigation into the function of these dorsal dI6 clusters is needed and may provide valuable insight into the cellular mechanisms of pain processing in the deep dorsal horn.

Synaptic inputs onto dI6 interneurons.

While a role for dI6 cells in pain processing is speculative, more conclusive evidence of the involvement of dI6 interneurons in sensory processing comes from our investigation of vGluT1 expression. Primary afferents from muscle mechanoreceptors are the sole source of vGluT1-immunoreactive terminals in the ventral spinal cord (Oliveira et al., 2003). Along the lumbar enlargement, dI6 interneurons situated lateral to the central canal displayed modest labelling for vGluT1. These interneurons were situated in a region corresponding to lamina VII (Sengul et al., 2012). In contrast to the strikingly dense innervation of clusters of $V0_D$ we have described previously (Griener et al., 2015), the relatively sparse input from proprioceptive afferents implies that the primary role of ventrally located dI6 interneurons is not sensory processing. Numerous studies have implicated interneurons located in lamina VII of the cat lumbar enlargement in reflex pathways (see Jankowska, 1992). Unfortunately, methodological limitations currently preclude our electrophysiological analysis of the functional significance of these sensory inputs onto ventral dI6 interneurons.

This study also provides the first evidence serotonergic input onto dI6 interneurons located in the ventral lumbar spinal cord. Serotonin modulates a plethora of functions in the mammalian spinal cord (reviewed in Schmidt & Jordan, 2000). Classically, investigations of the effects of 5-HT on locomotion have relied on measuring the network response to various pharmacological agents. The major drawback of such an approach is that the precise cellular targets of 5-HT cannot be readily distinguished. Intracellular recording from genetically labelled interneurons is beginning to disentangle the neuromodulatory effects of 5-HT on motorneurons from those on CPG interneurons. Recent investigation in adult mice has demonstrated the emergence of bistable membrane properties in V2a interneurons in the presence of 5-HT (Husch et al., 2015). The development of such an intrinsic property fundamentally alters the significance of synaptic drive to this subset of the V2a population and thus

alters functional integration of these cells within the locomotor CPG. Our demonstration that dI6 interneurons receive 5-HT innervation in the neonatal animal reveal them to be an additional target of serotonergic neuromodulation and warrants further investigation.

Projection pattern and synaptic targets of dI6 interneurons.

The overwhelming majority of dI6 cells to take up the dextran tracer applied at either the L2 or L4 segment are commissural interneurons (CINs). Previous description of the projection pattern of DMRT3^{+} dI6 interneurons in the E15.5 embryo indicated 22% of these cells are ipsilateral and only 39% are commissural (Andersson et al., 2015). The discrepancy between their reported proportion and our finding that 84% of dI6 cells are commissural is likely due to maturation of CINs during the final stages of embryonic development. Recently, detailed analysis of the developmental timeline of the axonal projections of the excitatory commissural V3 population revealed a progressive increase in commissural projections from E12.5 to P0 (Blacklaws et al., 2015). It stands to reason that a similar maturation occurs in the commissural dI6 population.

CINs in the ventro-medial spinal cord have been classified into four populations based on the direction of their axonal projections; axons of intrasegmental CINs (sCINs) are restricted to within 1.5 segments of their cell bodies, while three populations of intersegmental CINs project farther and are distinguished by ascending (*a*CINs), descending (*d*CINs), or bifurcating (*ad*CINs) axons (Eide et al., 1999, Stokke et al., 2002). The dI6 interneurons located in rostral lumbar segments that were labelled by dextran dye application to the L4 segment represent *d*CINS and/or *ad*CINs. Conversely, dextran labelled dI6 interneurons located in caudal lumbar segments following dye application to the L2 segment are *a*CINs and/or *ad*CINs. The equal

number of ipsilaterally located dextran labelled dI6 cells provides us with confidence that overall tracer uptake was consistent between the L2 *versus* L4 treatments. Therefore, since we found more tracer uptake into dI6 cells following application to the L4 segment, we conclude that within the lumbar enlargement dI6 cells are predominantly *d*CINS and/or *ad*CINs.

In light of our finding that nearly all retrogradely labelled dI6 cells are situated contralateral to the site of dextran application, the results of our viral synaptic tracing experiments are surprising. While 84% of the dextran-labelled dI6 cells are commissural, at 38 h after PRV-152 injection into the TA or GC muscles, respectively only 24% or 56% of the infected dI6 cells were located contralaterally to the injected limb. As this incubation period allows labelling of interneurons monosynaptically connected to motorneurons (Jovanovic et al., 2010), these results suggest that premotor dI6 interneurons are unique among the broader population of dI6 cells in that they are more likely to have ipsilateral targets. While it is possible that premotor dI6 interneurons are distinct from the general dI6 population, it cannot be excluded that premotor dI6 cells may also extend rostrally or caudally directed contralateral projections. Nevertheless, these results demonstrate that the dI6 interneurons are relatively unique among the genetically identified neuronal populations in that only the V3 (Zhang et al., 2008, Blacklaws et al., 2015) and $V0_C$ (Zagoraiou et al., 2009, Stepien et al., 2010, Coulon et al., 2011) populations have also been demonstrated to target motorneurons on either side of the spinal cord.

Premotor dI6 interneurons visualized 38 h after PRV-152 injection were nearly exclusively located within approximately 600μm (i.e., 1 segment) of their target motorneuron and as such can be considered segmental interneurons. Quinlan & Kiehn (2007) have proposed a dual-inhibitory system through which segmental CINs inhibit contralateral motorneurons. In this system inhibition occurs both directly and indirectly

via 1) inhibitory sCINs that form monosynaptic inhibitory contacts onto motorneurons, and 2) excitatory sCINs that synapse onto inhibitory premotor interneurons which are themselves located ipsilateral to the target motorneuron. Results from our synaptic tracing experiments suggest that dI6 interneurons may be involved in both pathways of this system. As premotor dI6 cells are found on both sides of the spinal cord some are therefore sCINs and since they are likely inhibitory, they could mediate the direct monosynaptic inhibition of contralateral motorneurons. Furthermore, the ipsilaterally located premotor dI6 cells may be the target inhibitory interneuron of the excitatory sCIN in the indirect pathway.

By 48 h post-injection PRV-152 labels neurons disynaptically connected to motorneurons (Jovanovic et al., 2010). In the upper lumbar segments, PRV-labelled dI6 interneurons were evenly distributed on either side of the midline following virus injection into the either TA or GC muscles. Again, this finding is in stark contrast to the predominantly commissural nature of the entire dI6 population demonstrated via dextran-labelling. It thus appears that dI6 interneurons located in rostral lumbar segments may project to last-order premotor interneurons located on either side of the spinal cord which are themselves, either ipsi- or contralaterally projecting. While the identity of these premotor targets cannot currently be ascertained, the absence of significant PRV-labelling in the rostral lumbar segments at 38 h post-injection leads us to believe they are likely to be segmentally restricted cells.

Interpretation of viral labelling in the L4 and L5 segments at this time point is problematic. First, this technique cannot differentiate premotor interneurons identified in the first wave of retrograde labelling from subsequently labelled disynaptically connected cells. As these caudal segments already contained many PRV-labelled dI6 interneurons at 38 h incubation, viral labelling cannot exclusively identify disynaptically connected dI6 cells. Second, prolonged exposure to PRV causes neurodegeneration,

elicits an inflammatory response, and allows spurious viral spread into nearby glial cells (Ugolini, 2010). In our experiments, by 48 h non-specific GFP-labelling within the ipsilateral spinal cord was frequently seen in the L4 and L5 segments which impaired accurate assessment of connections between spinal neurons. Results of our cell counts are presented for completeness, however interpretation must proceed with caution. To obviate these limitations, we restricted our analysis to the L1-L2 segments. Our data following 38 h incubation revealed that only 1 and 3 PRV^+ dI6 cells were located in these segments upon viral injection into the TA and GC muscles, respectively. Thus, counts of PRV^+ dI6 interneurons observed 48 h post-injection are unlikely to be significantly contaminated by premotor dI6 cells. Furthermore, the relative paucity of PRV in these rostral segments gives us confidence that this region was still free of viral-induced cellular deterioration (data not shown).

Neurotransmitter phenotype of dI6 interneurons.

The dI6 interneurons have long been speculated to be an inhibitory population (Lanuza et al., 2004, Goulding et al., 2006, Rabe et al., 2009). Data presented in the current study which show that only 19.5 ± 7.6% of ventrally located dI6 cells are glycinergic are surprising given the recent report that $DMRT3^+$ dI6 interneurons exclusively express the inhibitory marker *viaat* and not the excitatory marker *vglut2* in postnatal animals (Andersson et al., 2012). Several possibilities exist to explain this discrepancy. While *viaat* is used to identify inhibitory cells in the spinal cord, it is a vesicular transporter involved in the uptake of both GABA and glycine into synaptic vesicles and can therefore not differentiate between the two inhibitory transmitters (Burger et al., 1991). It is possible that the entire dI6 population is inhibitory but the majority of cells within the ventral horn utilize GABA, either alone or in conjunction with glycine. Prior analysis of the neurotransmitter phenotype of commissural interneurons in the lumbar spinal cord revealed a significant proportion of cells that

utilize GABA or glycine, and a small number of cells that utilize both (Restrepo et al., 2009).

Alternately, the existence of a previously undescribed subpopulation of excitatory dI6 interneurons cannot be excluded. Previous description of the inhibitory nature of the dI6 cells has relied on cells identified via DMRT3 and/or Wt1 (Andersson et al., 2013, Hendricks & Goulding, 2007, Goulding, 2006). As aforementioned, our TgDbx1^{Cre};R26^{EFP};Dbx1^{lacZ} mouse labels additional dI6 cells which are not captured by either alternate marker. It remains unclear what proportion of the total dI6 population is identified using either gene. The additional cells labelled in our transgenic model may not diversify in the same manner or display the same cellular characteristics as their DMRT3 and/or Wt1-expressing brethren. Differentiation of interneurons derived from a common progenitor domain into subpopulations characterized by distinct transcription factor profile corresponding to discrete neurotransmitter phenotype has been demonstrated for the V0 (Zagoraiou et al., 2009, Talpalar et al., 2013, Griener et al., 2015) and V2 populations (Peng et al., 2007) and thus cannot be discounted for the dI6 population.

Locomotor activity of dI6 interneurons.

Earlier work from our laboratory classified rhythmically active dI6 cells as loosely coupled (LC) or tightly coupled (TC) via their electrophysiological properties (Dyck et al., 2012). As the core of the locomotor CPG is postulated to be comprised of neurons whose intrinsic membrane properties support rhythm generation (see Brownstone & Wilson, 2008), LC dI6 cells were suggested to be involved in rhythm generation. As TC dI6 cells lacked these membrane properties, they were suggested to be involved in pattern formation (Dyck et al., 2012). The classification approach used in the current study differs from that used in the earlier work, instead identifying

putative rhythm generating (pRG) and putative pattern forming (pPF) dI6 cells according to their behaviour during non-resetting deletions. Several lines of reasoning prompted the adoption of new a classification approach. First, none of the proposed electrophysiological characteristics are exclusive to rhythm-generating cells, notably the presence of a riluzole-sensitive PIC. Second, these intrinsic membrane properties are not immutable and may be present under some experimental conditions but not others. Additionally, they may change during development. For instance, the bistability reported in V2a interneurons was not observed in until adulthood (Husch et al., 2015). As the current approach compares the behaviour of a cell to the ongoing activity of the locomotor CPG as a whole, we feel it provides a superior classification system.

In the current study, 28 dI6 interneurons were classified as either pRG or pPF based on either sustained or absent rhythmic activity during a non-resetting deletion of local ventral root ENG activity. We found approximately equal proportion of pPF and pRG cells, providing further support for the involvement of dI6 interneurons in diverse aspects locomotor network function. Analysis of the distribution of pRG and pPF dI6 interneurons along the medio-lateral plane of the spinal cord indicated that pPF cells were more likely to be located laterally. The pPF dI6 cells were also found to be significantly larger than the pRG cells. Both of these findings are in accordance with prior reports that the proposed pattern forming TC dI6 interneurons are larger and located farther from the midline than their LC counterparts (Dyck et al., 2012). Furthermore, in the previous publication, non-resetting deletions were observed while recording from 4 TC dI6 interneurons (Dyck et al., 2012). It is worth noting that all four TC dI6 cells were located contralateral to the recorded ventral root and would therefore have been excluded from the present study, but nevertheless the behaviour of the dI6 cells were all consistent with a role in pattern formation. We therefore

examined whether pPF and pRG dI6 interneurons could also be differentiated based on the presence or absence of a persistent inward current (PIC) in response to an applied voltage ramp, as this was the primary characteristic used to distinguish TC from LC. PICs were recorded from both pPF and pRG dI6 interneurons, and each subpopulation contained cells which lacked a PIC. Therefore the two classification systems are not directly equivalent.

All rhythmically active dI6 cells displayed a preferred phase of firing which, once normalized to the ipsilateral L2 ventral root, most often occurred in phase with ENG output, consistent with earlier reports from our laboratory (Dyck et al., 2012). Consistent with our demonstration that many dI6 cells are *d*CINs, our current finding that 62% of the 86 rhythmic dI6 interneurons fire in phase with their local ventral root is remarkably similar to 64% previously reported from rhythmically active *d*CINS of unknown ontogeny (Butt et al., 2002*b*). As the examination of the strictly anatomically identified *d*CINs was able to target deep ventral interneurons (i.e., in lamina VIII), it seems plausible that our sampling of rhythmically active dI6 interneurons in lamina VII dorsal to the central canal may be representative of the entire ventromedially distributed population. While electrophysiological characterization of dI6 interneurons in lamina VIII is warranted, it is beyond the limitations of our current transgenic mouse model. Future experiments recording from Wt1 and/or DMRT3-expressing dI6 interneurons may prove fruitful.

The difference between the preferred firing phase of pPF and pRG dI6 interneurons is interesting in light of their proposed functions within the locomotor CPG. Motorneurons are the proposed synaptic targets of members of the pattern forming layer, whereas rhythm generating interneurons are not premotor, but instead target other CPG interneurons (see Brownstone & Wilson, 2008, Brownstone & Bui, 2010). As the spinal target of rhythm generating cells cannot be ascertained, it is

unsurprising that pRG dI6 cells are equally likely to be active during either locomotor phase. The bias of pPF dI6 interneurons towards firing in phase with their local ventral root is, however, interesting. Though admittedly we cannot identify the target of pPF dI6 cells, it is surprising that this purportedly inhibitory population fires predominantly during the active locomotor phase. The results from our trans-synaptic tracing indicate that premotor dI6 interneurons (which theoretically may be members of the pattern forming layer) are found primarily ipsilateral to their target motorneuron, within adjacent spinal segments, thus it seems unlikely that pPF dI6 cells inhibit contralateral or antagonist motor pools. Although the dominant output of the L2 root is flexor-related, the L2 segment contains motorneurons of both flexors and extensors (Cowley & Schmidt, 1994*b*), thus pPF dI6 cells in the L2 segment may target ipsilateral local extensor motorneurons. However, we failed to demonstrate preferential targeting of extensor *versus* flexor motorneurons by premotor dI6 interneurons. Therefore, the most parsimonious explanation is that some pPF dI6 interneurons are, in fact, excitatory. As aforementioned, the dI6 interneurons have dogmatically been viewed as inhibitory, however the results of our electrophysiological analysis demonstrate that more thorough examination of their neurotransmitter phenotype is necessary.

Anatomical reconstruction of pRG and pPF dI6 interneurons.

The results of our anatomical reconstruction revealed no difference between the cellular morphology of the pRG and pPF dI6 cells. Previous examination of unidentified rhythmically active lumbar interneurons indicated PRG cells were clustered medially and extended short axons medially or caudally, presumably towards nearby CPG interneurons (Griener et al., 2013). PPF interneurons, in contrast, were generally located at a greater distance from the midline and tended to extend a long axon laterally. Unfortunately, in the present experiments we were only able to reconstruct a very small number of pRG dI6 cells, all of which happened to be laterally located.

These cells, as well as the laterally located pPF dI6 cells, displayed a generally similar morphology to that which has previously been published for lateral PPF cells (Griener et al., 2013). While further analysis of medially located dI6 cells is definitely required, it currently appears that within the dI6 population the location of a cell along the medio-lateral plane is a better predictor of morphology than the proposed locomotor function.

Conclusion.

Recently, the dogmatic view that individual genetically-defined populations execute distinct functions was impugned by the demonstration that reciprocal inhibition of antagonist motorneurons requires Ia inhibitory interneuron derived from both the V1 and the V2b populations (Zhang et al., 2014). It therefore seems likely that the execution of additional spinal functions will involve neurons born from several genetic populations. Isolated genetic ablation or silencing of each of the ventrally derived cardinal interneuron populations, as well as combined ablation of the V1 and V2b populations, have all failed to abolish locomotor rhythm generation (Lanuza et al., 2004, Gosgnach et al., 2006, Crone et al., 2008, Zhang et al., 2008, Dougherty et al., 2013, Zhang et al., 2014). This resiliency strongly argues that the neural network that elicits the basic locomotor rhythm is comprised of interneurons derived from multiple embryonic populations. Likewise, interneurons involved in pattern formation and motorneuron recruitment undoubtedly derive from numerous embryonic sources. Each of the dI3, V0, V1, V2a, V2b, and V3 populations include last-order premotor interneurons (Bui et al., 2013, Al-Mosawie et al., 2007, Zagoraiou et al., 2009, Zhang et al., 2008, Zhang et al., 2014). Presently, we have demonstrated that the dI6 population display the physical cellular characteristics and firing behaviour which support their role in both locomotor rhythm generation and pattern formation.

4.6 References

Al-Mosawie A, Wilson JM, Brownstone RM. (2007) Heterogeneity of V2-derived interneurons in the adult mouse spinal cord. Eur J Neurosci. 26:3003-15.

Andersson LS, Larhammar M, Memic F, Wootz H, Schwochow D, Rubin, CJ, Patra K, Arnason T, Wellbring L, Hjalm G, Imsland F, Petersen JL, McCue ME, Mickelson JR, Cothran G, Ahituv N, Roepstorff L, Mikko S, Vallstedt A, Lindgren G, Andersson, Kullander K. (2012) Mutations in DMRT3 affect locomotion in horses and spinal circuit function in mice. Nature. 488:642-46.

Blacklaws J, Deska-Gauthier D, Jones CT, Petracca YL, Liu M, Zhang H, Fawcett JP, Glover JC, Lanuza GM, Zhang Y. (2015) Sim1 is required for the migration and axonal projections of V3 interneurons in the developing mouse spinal cord. Dev Neurobiol. 75:1003-17.

Brownstone RM, Bui TV. (2010) Spinal interneurons providing input to the final common path during locomotion. Prog Brain Res. 187:81-95.

Brownstone R, Wilson J. (2008) Strategies for delineating spinal locomotor rhythm-generating networks and the possible role of Hb9 interneurones in rhythmogenesis. Brain Res. Rev. 57:64-76.

Bui TV, Akay T, Loubani O, Hnasko TS, Jessell TM, Brownstone RM. (2013) Circuits for grasping: spinal dI3 interneurons mediate cutaneous control of motor behavior. Neuron. 78:191-204.

Burger PM, Hell J, Mehl E, Krasel C, Lottspeich F, Jahn R. (1991) GABA and glycine in synaptic vesicles: storage and transport characteristics. Neuron. 7:287-93.

Butt SJ, Lebret JM, Kiehn O. (2002*a*). Organization of left-right coordination in the mammalian locomotor network. Brain Res Rev. 40:107-17.

Butt SJ, Harris-Warrick RM, Kiehn O. (2002*b*). Firing properties of identified interneuron populations in the mammalian hindlimb central pattern generator. J Neurosci. 22:9961-71.

Cazalets JR, Sqalli-Houssaini Y, Clarac F. (1992) Activation of the central pattern generators for locomotion by serotonin and excitatory amino acids in neonatal rat. J Physiol. 455:187-204.

Coulon P, Bras H, Vinay L. 2011. Characterization of last-order premotor interneurons by transneuronal tracing with rabies virus in the neonatal mouse spinal cord. J Comp Neurol. 519:3470-3487.

Cowley KC, Schmidt BJ. (1994*a*) A comparison of motor patterns induced by N-methyl-D-aspartate, acetylcholine and serotonin in the in vitro neonatal rat spinal cord. Neurosci Lett. 171:147-50.

Cowley KC, Schmidt BJ. (1994*b*) Some limitations of ventral root recordings for monitoring locomotion in the in vitro neonatal rat spinal cord preparation. Neurosci Lett. 171:142-6.

Cowley KC, Schmidt BJ. (1997) Regional distribution of the locomotor pattern-generating network in the neonatal rat spinal cord. J Neurophysiol. 77: 247–259.

Drew T, Doucet S. (1991). Application of circular statistics to the study of neuronal discharge during locomotion. J Neurosci Methods. 38:171-181.

Dougherty KJ, Zagoraiou L, Satoh D, Rozani I, Doobar S, Arber S, Jessell TM, Kiehn O. (2013) Locomotor rhythm generation linked to the output of spinal shox2 excitatory interneurons. Neuron. 80:920-33.

Dyck J, Gosgnach, S (2009) Whole cell recordings from visualized neurons in the inner laminae of the functionally intact spinal cord. J Neurophys. 102:590-597.

Dyck J, Lanuza GM, Gosgnach S. (2012) Functional characterization of dI6 interneurons in the neonatal mouse spinal cord. J Neurophysiol. 107:3256-3266

Eide AL, Glover J, Kjaerulff O, Kiehn O. (1999). Characterization of commissural interneurons in the lumbar region of the neonatal rat spinal cord. J Comp Neurol. 403:332-45.

Endo T, Kiehn O. (2008) Asymmetric operation of the locomotor central pattern generator in the neonatal mouse spinal cord. J Neurophysiol. 100:3043-54.

Gosgnach S, Lanuza GM, Butt SJ, Saueressig H, Zhang Y, Velasquez T, Riethmacher D, Callaway EM, Kiehn O, Goulding M. (2006) V1 spinal neurons regulate the speed of vertebrate locomotor outputs. Nature. 440:215–19.

Goulding, M (2009) Circuits controlling vertebrate locomotion: moving in a new direction. Nat. Rev. Neurosci. 10:507-518.

Griener A, Dyck J, Gosgnach S. (2013) Regional distribution of putative rhythm-generating and pattern-forming components of the mammalian locomotor CPG. Neurosci. 10:644-50.

Griener A, Zhang W, Kao H, Wagner C, Gosgnach S. (2015) Probing diversity within subpopulations of locomotor-related V0 interneurons. Dev Neurobiol. 75:1189-203.

Gross MK, Dottori M, Goulding M. (2002) Lbx1 specified somatosensory association interneurons in the dorsal spinal cord. Neuron. 34:535-49.

Hendricks, TJ, Goulding MD. (2007) Program No. 132.11/E3. 2007 Neuroscience Meeting Planner. San Diego, CA: Society for Neuroscience, 2007. Online.

Hochman S, Schmidt BJ. (1998) Whole cell recordings of lumbar motoneurons during locomotor-like activity in the in vitro neonatal rat spinal cord. J Neurophysiol. 79:743-52.

Husch A, Dietz SB, Hong DN, Harris-Warrick RM. (2015) Adult spinal V2a interneurons show increased excitability and serotonin-dependent bistability. J Neurophysiol. 113:1124-34.

Jan YN, Jan LY. (2010) Branching out: mechanisms of dendritic arborization. Nat Rev Neurosci. 11:316-328.

Jankowska E. (1992) Interneuronal relay in spinal pathways from proprioreceptors. Prog Neurobiol. 38:355-78.

Jovanovic K, Pastor AM, O'Donovan MJ. (2010) The use of PRV-Bartha to define premotor inputs to lumbar motoneurons in the neonatal spinal cord of the mouse. PLoS One. 5:e11743.

Kerman, I. A., Enquist, L.W., Watson, S.J. & Yates, B.J. 2003. Brainstem substrates of sympatho-motor circuitry identified using trans-synaptic tracing with pseudorabies virus recombinants. J. Neurosci. 23, 4657-4666.

Kjaerulff O, Kiehn O. (1996) Distribution of networks generating and coordinating locomotor activity in the neonatal rat spinal cord in vitro: a lesion study. J. Neurosci. 16:5777–5794.

Kjaerulff O, Kiehn O. (1998) Distribution of networks generating and coordinating locomotor activity in the neonatal rat spinal cord in vitro: a lesion study. J Neurosci: 16:5777-94.

Kriellaars DJ, Brownstone RM, Noga BR, Jordan LM. (1994). Mechanical entrainment of fictive locomotion in the decerebrate cat. J Neurophysiol. 71:2074-2086.

Lafreniere-Roula, M, McCrea, DA (2005) Deletions of rhythmic motoneuron activity during fictive locomotion and scratch provide clues to the organization of the mammalian central pattern generator. J. Neurophysiol. 94:1120–1132.

Lanuza GM, Gosgnach S, Pierani A, Jessell TM, Goulding M (2004). Genetic identification of spinal interneurons that coordinate left-right locomotor activity necessary for walking movements. Neuron 42:375–386.

Longair MH, Baker DA, Armstrong JD. (2011) Simple Neurite Tracer: open source software for reconstruction, visualization and analysis of neuronal processes. Bioinformatics. 27:2453-2454.

McCrea DA, Rybak IA. (2008) Organization of mammalian locomotor rhythm and pattern generation. Brain Res Rev. 57:134-146.

Oliveira AL, Hydling F, Olsson E, Shi T, Edwards RH, Fujiyama F, Kaneko T, Hökfelt T, Cullheim S, Meister B. (2003) Cellular localization of three vesicular glutamate transporter mRNAs and proteins in rat spinal cord and dorsal root ganglia. Synapse. 50:117-29.

Peng CY, Yajima H, Burns CE, Zon LI, Sisodia SS, Pfaff SL, Sharma K. (2007) Notch and MAML signaling drives Scl-dependent interneuron diversity in the spinal cord. Neuron. 53:813-27.

Pierani A, Moran-Rivard L, Sunshine MJ, Littman DR, Goulding M, Jessell TM. (2001). Control of interneuron fate in the developing spinal cord by the progenitor domain homeodomain protein Dbx1. Neuron. 29: 367-84.

Quinlan KA, Kiehn O. (2007) Segmental, synaptic actions of commissural interneurons in the mouse spinal cord. J Neurosci. 27:6521-30.

Rabe N, Gezelius H, Vallstedt A, Memic F, Kullander K. (2009) Netrin-1-dependent spinal interneuron subtypes are required for the formation of left-right alternating locomotor circuitry. J Neurosci. 29:15642-9.

Restrepo CE, Lundfald L, Szabó G, Erdélyi F, Zeilhofer HU, Glover JC, Kiehn O. (2009) Transmitter-phenotypes of commissural interneurons in the lumbar spinal cord of newborn mice. J Comp Neurol. 517:177-92.

Schmidt BJ, Jordan LM. (2000) The role of serotonin in reflex modulation and locomotor rhythm production in the mammalian spinal cord. Brain Res Bull. 53:689-710.

Sengul G, Puchalski RB, Watson C. (2012) Cytoarchitecture of the spinal cord of the postnatal (P4) mouse. Anat Rec (Hoboken). 295: 837-45.

Stepien AE, Tripodi M, Arber S. (2010) Monosynaptic rabies virus reveals premotor network organization and synaptic specificity of cholinergic partition cells. Neuron. 68:456-472.

Stokke MF, Nissen UV, Glover JC, Kiehn O. (2002) Projection patterns of commissural interneurons in the lumbar spinal cord of the neonatal rat. J Comp Neurol. 446:349-59.

Talpalar AE, Bouvier J, Borgius L, Fortin G, Pierani A, Kiehn O. (2013) Dual-mode operation of neuronal networks involved in left-right alternation. Nature. 500:85-88.

Ugolini G. (2010) Advances in viral transneuronal tracing. J Neurosci Methods. 194:2-20.

Zagoraiou L, Akay T, Martin JF, Brownstone RM, Jessell TM, Miles GB. (2009) A cluster of cholinergic premotor interneurons modulates mouse locomotor activity. Neuron. 64:645-62.

Zar JH. Circular distribution. In: *Biostatistical Analysis.* Englewood Cliffs, NJ: Prentice Hall, 1974, p. 310-27.

Zhang J, Lanuza GM, Britz O, Wang Z, Siembab VC, Zhang Y, Velasquez T, Alvarez FJ, Frank E, Goulding M. (2014) V1 and v2b interneurons secure the alternating flexor-extensor motor activity mice require for limbed locomotion. Neuron. 82:138-50.

Zhang Y, Narayan S, Geiman E, Lanuza GM, Velasquez T, Shanks B, Akay T, Dyck J, Pearson K, Gosgnach S, Fan CM, Goulding M. (2008) V3 spinal neurons establish a robust and balanced locomotor rhythm during walking. Neuron. 60:84-96.

Zhong G, Shevtsova NA, Rybak IA, Harris-Warrick RM. (2012) Neuronal activity in the isolated mouse spinal cord during spontaneous deletions in fictive locomotion:

insights into locomotor central pattern generator organization. J Physiol. 590:4735-4759.

Table 4.1. Distribution of dI6 interneurons in the TgDbx1^{Cre}; R26^{EFP}; Dbx1^{lacZ} neonatal mouse spinal cord

Spinal Cord Segment	*n*	$\bar{x}$ dI6 cells ± SD	Area ± SD (mm^2)
Cervical	2	92.8 ± 16.6*	0.635 ± 0.07*
Thoracic	2	95.3 ± 14.0	0.833 ± 0.05
T12	5	60.4 ± 11.02	0.795 ± 0.10
L1	6	60.3 ± 6.7	0.884 ± 0.06
L2	6	61.8 ± 9.1	0.982 ± 0.07
L3	6	62.4 ± 7.7	0.984 ± 0.09
L4	5	63.6 ± 7.7	0.984 ± 0.11
L5	6	64.6 ± 8.7	0.816 ± 0.10
Sacral	2	45.3 ± 5.7	0.582 ± 0.03

*cell count and surface area measurement taken from spinal hemisegments

4.7 Figures

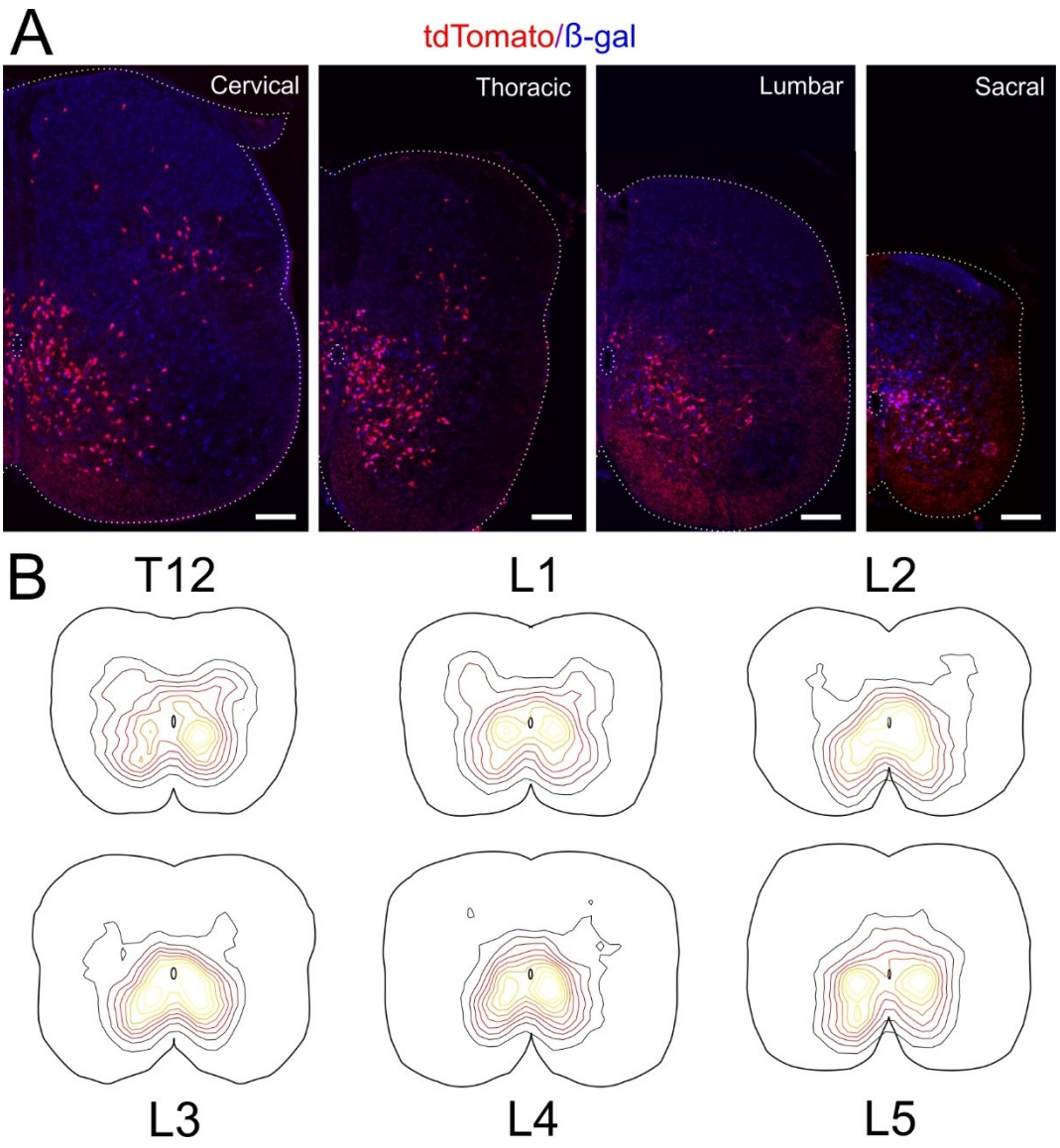

Figure 1. *Distribution of dI6 interneurons in the mouse spinal cord.* A. 20µm sections cut from P0 $Dbx1^{Cre}$;$R26^{EFP}$;$Dbx1^{lacZ}$ mouse spinal cords and labelled for β-gal (blue) and EFP (red). Three interneuronal populations are labelled: dI6 interneurons appear red (EFP^+/ $\beta\text{-gal}^-$), $V0_D$ cells appear magenta (EFP^+/ $\beta\text{-gal}^+$), and $V0_V$ cells appear blue (EFP^-/ $\beta\text{-gal}^+$). Representative cervical, thoracic, lumbar, and sacral half-sections show

the laminar distribution of dI6 interneurons along the rostro-caudal extent of the spinal cord. Scale bar 100 μm. B. Topographical maps representing the distribution of dI6 interneurons at each spinal segment from T12 to L5. Black contour represents lowest density. Yellow contour represents highest density.

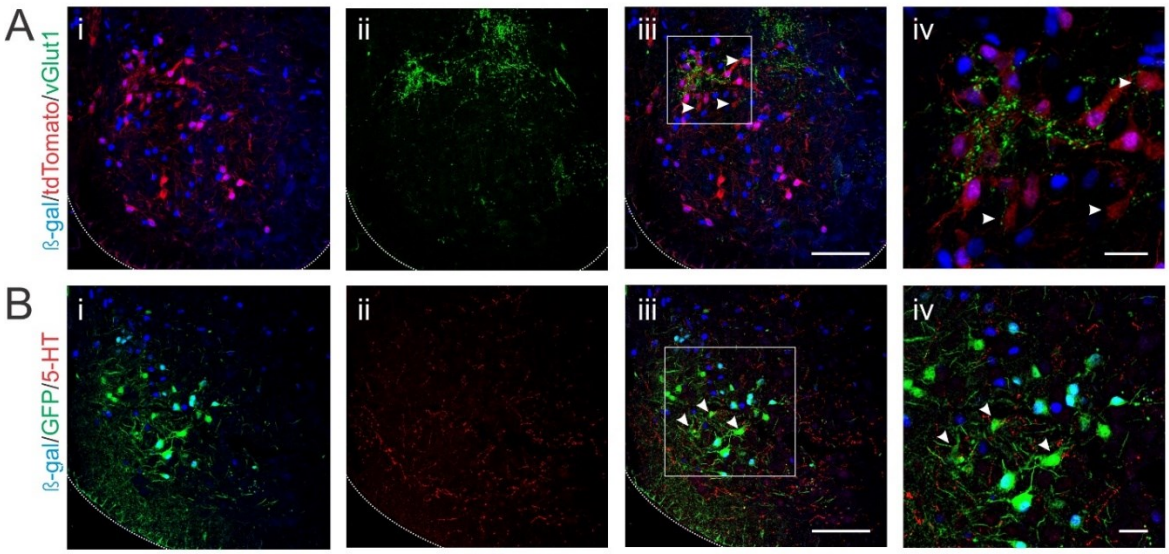

Figure 2. *dI6 interneurons receive primary afferent and descending serotonergic input.* A. 6μm ventral quarter sections cut from a P0 $Dbx1^{Cre}$;$R26^{tdTomato}$;$Dbx1^{lacZ}$ mouse spinal cord and labelled for β-gal (blue) and vGlut1 (green). In all sections, tdTomato (red) cells can be seen without an antibody. Midline is to the left, lateral edge is to the right. Dashed lines outline the ventral perimeter. A.i dI6 interneurons appear red ($tdTomato^+$/ $\beta\text{-}gal^-$), while $V0_D$ interneurons appear magenta ($tdTomato^+$/ $\beta\text{-}gal^+$). A.ii. Dense vGlut1 labelling is seen in the intermediate spinal cord, lateral to the central canal, with additional labelling ventrally and laterally, presumably in the motor nuclei. A.iii. vGlut1-immunoreactive terminals are seen in close apposition to dI6 interneurons in the intermediate spinal cord (white arrowheads). A.iv. Magnification of the boxed region in A.iii. Scale bar A.i-iii. 100 μm. Scale bar A.iv. 25 μm. B. 6μm ventral quarter sections cut from a P0 $Dbx1^{Cre}$;$R26^{EYFP}$;$Dbx1^{lacZ}$ mouse spinal cord and labelled for β-gal (blue), GFP (green), and 5-HT (red). B.i. dI6 interneurons appear green (GFP^+/ $\beta\text{-}gal^-$), while $V0_D$ appear turquoise (GFP^+/$\beta\text{-}gal^+$). B.iii. Serotonergic varicosities are found in close proximity to dI6 interneurons in the ventro-medial

lumbar spinal cord (white arrowheads). B.iv. Magnification of the boxed region in B.iii. Scale bar B.i-iii. 100 μm. Scale bar B.iv. 25 μm.

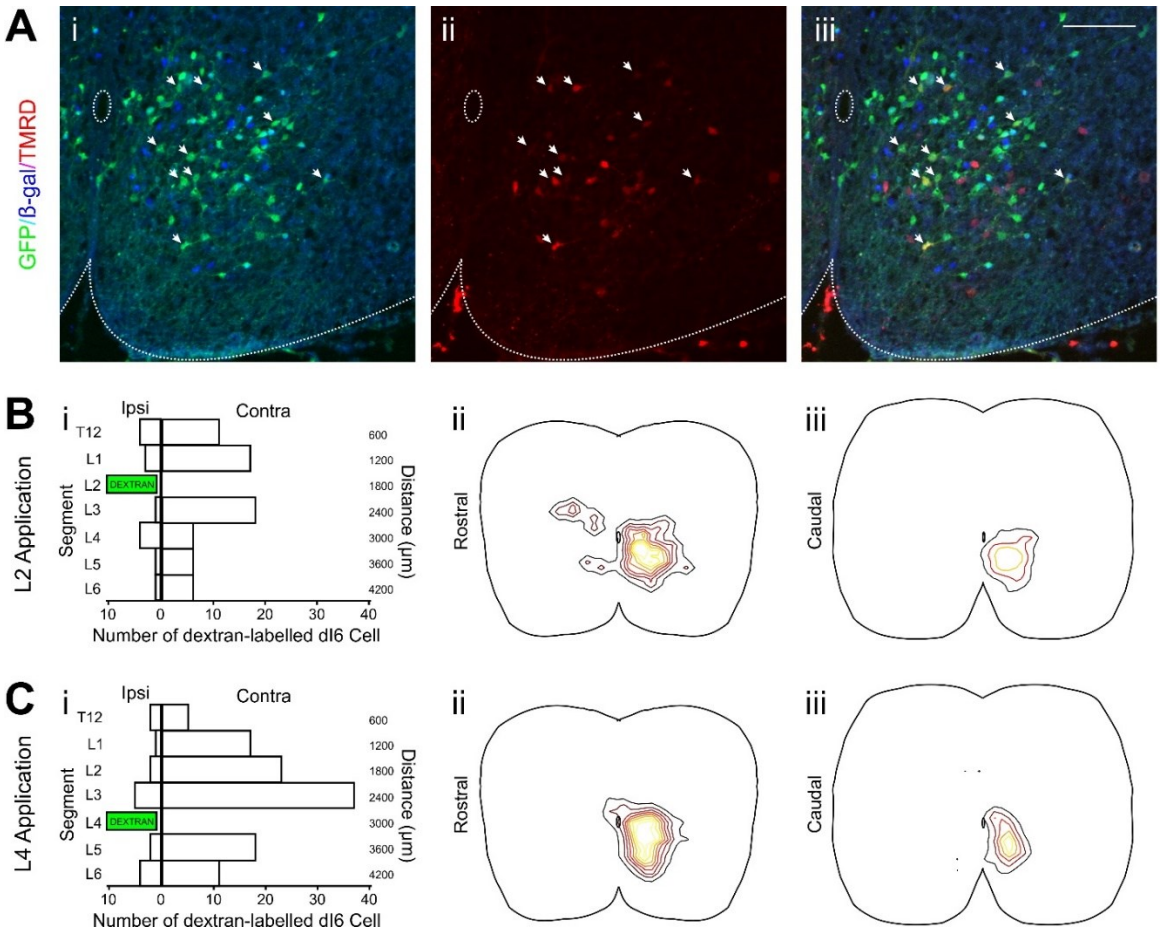

Figure 3. *The majority of dI6 interneurons are commissural.* A. Representative section from a spinal cord of a P0 $Dbx1^{Cre}$;$R26^{EFP}$;$Dbx1^{lacZ}$ mouse injected with TMRD at the L4 segment. A.i. Antibodies to EFP (green) and β-gal (blue) distinguish the dI6 cells (green; GFP^+/ $\beta\text{-gal}^-$) from the $V0_D$ (turquoise; $GFP^+/\beta\text{-gal}^+$). A.ii. TMRD-labelled cells (red) located rostral and contralateral to the injection site. A.iii. Composite image reveals TRMD-labelled dI6 interneurons (arrow heads). Scale bar 100 μm. B *and* C. Location of dextran labelled dI6 interneurons following unilateral dye application to the L2 (B) or L4 (C) segment. i. Bar graph of the total number of dextran labelled dI6 cells in each lumbar segment. ii. Topographical maps representing the distribution of dI6 interneurons rostral to the dye application at either the L2 (B.ii.) or L4 (C.ii.) segment. iii. Topographical maps showing the distribution of dI6 interneurons caudal to the dye

application at either the L2 (B.iii.) or L4 (C.iii.) segment. Black contour represents lowest density. Yellow contour represents highest density.

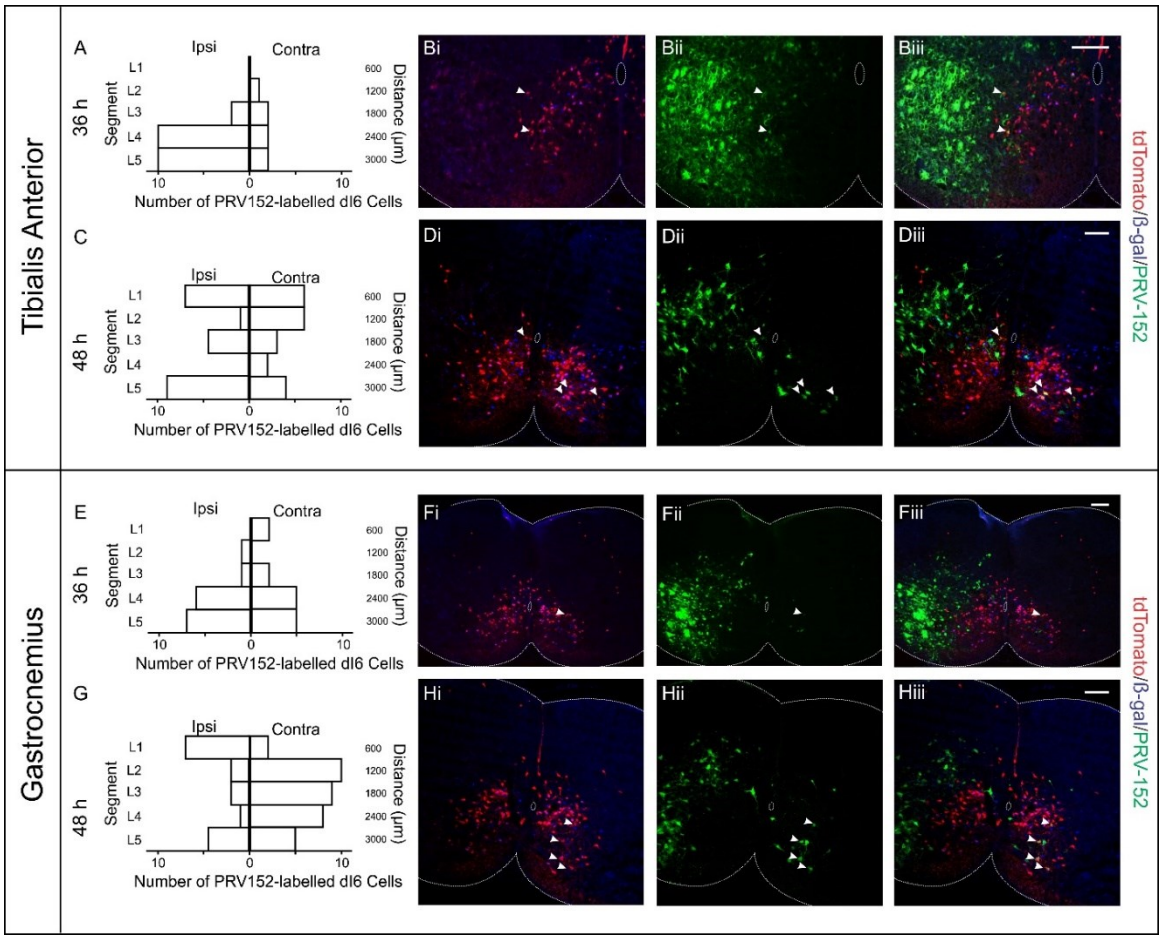

Figure 4. *dI6 interneurons form mono- and disynaptic contacts on flexor and extensor motorneurons bilaterally.* A–D. Synaptic tracing between dI6 interneurons and ankle flexor (tibialis anterior, TA) motorneurons. A and C. Bar graphs showing the number of dI6 interneurons labelled 36-38 h (A) or 48 h (C) after PRV-152 injection counted in each of the lumbar segments (L1 to L5) both ipsi- and contralaterally. B and D. 20 µm transverse sections cut from TgDbx1^{Cre}; R26^{EFP};Dbx1^{lacZ} mouse spinal cords harvested 38 h (B) or 48 h (D) after unilateral injection of PRV-152 into the TA muscle. Tissue was processed for β-gal (blue) and GFP (green), while tdTomato was visible without an antibody. The composite images (iii) reveal PRV-152 labelled dI6 interneurons (GFP^{+}/tdTomato^{+}/β-gal^{-}) in both the ipsilateral and contralateral spinal cord (white arrowheads). Scale bar 100 µm. E–H. Synaptic tracing between dI6

interneurons and ankle extensor (gastrocnemius, GC), motorneurons. E and G. Bar graphs summarizing the segmental and bilateral distribution of PRV-152 infected dI6 interneurons counted 36-38 h (E) or 48 h (G) post-injection. F and H. 20 Transverse sections cut from TgDbx1^{Cre}; R26^{EFP};Dbx1^{lacZ} mouse spinal cords collected 38 h (F) or 48 h (H) after unilateral injection of PRV-152 into the GC muscle. Tissue was processed for β-gal (blue) and GFP (green), while tdTomato was visible without an antibody. The composite images (iii) reveal PRV-152 labelled dI6 interneurons (GFP^{+}/tdTomato^{+}/β-gal^{-}) in both the ipsilateral and contralateral spinal cord (white arrowheads). Scale bar 100 μm.

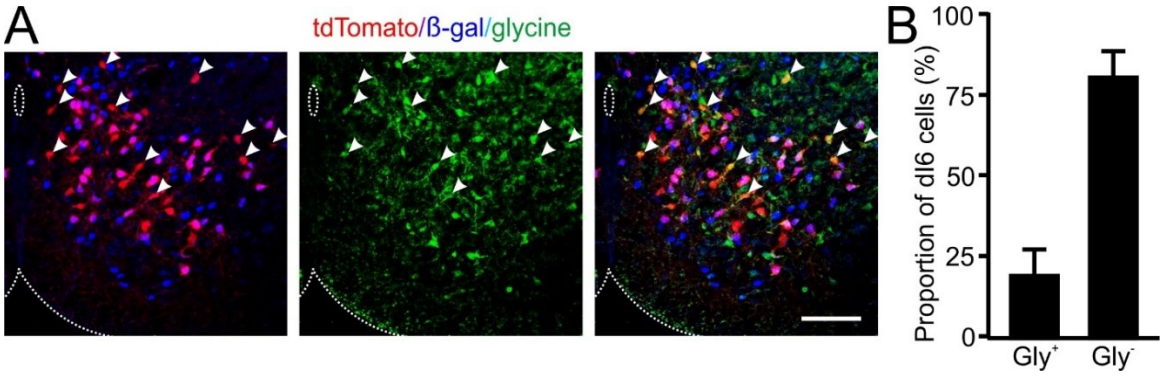

Figure 5. *A minority of dI6 interneurons are glycinergic.* A. View of the ventral quarter of a 20µm transverse section of a P0 $Dbx1^{Cre}$;$R26^{tdTomato}$;$Dbx1^{lacZ}$ mouse spinal cord. TdTomato (red) can be visualized without an antibody, and tissue was processed for β-gal (blue), and glycine (green). dI6 interneurons appear red ($tdTomato^{+}$/ $\beta\text{-}gal^{-}$). Antibody labelling of glycinergic cell bodies in the ventral spinal cord. White arrowheads indicate glycinergic dI6 interneurons. Dashed white lines delineated central canal and ventral edge. Scale bar 100 µm. B. Bar graph of the mean percentage of glycinergic dI6 interneurons in the ventral spinal cord.

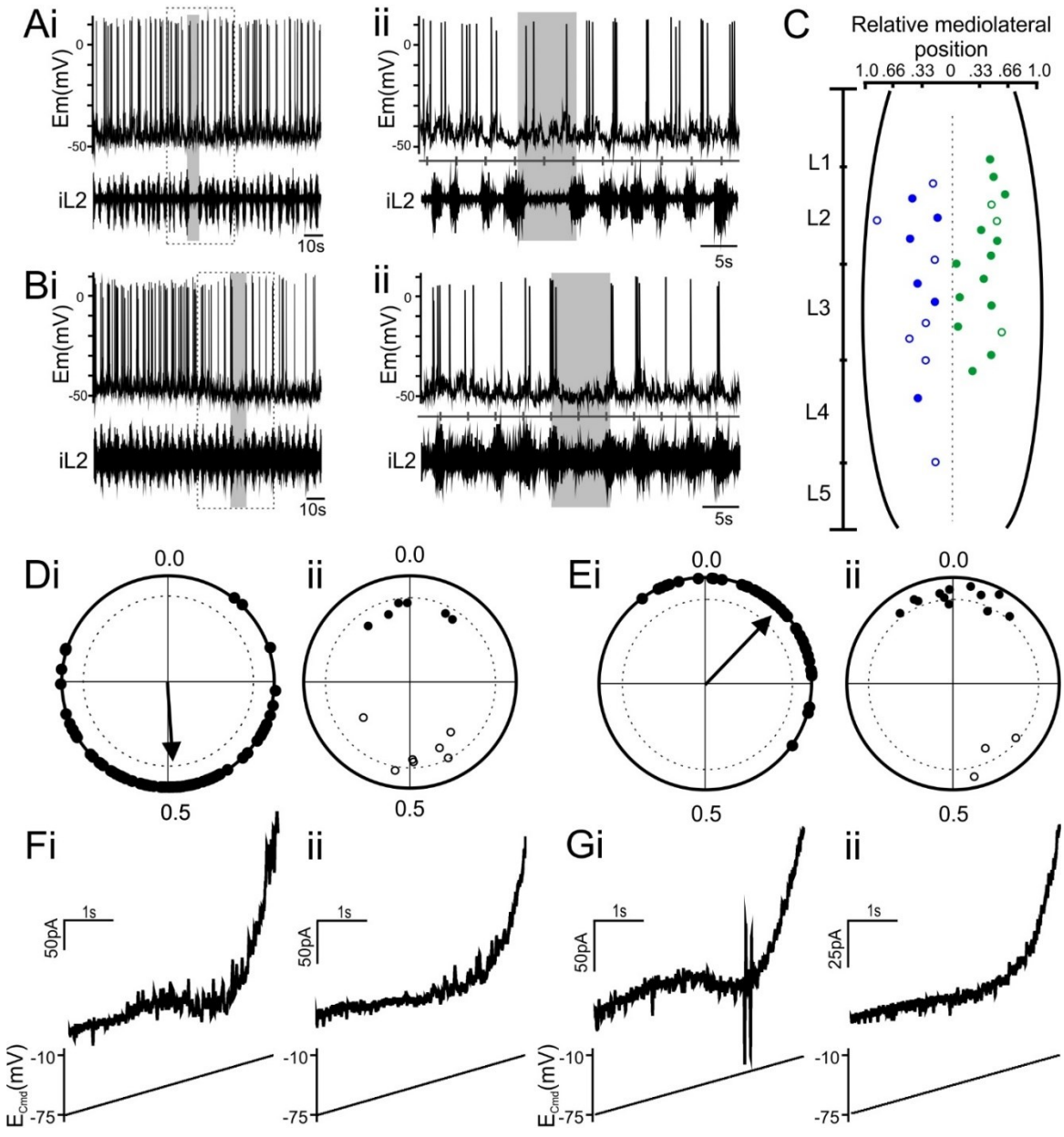

Figure 6. *Firing behaviour and location of putative RG and PF dI6 interneurons.* Panels A and B show typical intracellular recordings (top trace of each panel) from rhythmically active dI6 interneurons during which a non-resetting deletion (grey boxed region) was observed on the ipsilateral L2 ventral root (bottom trace of each panel). A. A putative rhythm generating (pRG) dI6 interneuron which fires out of phase with its local ventral root continues to oscillate during the non-resetting deletion (solid grey box).Dashed box in Ai shown in expanded timescale in A.ii. B. A putative pattern forming (pPF) dI6

interneuron fires in phase with its local ventral root and fails to fire during a non-resetting deletion (solid grey box). Dashed box in B.i. shown in expanded timescale in B.ii. C. Schematic of the neonatal mouse spinal cord showing the segmental and relative medio-lateral location of each dI6 interneuron classified as pRG or pPF. Recordings of each cell type were obtained from either side of the spinal cord, but all pRG cells are represented on the left (blue) and all pPF cells are on the right (green). Filled or hollow circles represent cells that fire in- or out of phase with their local ventral root, respectively. D.i. Polar plot for the pRG dI6 cell shown in A compares the onset of the ventral root burst with that of the cell. Points clustered about 0.5 indicate the cell fires out of phase. D.ii. Group polar plot of all pRG dI6 cells shows they fire either in phase or out of phase with ventral root activity. E.i. Polar plot for the pPF dI6 cell shown in B indicates it fires in phase with ventral root activity. E.ii. Group polar plot of all pPF dI6 cells demonstrates the majority of cells fire in phase with their local ventral root. F & G. Current responses to a slow voltage ramp (bottom trace) applied to either pRG (F) or pPF (G) dI6 interneurons show persistent inward currents (PICs) can be found in either subpopulation (F.i. & G.i.). A subset of cells in either subpopulation lack a PIC (F.ii. & G.ii.).

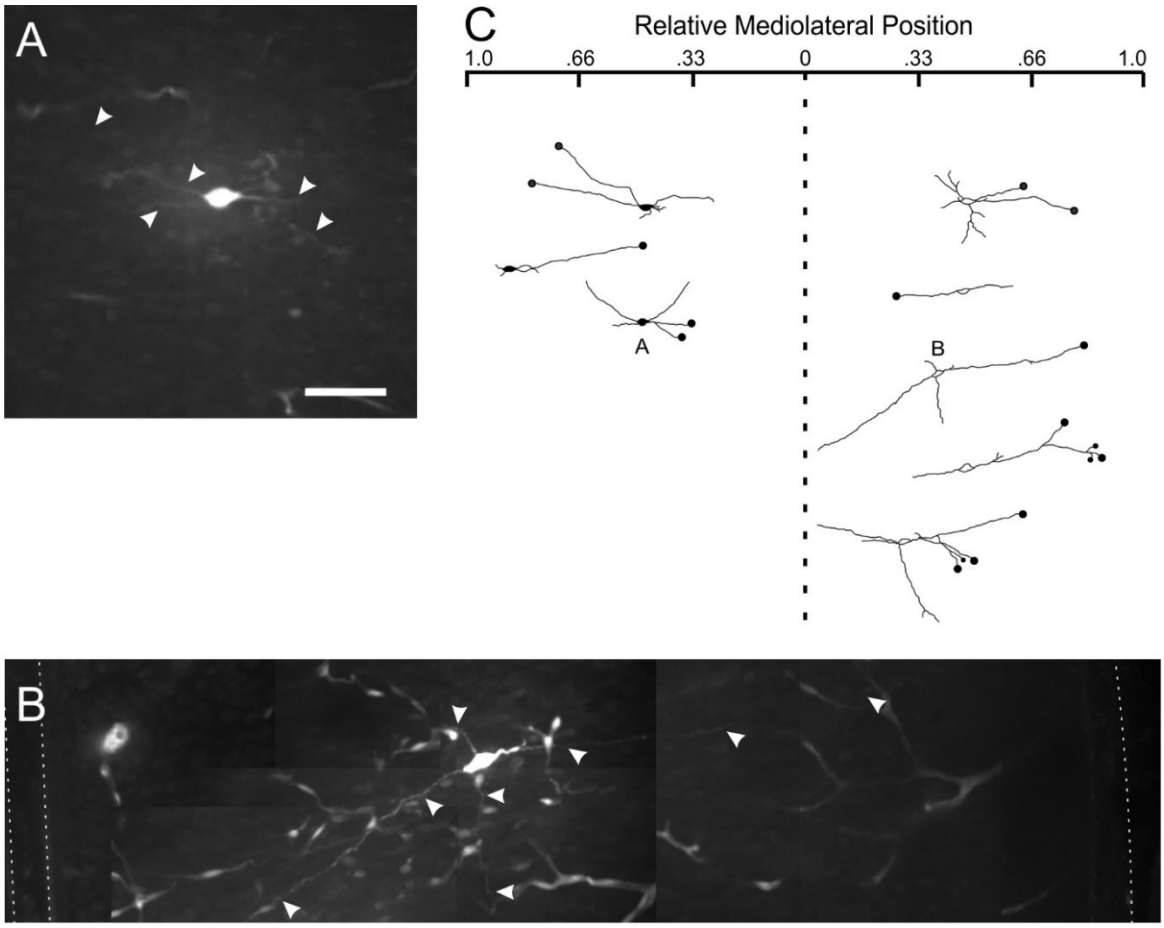

Figure 7. *Morphological reconstruction of pRG and pPF dI6 interneurons.* A-B. Reconstruction of Neurobiotin-filled dI6 interneurons classified as pRG (A) or pPF (B) during whole cell recording. Scale bars represent 50μm. Processes are indicated by white arrowheads. C. Schematic of neonatal mouse spinal cord displaying all pRG dI6 cells (black somas to the left of the midline) and pPF dI6 cells (white somas to the right) cells that were filled and reconstructed. Cells illustrated in panels A and B are identified. Axons are indicated by neurites terminating with black dot.

Chapter 5 – General Discussion

5.1 Summary

Work undertaken in this thesis addressed the general organizational principles that govern the interneurons of the locomotor CPG. Electrophysiological and morphological examination of rhythmically active unidentified interneurons in lamina VII provided evidence that cells contributing to rhythm generation are located in different areas of the spinal cord and have distinct projection patterns in comparison cells contributing to locomotor pattern formation. Experiments conducted in the neonatal TgDbx1^{Cre}:Rosa26EFP:Dbx1^{lacZ} mouse provided valuable insight into the anatomy and function of three distinct populations of ventrally-located interneurons, namely the V0$_V$, V0$_D$, and dI6. These experiments described the distribution of all three populations within the lumbar enlargement, as well as defined their upstream and downstream synaptic partners. Each of their roles in locomotor rhythm generation were analyzed using either electrophysiological or immunohistochemical approaches. Together, these experiments advanced our understanding of the architecture and operation of the locomotor CPG and pose additional questions that can direct future research.

5.2 Discussion & Future Directions

Our investigation into the laminar distribution of each of the three genetically labelled interneuron populations indicated all three are most densely distributed in the ventro-medial spinal cord, an area of particular significance to the locomotor CPG. Investigation of the distribution of dI6 interneurons revealed a previously undescribed population of dI6 cells which settle in the dorsal spinal cord, laterally in lamina V. Significantly, these cells have not been reported in studies on the DMRT3-expressing

dI6 cells (Andersson et al., 2012) or Wt1 expressing cells. Therefore, further studies into the function of these dorsally situated dI6 cells must be performed using the TgDbx1^{Cre}:Rosa26EFP:Dbx1^{lacZ} mouse model. Neurons situated in lamina V are implicated in pain processing, particularly with respect to nociceptive information conveyed via C and Aδ fibres (reviewed in Millan, 1999). Wide dynamic range neurons, found in abundance in lamina V, encode stimulus intensity from cutaneous, visceral, and muscle afferents and have been implicated in pain sensitization. Further study of the dI6 interneurons situated postnatally in lamina V may reveal the embryonic origin of this unique cell type and may provide an avenue into the investigation of pain processing within the spinal cord.

In addition to the novel implication of dI6 interneurons in the processing of sensory information, the existence of this dorsally situated cluster reveals that the TgDbx1^{Cre}:Rosa26EFP:Dbx1^{lacZ} mouse labels additional dI6 interneurons which have not been investigated in experiments from other laboratories which employed the DMRT3 or Wt1 molecular markers. Therefore, prior characterization of dI6 cells cannot be assumed to accurately represent the total population of dI6 cells, nor specifically those cells investigated here. As our additional dI6 cells do not express the same transcription factors, it is possible that they do not follow identical developmental paths as the DMRT3 and/or Wt1 expressing cells. While many of our findings concerning the commissural projections and bilaterally distributed premotor dI6 interneurons are consistent with those previously reported (Andersson et al., 2012), it remains to be seen whether novel subpopulations of dI6 cells are identified in the TgDbx1^{Cre}:Rosa26^{EFP}:Dbx1^{lacZ} mouse

Examination of the sensory input onto dI6 interneurons and V0 subpopulations revealed vGlut1-immunopositive terminals surrounding each. The most striking finding was the dense innervation of small clusters of V0$_D$ interneurons immediately lateral to

the central canal. Although examination of the functional significance of these synaptic contacts was beyond the scope of our examination, it seems likely that $V0_D$ interneurons are of particular importance in processing proprioceptive feedback during locomotor tasks. Currently, all available genetic knock-out models which target $V0_D$ interneurons result in perinatal death due to respiratory deficits, and as such experiments in the adult animal are unfeasible (Lanuza et al., 2004, Talpalar et al., 2013). While knock-out experiments must await the development of an improved transgenic model, further research into the sensory functions $V0_D$ cells can be envisioned through the use of activity dependent c-fos labelling in the $TgDbx1^{Cre}$: $R26^{EFP}$:$Dbx1^{lacZ}$ mouse. Unfortunately, the loss of β-gal and $ROSA26^{EFP}$ reporter expression by adulthood restricts identification of the dI6, $V0_D$, and $V0_V$ cell populations to young, functionally immature animals. Nevertheless, dorsal root stimulation in the intact isolated spinal cord preparation combined with c-fos labelling would reveal whether genetically-labelled cells increase action potential firing in response to sensory input in the newborn. The persistence of the two molecular markers until at least P7 (A. Griener, unpublished observation), a stage at which pups are able to support their own body weight (Andersson et al., 2012), would allow investigation of dI6, $V0_D$, and $V0_V$ cellular activity in response to loading of the limbs and to rudimentary locomotor tasks. The function of the densely innervated $V0_D$ clusters can potentially be characterized in the adult animal, as their anatomical uniqueness and exclusive cell type (i.e., no dI6 cells were observed) would allow their discrimination in the absence of the β-gal reporter. By adopting an alternate reporter line in which Cre-mediated EFP expression does not decline postnatally (Novak et al., 2000), c-fos labelling could be used to visualise the response of these clusters to diverse sensory stimuli. For instance, their involvement in spinal reflex pathways could be investigated by examining increased activity in response to dorsal root stimulation. Alternatively, to specifically address their role in sensory processing during locomotion, changes in c-

fos expression could be examined following weight-bearing overground walking in comparison to non-weight bearing tasks such as swimming, as has been performed recently for the V3 interneurons (Borowska et al., 2013).

Mutations in the DMRT3 gene were first discovered through genetic analysis of Icelandic horses which display an atypical 'pacing' gait wherein the fore- and hindlimbs of one side of the body move synchronously (Andersson et al., 2012). As left-right and flexor-extensor alternation are largely unimpaired within each pair of limbs, it stands to reason that mutations to this gene cause abnormalities in the cellular circuitry which coordinate activity between cervical and lumbar locomotor networks. Future research on the dI6 interneurons should therefore be designed to explain the altered coupling between fore- and hindlimbs. Particularly, it would be of interest to know whether dI6 interneurons themselves are long ascending interneurons which project from lumbar segments up into the cervical spinal cord, or whether they are merely locally restricted cells involved in relaying such information.

One of the main outstanding questions from the research presented here concerns the neurotransmitter phenotype of the dI6 interneuron population. Previous reports indicating dI6 cells are inhibitory have relied on the DMRT3 or Wt1 genetic markers (Andersson et al., 2012, Goulding, 2009). As it is unclear what proportion of the total dI6 population either of these markers captures, it cannot be concluded that the dI6 population is exclusively inhibitory. Methodological limitations of performing *in situ* hybridization in combination with immunohistochemistry for two proteins (EYFP and β-gal) has prevented our investigation of possible excitatory dI6 interneurons. Further experiments will obviate such limitations based on two lines of reasoning. First, results presented herein (Chapter 3) as well as published findings from the Kiehn laboratory (Talpalar et al., 2013) have indicated that the $V0_D$ subpopulation is inhibitory, utilizing either GABA, glycine or both. Secondly, previous characterization

of the TgDbx1^{Cre}:R26^{EFP}:Dbx1^{lacZ} mouse has indicated that almost all EFP^{+} cells located above the central canal are β-gal^{-} and are thus dI6 interneurons (Dyck et al., 2012). This finding has been presented as evidence that dI6 cells are preferentially targeted during electrophysiological recordings from EFP^{+} cells in the semi-intact preparation using either the TgDbx1^{Cre}R26^{EFP} or TgDbx1^{Cre}:R26^{EFP}:Dbx1^{lacZ} mouse. Since *in situ* hybridization combined with immunohistochemistry for only one protein should be possible, future experiments searching for excitatory dI6 cells will address vGluT2 mRNA expression in EFP^{+} cells in spinal cord sections from neonatal TgDbx1^{Cre}:R26^{EFP} mice. As V0$_{D}$ interneurons are inhibitory, any vGluT2^{+}/EFP^{+} interneurons must represent excitatory dI6 cells. Additionally, as few V0$_{D}$ cells are found dorsal to the central canal, any dorsally located vGluT2^{+}/EFP^{+} interneurons would provide evidence for the existence of excitatory dI6 cells. Of particular interest would be any excitatory dI6 cells within approximately 100μm of the central canal, as these would suggest excitatory dI6 cells were among those targeted for electrophysiological recordings.

Based on our conclusion that cells which fall silent during non-resetting deletions in activity of their local ventral root are members of the pattern forming layer and are thus premotor interneurons, an exclusively inhibitory nature for the dI6 population is surprising given that the majority of pPF dI6 cells fire in phase with ENG activity. Without a definitive identification of their downstream targets, several possibilities may explain this apparent discrepancy. As the dominant output from the L2 root is flexor-related, it is possible that pPF dI6 cells are inhibitory last-order CPG interneurons which synapse preferentially onto ipsilateral extensor motorneurons. Alternatively, pPF dI6 cells may inhibit contralateral flexor motorneurons. While neither explanation can be discounted, neither is entirely satisfactory given the results of our retrograde trans-synaptic tracing experiments. PRV-152 injection into the TA and GC muscles revealed no preferential innervation of extensor over flexor

motorneurons (nor *vice versa*). Moreover, the majority of the premotor dI6 cells were located within 1-2 segments of their target motorneuron and as such, it is unlikely that pPF dI6 cells project ipsilaterally to inhibit extensor motorneurons located in distal segments. It also seems unlikely that the pPF dI6 cells are predominantly commissural as the majority, though admittedly not all, of the last-order premotor dI6 interneurons identified at 38 h post-injection were located ipsilateral to the injected limb. The majority of the commissural interneurons in the spinal cord are located in lamina VIII. The *in vitro* semi-intact preparation employed to record from dI6 interneurons only grants access to EFP^+ cells located within 60um of the central canal. As such, more ventrally located interneurons, such as those situated in lamina VIII, would be inaccessible for intracellular recording. The most parsimonious explanation is that last-order premotor dI6 interneurons located in the upper lumbar segments synapse locally onto ipsilateral flexor motorneurons, and are therefore predicted to be excitatory. In the absence of any conclusive evidence that the dI6 population does not include an excitatory contingent, such a possibility cannot be discounted.

Examination of presumptive serotonergic varicosities in the spinal cord indicated that all three genetically-defined populations investigated are potential targets for neuromodulation from descending projections. Given the wealth of information available addressing serotonergic neuromodulation at the network level, further exploration of the effect of serotonin on the dI6, $V0_D$ and $V0_V$ interneurons will grant considerable insight into the cellular mechanisms through which monoamines modulate the locomotor rhythm. Future experiments addressing the serotonin receptor subtypes expressed by each population will direct future pharmacological research into the manner in which serotonin modulates the activity of these CPG interneurons. Such an approach has recently been adopted in the investigation of the

V2a interneurons, and has revealed subtleties about the maturation and function of this population (Husch et al., 2015).

Recent reports by Jovanovic et al. (2010) of the time course of virus transport following PRV-152 injection into the hindlimb musculature of the newborn rodent necessitated the re-evaluation of monosynaptic connectivity between V0 interneurons and contralaterally located motorneurons reported previously (Lanuza et al., 2004). Evaluation at the more conservative time point of 36 h post-injection indicated that V0 interneurons are not, in fact, monosynaptically connected to contralateral motorneurons. After a longer incubation to 48 h, PRV-152 infected contralateral V0 interneurons were found, indicating V0 interneurons form disynaptic contacts onto motorneurons. Findings reported here provide the first research into the connectivity between the two sub-populations of V0 interneurons and motorneurons. The finding that the majority of disynaptically connected V0 interneurons are of the ventral population is interesting in light of the fact that V2a interneurons contact $Evx1^{+}$ $V0_V$ interneurons (Crone et al., 2008).

Over the past 20 years, the advent of molecular genetic approaches has opened the door to rapid and substantive advances into understanding the development and inner workings of the mammalian locomotor CPG. By simply dividing the spinal cord into discrete populations, molecular genetics have fundamentally shifted the manner in which the spinal cord is studied. From their earliest discovery, transcription factors have provided a powerful tool for identifying, describing, and manipulating interneuron populations. The increasing array of elegant transgenic mouse lines create ever expanding opportunities for understanding the circuitry of the central nervous system. The present examination of $V0_V$, $V0_D$, and dI6 interneuron shed lights on the manner in which each is uniquely situated to serve specialized functions within the mammalian locomotor CPG.

References

Al-Mosawie A, Wilson JM, Brownstone RM. (2007) Heterogeneity of V2-derived interneurons in the adult mouse spinal cord. Eur J Neurosci. 26:3003-15.

Alvarez FJ, Jonas PC, Sapir T, Hartley R, Berrocal MC, Geiman EJ, Todd AJ, Goulding M. (2005) Postnatal phenotype and localization of spinal cord V1 derived interneurons. J Comp Neurol. 493:177-92.

Alvarez FJ, Villalba RM, Zerda R, Schneider SP. (2004) Vesicular glutamate transporters in the spinal cord, with special reference to sensory primary afferent synapses. J Comp Neurol. 472:257-80.

Andersson LS, Larhammar M, Memic F, Wootz H, Schwochow D, Rubin, CJ, Patra K, Arnason T, Wellbring L, Hjalm G, Imsland F, Petersen JL, McCue ME, Mickelson JR, Cothran G, Ahituv N, Roepstorff L, Mikko S, Vallstedt A, Lindgren G, Andersson, Kullander K. (2012) Mutations in DMRT3 affect locomotion in horses and spinal circuit function in mice. Nature. 488:642-46.

Angel MJ, Guertin P, Jiménez I, McCrea DA. (1996) Group I extensor afferents evoke disynaptic EPSPs in cat hindlimb extensor motorneurones during fictive locomotion. J Physiol. 494:851-61.

Angel MJ, Jankowska E, McCrea DA. (2005) Candidate interneurones mediating group I disynaptic EPSPs in extensor motoneurones during fictive locomotion in the cat. J Physiol. 563:597-610.

Arber S, Han B, Mendelsohn M, Smith M, Jessell TM, Sockanathan S. (1999) Requirement for the homeobox gene Hb9 in the consolidation of motor neuron identity. Neuron. 23:659-74.

Bermingham NA, Hassan BA, Wang VY, Fernandez M, Banfi S, Bellen HJ, Fritzsch B, Zoghbi HY. (2001) Proprioceptor pathway development is dependent on Math1. Neuron. 30:411-22.

Bertrand S, Cazalets JR. (2002) The respective contribution of lumbar segments to the generation of locomotion in the isolated spinal cord of newborn rat. Eur J Neurosci. 16:1741– 50.

Betley JN, Wright CV, Kawaguchi Y, Erdélyi F, Szabó G, Jessell TM, Kaltschmidt JA. (2009) Stringent specificity in the construction of a GABAergic presynaptic inhibitory circuit. Cell. 139:161-74.

Blacklaws J, Deska-Gauthier D, Jones CT, Petracca YL, Liu M, Zhang H, Fawcett JP, Glover JC, Lanuza GM, Zhang Y. (2015) Sim1 is required for the migration and axonal projections of V3 interneurons in the developing mouse spinal cord. Dev Neurobiol. 75:1003-17.

Bonnot A, Morin D. (1998) Hemisegmental localisation of rhythmic networks in the lumbosacral spinal cord of neonate mouse. Brain Res. 793:136–48.

Bonnot A, Whelan PJ, Mentis GZ, O'Donovan MJ. (2002) Locomotor-like activity generated by the neonatal mouse spinal cord. Brain Res Rev. 40:141–51.

Borowska J, Jones CT, Zhang H, Blacklaws J, Goulding M, Zhang Y. (2013) Functional subpopulations of V3 interneurons in the mature mouse spinal cord. J Neurosci. 33:18553-65.

Bracci E, Ballerini L, Nistri A. (1996) Localization of rhythmogenic networks responsible for spontaneous bursts induced by strychnine and bicuculline in the rat isolated spinal cord. J Neurosci. 16:7063–76.

Briscoe J, Ericson J. (2001) Specification of neuronal fates in the ventral neural tube. Curr Opin Neurobiol. 11:43-9.

Briscoe J, Sussel L, Serup P, Hartigan-O'Connor D, Jessell TM, Rubenstein JL, Ericson J. (1999) Homeobox gene Nkx2.2 and specification of neuronal identity by graded Sonic hedgehog signalling. Nature. 398:622-7.

Britz O, Zhang J, Grossmann KS, Dyck J, Kim JC, Dymecki S, Gosgnach S, Goulding M. (2015) A genetically defined asymmetry underlies the inhibitory control of flexor-extensor locomotor movements. Elife. 14;4.

Brown TG. (1911) The intrinsic factors in the act of progression in the mammals. Proc Roy Soc. 84:308.

Brownstone RM, Wilson JM. (2008) Strategies for delineating spinal locomotor rhythm-generating networks and the possible role of Hb9 interneurones in rhythmogenesis. Brain Res Rev. 57:64-76.

Buford JA, Smith JL. (1993) Adaptive control for backward quadrupedal walking. III. Stumbling corrective reactions and cutaneous reflex sensitivity. J Neurophysiol. 70:1102-14.

Bui TV, Akay T, Loubani O, Hnasko TS, Jessell TM, Brownstone RM. (2013) Circuits for grasping: spinal dI3 interneurons mediate cutaneous control of motor behavior. Neuron. 78:191-204.

Burrill JD, Moran L, Goulding MD, Saueressig H. (1997) PAX2 is expressed in multiple spinal cord interneurons, including a population of EN1+ interneurons that require PAX6 for their development. Development. 124:4493-503.

Butt SJ, Harris-Warrick RM, Kiehn O. (2002) Firing properties of identified interneuron populations in the mammalian hindlimb central pattern generator. J Neurosci. 22:9961-71.

Butt SJ, Kiehn O. (2003) Functional identification of interneurons responsible for left-right coordination of hindlimbs in mammals. Neuron. 38:953-63.

Butt SJ, Lebret JM, Kiehn O. (2002) Organization of left-right coordination in the mammalian locomotor network. Brain Res Rev. 40:107-17.

Carcagno AL, Di Bella DJ, Goulding M, Guillemot F, Lanuza GM. (2014) Neurogenin3 restricts serotonergic neuron differentiation to the hindbrain. J Neurosci 34:15223–33.

Carr PA, Alvarez FJ, Leman EA, Fyffe RE. (1998) Calbindin D28k expression in immunohistochemically identified Renshaw cells. Neuroreport. 9:2657-61.

Cazalets JR, Borde M, Clarac F. (1995) Localization and organization of the central pattern generator for hindlimb locomotion in newborn rat. J.Neurosci. 15:4943–51.

Cheng L, Arata A, Mizuguchi R, Qian Y, Karunaratne A, Gray PA, Arata S, Shirasawa S, Bouchard M, Luo P, Chen CL, Busslinger M, Goulding M, Onimaru H, Ma Q. (2004) Tlx3 and Tlx1 are post-mitotic selector genes determining glutamatergic over GABAergic cell fates. Nat Neurosci. 7:510-7.

Cheng L, Samad OA, Xu Y, Mizuguchi R, Luo P, Shirasawa S, Goulding M, Ma Q. (2005) Lbx1 and Tlx3 are opposing switches in determining GABAergic versus glutamatergic transmitter phenotypes. Nat Neurosci. 8:1510-5.

Conway BA, Hultborn H, Kiehn O. (1987) Proprioceptive input resets central locomotor rhythm in the spinal cat. Exp Brain Res. 68:643-56.

Coulon P, Bras H, Vinay L. (2011) Characterization of last-order premotor interneurons by transneuronal tracing with rabies virus in the neonatal mouse spinal cord. J Comp Neurol. 519:3470-87.

Cowley KC, Schmidt BJ. (1997) Regional distribution of the locomotor pattern-generating network in the neonatal rat spinal cord. J Neurophysiol. 77:247–59

Crone SA, Quinlan KA, Zagoraiou L, Droho S, Restrepo CE, Lundfald L, Endo T, Setlak J, Jessell TM, Kiehn O, Sharma K. (2008) Genetic ablation of V2a ipsilateral interneurons disrupts left-right locomotor coordination in mammalian spinal cord. Neuron. 60:70-83.

Crone SA, Zhong G, Harris-Warrick R, Sharma K. (2009) In mice lacking V2a interneurons, gait depends on speed of locomotion. J Neurosci. 29:7098-109.

Cullheim S, Kellerth JO. (1981) Two kinds of recurrent inhibition of cat spinal alpha-motoneurones as differentiated pharmacologically. J Physiol. 312:209-24.

Curtis DR. (1959) Pharmacological investigations upon inhibition of spinal motoneurones. J Physiol. 145:175-92.

Curtis DR, Hösli L, Johnston GA, Johnston IH. (1968) The hyperpolarization of spinal motoneurones by glycine and related amino acids. Exp Brain Res. 5:235-58.

Dyck J, Lanuza GM, Gosgnach S. (2012) Functional characterization of dI6 interneurons in the neonatal mouse spinal cord. J Neurophysiol. 107:3256-66

Ding YQ, Yin J, Kania A, Zhao ZQ, Johnson RL, Chen ZF. (2004) Lmx1b controls the differentiation and migration of the superficial dorsal horn neurons of the spinal cord. Development. 131:3693-703.

Dougherty KJ, Kiehn O. (2010) Functional organization of V2a-related locomotor circuits in the rodent spinal cord. Ann N Y Acad Sci. 1198:85-93.

Dueñas S, Rudomin P (1988) Excitability changes of ankle extensor group Ia and Ib fibers during fictive locomotion in the cat. Exp Brain Res 70:15–25.

Duysens J, Pearson KG. (1980) Inhibition of flexor burst generation by loading ankle extensor muscles in walking cats. Brain Res. 187:321-32.

Dueñas S, Rudomin P. (1993) Reversal of the effects of cutaneous afferents on PAD of Ib fibers during fictive locomotion. Soc Neurosci Abstr 19:225.

Eccles RM, Lundberg A. (1959) Synaptic actions in motoneurones by afferents which may evoke the flexion reflex. Arch Ital Biol. 97:199-221.

Eccles JC, Fatt P, Koketsu K. (1954) Cholinergic and inhibitory synapses in a pathway from motor-axon collaterals to motoneurones. J Physiol. 126:524-62.

Eccles JC, Kostyuk PG, Schmidt RF. (1962*a*) Central pathways responsible for depolarization of primary afferent fibres. J Physiol. 161:237-57.

Eccles JC, Kostyuk PG, Schmidt RF. (1962*b*) Presynaptic inhibition of the central actions of flexor reflex afferents. J Physiol. 161:258-81.

Eccles JC, Schmidt RF, Willis WD. (1962*c*) Presynaptic inhibition of the spinal monosynaptic reflex pathway. J Physiol. 161:282-97.

Eccles JC, Fatt P, Landgren S. (1956) Central pathway for direct inhibitory action of impulses in largest afferent nerve fibres to muscle. J Neurophysiol. 19:75-98.

Edgley SA, Jankowska E. (1987) An interneuronal relay for group I and II muscle afferents in the midlumbar segments of the cat spinal cord. J Physiol. 389:647-74.

Eide AL, Glover J, Kjaerulff O, Kiehn O. (1999) Characterization of commissural interneurons in the lumbar region of the neonatal rat spinal cord. J Comp Neurol. 403:332–45.

Engberg I, Lundberg A. (1969) An electromyographic analysis of muscular activity in the hindlimb of the cat during unrestrained locomotion. Acta Physiol Scand. 75:614-30.

English AW. (1978) An electromyographic analysis of forelimb muscles during overground stepping in the cat. J Exp Biol. 76:105-22.

Ericson J, Rashbass P, Schedl A, Brenner-Morton S, Kawakami A, van Heyningen V, Jessell TM, Briscoe J. (1997) Pax6 controls progenitor cell identity and neuronal fate in response to graded Shh signaling. Cell. 90:169-80.

Feldman AG, Orlovsky GN. (1975) Activity of interneurons mediating reciprocal 1a inhibition during locomotion. Brain Res. 84:181-94.

Forssberg H. (1979) Stumbling corrective reaction: a phase-dependent compensatory reaction during locomotion. J Neurophysiol. 42:936-53.

Forssberg H, Grillner S, Rossignol S. (1977) Phasic gain control of reflexes from the dorsum of the paw during spinal locomotion. Brain Res 132: 121–39.

Geertsen SS, Stecina K, Meehan CF, Nielsen JB, Hultborn H. (2011) Reciprocal Ia inhibition contributes to motoneuronal hyperpolarisation during the inactive phase of locomotion and scratching in the cat. J Physiol. 589:119-34.

Glasgow SM, Henke RM, MacDonald RJ, Wright CVE, Johnson JE. (2005) Ptf1a determines GABAergic over glutamatergic neuronal cell fate in the spinal cord dorsal horn. Development 2005 132: 5461-9.

Goetz C, Pivetta C, Arber S. (2015) Distinct limb and trunk premotor circuits establish laterality in the spinal cord. Neuron. 85:131-44.

Gosgnach S, Lanuza GM, Butt SJ, Saueressig H, Zhang Y, Velasquez T, Riethmacher D, Callaway EM, Kiehn O, Goulding M. (2006) V1 spinal neurons regulate the speed of vertebrate locomotor outputs. Nature. 440:215–19.

Gosgnach S, Quevedo J, Fedirchuk B, McCrea DA. (2000) Depression of group Ia monosynaptic EPSPs in cat hindlimb motoneurones during fictive locomotion. J Physiol. 526:639-52.

Gossard JP. (1996) Control of transmission in muscle group Ia afferents during fictive locomotion in the cat. J Neurophysiol 76:4104–12

Goulding M. (2009) Circuits controlling vertebrate locomotion: moving in a new direction. Nat Rev Neurosci. 10:507-18.

Goulding M, Lanuza G, Sapir T, Narayan S. (2002) The formation of sensorimotor circuits. Curr Opin Neurobiol. 12:508–15.

Gowan K, Helms AW, Hunsaker TL, Collisson T, Ebert PJ, Odom R, Johnson JE. (2001) Crossinhibitory activities of Ngn1 and Math1 allow specification of distinct dorsal interneurons. Neuron. 31:219-32.

Grillner S, Rossignol S. (1978) On the initiation of the swing phase of locomotion in chronic spinal cats. Brain Res. 146:269-77.

Grillner S, Zangger P. (1979) On the central generation of locomotion in the low spinal cat. Exp Brain Res. 34:241–61.

Gross MK, Dottori M, Goulding M. (2002) Lbx1 specifies somatosensory association interneurons in the dorsal spinal cord. Neuron. 34:535-49.

Guertin PA. (2014) Preclinical evidence supporting the clinical development of central pattern generator-modulating therapies for chronic spinal cord-injured patients. Front Hum Neurosci. 8:272. eCollection

Guertin P, Angel MJ, Perreault MC, McCrea DA. (1995) Ankle extensor group I afferents excite extensors throughout the hindlimb during fictive locomotion in the cat. J Physiol. 487:197-209.

Hägglund M, Dougherty KJ, Borgius L, Itohara S, Iwasato T, Kiehn O. (2013) Optogenetic dissection reveals multiple rhythmogenic modules underlying locomotion. Proc Natl Acad Sci U S A. 110:11589-94.

Hargrave M, Karunaratne A, Cox L, Wood S, Koopman P, Yamada T. (2000) The HMG box transcription factor gene Sox14 marks a novel subset of ventral interneurons and is regulated by sonic hedgehog. Dev Biol. 219:142-53.

Harkema SJ. (2001) Neural plasticity after human spinal cord injury: application of locomotor training to the rehabilitation of walking. Neuroscientist. 7:455-68.

Helms AW, Battiste J, Henke RM, Nakada Y, Simplicio N, Guillemot F, Johnson JE. (2005) Sequential roles for Mash1 and Ngn2 in the generation of dorsal spinal cord interneurons. Development. 132:2709-19.

Helms AW, Johnson JE. (1998) Progenitors of dorsal commissural interneurons are defined by MATH1 expression. Development. 125:919-28.

Helms AW, Johnson JE. (2003) Specification of dorsal spinal cord interneurons. Curr Opin Neurobiol. 13:42-9.

Hiebert GW, Whelan PJ, Prochazka A, Pearson KG. (1996) Contribution of hind limb flexor muscle afferents to the timing of phase transitions in the cat step cycle. J Neurophysiol. 75:1126-37.

Hinckley CA, Ziskind-Conhaim L. (2006) Electrical coupling between locomotor-related excitatory interneurons in the mammalian spinal cord. J Neurosci. 26:8477-83.

Hinckley CA, Hartley R, Wu L, Todd A, Ziskind-Conhaim L. (2005) Locomotor-like rhythms in a genetically distinct cluster of interneurons in the mammalian spinal cord. J Neurophysiol. 93:1439-49.

Hinckley CA, Wiesner EP, Mentis GZ, Titus DJ, Ziskind-Conhaim L. (2010) Sensory modulation of locomotor-like membrane oscillations in Hb9-expressing interneurons. J Neurophysiol. 103:3407-23.

Holmqvist B, Lundberg A. (1961) Differential supraspinal control of synaptic actions evoked by volleys in the flexion reflex afferents in alpha motoneurones. Acta Physiol Scand. 54:1-51.

Hultborn H, Illert M, Santini M. (1976) Convergence on interneurones mediating the reciprocal Ia inhibition of motoneurones. I. Disynaptic Ia inhibition of Ia inhibitory interneurones. Acta Physiol Scand. 96: 193-201.

Hultborn H, Jankowska E, Lindström S. (1971) Recurrent inhibition of interneurones monosynaptically activated from group Ia afferents. J Physiol. 215:613-36.

Husch A, Dietz SB, Hong DN, Harris-Warrick RM. (2015) Adult spinal V2a interneurons show increased excitability and serotonin-dependent bistability. J Neurophysiol. 113:1124-34.

Ito M. (2002) Historical review of the significance of the cerebellum and the role of Purkinje cells in motor learning. Ann N Y Acad Sci. 978:273-88.

Jankowska E, Jukes MG, Lund S, Lundberg A. (1967*a*) The effect of DOPA on the spinal cord. 5. Reciprocal organization of pathways transmitting excitatory action to alpha motoneurones of flexors and extensors. Acta Physiol Scand.70:369-88.

Jankowska E, Jukes MG, Lund S, Lundberg A. (1967*b*) The effect of DOPA on the spinal cord. 6. Half-centre organization of interneurones transmitting effects from the flexor reflex afferents. Acta Physiol Scand. 70:389-402.

Jankowska E. (1992) Interneuronal relay in spinal pathways from proprioceptors. Prog Neurobiol. 38:335-78.

Jankowska E, Lindström S. (1971) Morphological identification of Renshaw cells. Acta Physiol Scand. 81:428-30.

Jankowska E, McCrea D, Mackel R. (1981) Pattern of 'non-reciprocal' inhibition of motoneurones by impulses in group Ia muscle spindle afferents in the cat. J Physiol. 316:393-409.

Jankowska E, McCrea D, Rudomin P, Sykova E. (1981) Observations on neuronal pathways subserving primary afferent depolarization. J Neurophysiol 46:506–516.

Jankowska E, Riddell JS. (1998) Neuronal systems involved in modulating synaptic transmission from group II muscle afferents. In: Rudomin P, Romo R, Mendell L (eds) Presynaptic inhibition and neural control. Oxford University Press, New York, pp 315–328.

Jankowska E, Slawinska U, Hammar I. (2002) On organization of a neuronal network in pathways from group II muscle afferents in feline lumbar spinal segments. J Physiol. 542:301-14.

Kam K, Worrell JW, Ventalon C, Emiliani V, Feldman JL. (2013) Distinct inspiratory rhythm and pattern generating mechanisms in the preBötzinger complex. J Neurosci. 33:9235-45.

Karunaratne A, Hargrave M, Poh A, Yamada T. (2002) GATA proteins identify a novel ventral interneuron subclass in the developing chick spinal cord. Dev Biol. 249:30-43.

Kiehn O, Butt SJ. (2003) Physiological, anatomical and genetic identification of CPG neurons in the developing mammalian spinal cord. Prog Neurobiol. 70:347–61.

Kjaerulff O, Barajon I, Kiehn O. (1994) Sulphorhodamine-labeled cells in the neonatal rat spinal cord following chemically induced locomotor activity in vitro. J Physiol. 478:265–73.

Kjaerulff O, Kiehn O. (1996) Distribution of networks generating and coordinating locomotor activity in the neonatal rat spinal cord in vitro: a lesion study. J Neurosci. 16:5777–94.

Kjaerulff O, Kiehn O. (1997) Crossed rhythmic synaptic input to motorneurons during selective activation of the contralateral spinal locomotor network. J Neurosci. 17:9433–47.

Kremer E, Lev-Tov A. (1997) Localization of the spinal network associated with generation of hindlimb locomotion in the neonatal rat and organization of its transverse coupling system. J Neurophysiol. 77:1155–70.

Kiehn O, Kjaerulff O. (1998) Distribution of central pattern generators for rhythmic motor outputs in the spinal cord of limbed vertebrates. Ann NY Acad Sci. 860:110–29.

Kriellaars DJ, Brownstone RM, Noga BR, Jordan LM. (1994) Mechanical entrainment of fictive locomotion in the decerebrate cat. J Neurophysiol. 71:2074-86.

Kudo N, Yamada T. (1987) N-methyl-D,L-aspartate-induced locomotor activity in a spinal cord-hindlimb muscles preparation of the newborn rat studied in vitro. Neurosci Lett. 75:43–48.

Kwan AC, Dietz SB, Webb WW, Harris-Warrick RM. (2009) Activity of Hb9 interneurons during fictive locomotion in mouse spinal cord. J Neurosci. 29:11601-13.

Lafreniere-Roula M, McCrea DA. (2005) Deletions of rhythmic motoneuron activity during fictive locomotion and scratch provide clues to the organization of the mammalian central pattern generator. J Neurophysiol. 94:1120–32.

Lanuza GM, Gosgnach S, Pierani A, Jessell TM, Goulding M. (2004) Genetic identification of spinal interneurons that coordinate left-right locomotor activity necessary for walking movements. Neuron. 42:375-86.

Lee KJ, Jessell TM. (1999) The specification of dorsal cell fates in the vertebrate central nervous system. Annu Rev Neurosci. 22:261-94.

Lev-Tov, A., Delvolvé, I., and Kremer, E. (2000) Sacrocaudal afferents induce rhythmic efferent bursting in isolated spinal cords of neonatal rats. J Neurophysiol. 83, 888-94.

Liem KF, G. Tremml, T.M. Jessell. (1997) A role for the roof plate and its resident TGFbeta-related proteins in neuronal patterning in the dorsal spinal cord. Cell. 91:127–38.

Lundberg A, Malmgren K, Schomburg ED. (1977) Comments on reflex actions evoked by electrical stimulation of group II muscle afferents. Brain Res. 122:551-5.

Lundfald L, Restrepo CE, Butt SJ, Peng CY, Droho S, Endo T, Zeilhofer HU, Sharma K, Kiehn O. (2007) Phenotype of V2-derived interneurons and their relationship to the axon guidance molecule EphA4 in the developing mouse spinal cord. Eur J Neurosci. 26:2989-3002.

Magnuson DS, Lovett R, Coffee C, Gray R, Han Y, Zhang YP, Burke DA. (2005) Functional consequences of lumbar spinal cord contusion injuries in the adult rat. J Neurotrauma. 22:529–43.

Marchetti C, Beato M, Nistri A. (2001) Alternating rhythmic activity induced by dorsal root stimulation in the neonatal rat spinal cord in vitro. J Physiol. 530:105-12.

McCrea DA. (2001) Spinal circuitry of sensorimotor control of locomotion. J Physiol. 533:41-50.

McCrea DA, Pratt CA, Jordan LM. (1980) Renshaw cell activity and recurrent effects on motoneurons during fictive locomotion. J Neurophysiol. 44:475-88.

McCrea DA, Rybak IA. (2008) Organization of mammalian locomotor rhythm and pattern generation. Brain Res Rev. 57:134-46.

Meehan CF, Grondahl L, Nielsen JB, Hultborn H. (2012) Fictive locomotion in the adult decerebrate and spinal mouse in vivo. J Physiol. 590:289-300.

Miller S, Scott PD. (1977) The spinal locomotor generator. Exp Brain Res. 30:387-403.

Miesegaes GR, Klisch TJ, Thaller C, Ahmad KA, Atkinson RC, Zoghbi HY. (2009) Identification and subclassification of new Atoh1 derived cell populations during mouse spinal cord development. Dev Biol. 327:339-51.

Millan MJ. (1999) The induction of pain: an integrative review. Prog Neurobiol. 57:1-164.

Moran-Rivard L, Kagawa T, Saueressig H, Gross MK, Burrill J, Goulding M. (2001) Evx1 is a postmitotic determinant of V0 interneuron identity in the spinal cord. Neuron. 29:385-99.

Müller T, Brohmann H, Pierani A, Heppenstall PA, Lewin GR, Jessell TM, Birchmeier C. (2002) The homeodomain factor lbx1 distinguishes two major programs of neuronal differentiation in the dorsal spinal cord. Neuron. 34:551-62.

Nakanishi ST, Whelan PJ. (2012) A decerebrate adult mouse model for examining the sensorimotor control of locomotion. J Neurophysiol. 2012 107:500-15.

Nishimaru H, Restrepo CE, Kiehn O. (2006) Activity of Renshaw cells during locomotor-like rhythmic activity in the isolated spinal cord of neonatal mice. J Neurosci. 26:5320-8.

Noga BR, Shefchyk SJ, Jamal J, Jordan LM. (1987) The role of Renshaw cells in locomotion: antagonism of their excitation from motor axon collaterals with intravenous mecamylamine. Exp Brain Res. 66:99-105.

Novak A, Guo C, Yang W, Nagy A, Lobe CG. (2000) Z/EG, a double reporter mouse line that expresses enhanced fluorescent protein upon Cre-mediated excision. Genesis. 28:147-55.

Oliveira AL, Hydling F, Olsson E, Shi T, Edwards RH, Fujiyama F, Kaneko T, Hökfelt T, Cullheim S, Meister B. (2003) Cellular localization of three vesicular glutamate transporter mRNAs and proteins in rat spinal cord and dorsal root ganglia. Synapse. 50:117-29.

Panayi H, Panayiotou E, Orford M, Genethliou N, Mean R, Lapathitis G, Li S, Xiang M, Kessaris N, Richardson WD, Malas S. (2010) Sox1 is required for the specification of a novel p2-derived interneuron subtype in the mouse ventral spinal cord. J Neurosci. 30:12274-80.

Peng CY, Yajima H, Burns CE, Zon LI, Sisodia SS, Pfaff SL, Sharma K. (2007) Notch and MAML signaling drives Scl-dependent interneuron diversity in the spinal cord. Neuron. 53:813-27.

Pfaff SL, Mendelsohn M, Stewart CL, Edlund T, Jessell TM. (1996) Requirement for LIM homeobox gene Isl1 in motor neuron generation reveals a motor neuron-dependent step in interneuron differentiation. Cell. 84:309-20.

Piercey MF, Goldfarb J. (1974) Discharge patterns of Renshaw cells evoked by volleys in ipsilateral cutaneous and high-threshold muscle afferents and their relationship to reflexes recorded in ventral roots. J Neurophysiol. 37:294-302.

Pierani A, Moran-Rivard L, Sunshine MJ, Littman DR, Goulding M, Jessell TM. (2001) Control of interneuron fate in the developing spinal cord by the progenitor homeodomain protein Dbx1. Neuron. 29:367-84.

Pillai A, Mansouri A, Behringer R, Westphal H, Goulding M. (2007) Lhx1 and Lhx5 maintain the inhibitory-neurotransmitter status of interneurons in the dorsal spinal cord. Development. 134:357-66.

Pratt CA, Buford JA, and Smith JL. (1996) Adaptive control for backward quadrupedal walking V. Mutable activation of bifunctional thigh muscles. J Neurophysiol 75: 832–842.

Pratt CA, Jordan LM. (1987) Ia inhibitory interneurons and Renshaw cells as contributors to the spinal mechanisms of fictive locomotion. J Neurophysiol. 57:56-71.

Prochazka A, Sontag KH, and Wand P. (1978) Motor reactions to perturbations of gait: proprioceptive and somesthetic involvement. Neurosci Lett 7: 35–39.

Quevedo J, Stecina K, and McCrea DA. (2005*a*) Intracellular analysis of reflex pathways underlying the stumbling corrective reaction during fictive locomotion in the cat. J Neurophysiol 94: 2053–2062.

Quevedo J, Stecina K, Gosgnach S, McCrea DA. (2005*b*) Stumbling corrective reaction during fictive locomotion in the cat. J Neurophysiol. 94:2045-52.

Quinlan KA, Kiehn O. (2007) Segmental, synaptic actions of commissural interneurons in the mouse spinal cord. J Neurosci. 27:6521-30.

Rabe N, Gezelius H, Vallstedt A, Memic F, Kullander K. (2009) Netrin-1-dependent spinal interneuron subtypes are required for the formation of left-right alternating locomotor circuitry. J Neurosci. 29:15642-9.

Rossignol, S. (1996) Neural control of stereotypic limb movements. In Handbook of Physiology, section 12, Exercise: Regulation and Integration of Multiple Systems, ed. Rowell, L. & Shepherd, J., pp. 173–216. American Physiological Society, New York.

Rudomin P. (1990) Presynaptic inhibition of muscle spindle and tendon organ afferents in the mammalian spinal cord. Trends Neurosci. 13:499-505.

Rudomin P, Jiménez I, Solodkin M, Dueñas S. (1983) Sites of action of segmental and descending control of transmission on pathways mediating PAD of Ia- and Ib-afferent fibers in cat spinal cord. J Neurophysiol. 50:743–769.

Rudomin P, Jiménez I, Quevedo J, Solodkin M. (1990) Pharmacologic analysis of inhibition produced by last-order intermediate nucleus interneurons mediating nonreciprocal inhibition of motoneurons in cat spinal cord. J Neurophysiol. 63:147-60.

Rudomin P, Schmidt RF. (1999) Presynaptic inhibition in the vertebrate spinal cord revisited. Exp Brain Res. 129:1-37.

Ryall RW. (1981) Patterns of recurrent excitation and mutual inhibition of cat Renshaw cells. J Physiol. 316:439-52.

Ryall RW, Piercey MF. (1971) Excitation and inhibition of Renshaw cells by impulses in peripheral afferent nerve fibers. J Neurophysiol. 34:242-51.

Sapir T, Geiman EJ, Wang Z, Velasquez T, Mitsui S, Yoshihara Y, Frank E, Alvarez FJ, Goulding M. (2004) Pax6 and engrailed 1 regulate two distinct aspects of renshaw cell development. J Neurosci. 24:1255-64.

Saueressig H, Burrill J, Goulding M. (1999) Engrailed-1 and netrin-1 regulate axon pathfinding by association interneurons that project to motor neurons. Development. 126:4201-12.

Sherrington CS. (1910) Flexion-reflex of the limb, crossed extension-reflex, and reflex stepping and standing. J Physiol. 40:28-121.

Shik M, Severin F, Orlovsky G. (1966) Control of walking and running by means of electrical stimulation of the mid-brain. Biophysics. 11:756-65.

Stepien AE, Tripodi M, Arber S. (2010) Monosynaptic rabies virus reveals premotor network organization and synaptic specificity of cholinergic partition cells. Neuron. 68:456-72.

Stokke MF, Nissen UV, Glover JC, Kiehn O. (2002) Projection patterns of commissural interneurons in the lumbar spinal cord of the neonatal rat. J Comp Neurol. 446:349–59.

Szabo NE, da Silva RV, Sotocinal SG, Zeilhofer HU, Mogil JS, Kania A. (2015) Hoxb8 intersection defines a role for Lmx1b in excitatory dorsal horn neuron development, spinofugal connectivity, and nociception. J Neurosci. 35:5233-46.

Talpalar AE, Bouvier J, Borgius L, Fortin G, Pierani A, Kiehn O. (2013) Dual-mode operation of neuronal networks involved in left-right alternation. Nature. 500:85-8.

Wand P, Prochazka A, Sontag KH. (1980) Neuromuscular responses to gait perturbations in freely moving cats. Exp Brain Res 38: 109–114.

Wang Z, Li L, Goulding M. (2008) Early postnatal development of reciprocal Ia inhibition in the murine spinal cord. J Neurophysiol. 100: 185-96.

Whelan PJ. (1996) Control of locomotion in the decerebrate cat. Prog Neurobiol. 49:481-515.

Whelan P, Bonnot A, O'Donovan MJ. (2000) Properties of rhythmic activity generated by the isolated spinal cord of the neonatal mouse. J Neurophysiol. 84:2821-33.

Wilson JM, Cowan AI, Brownstone RM. (2007) Heterogeneous electrotonic coupling and synchronization of rhythmic bursting activity in mouse Hb9 interneurons. J Neurophysiol. 98:2370-81.

Wilson JM, Hartley R, Maxwell DJ, Todd AJ, Lieberam I, Kaltschmidt JA, Yoshida Y, Jessell TM, Brownstone RM. (2005) Conditional rhythmicity of ventral spinal interneurons defined by expression of the Hb9 homeodomain protein. J Neurosci. 25:5710-9.

Wilson SI, Shafer B, Lee KJ, Dodd J. (2008) A molecular program for contralateral trajectory: Rig-1 control by LIM homeodomain transcription factors. Neuron. 59:413-24.

Wilson VJ, Kato M. (1956) Excitation of extensor motorneurons by group II afferent fibres in ipsilateral muscle nerves. J Neurophysiol. 28:545-54.

Wilson VJ, Talbot WH, Kato M. (1964) Inhibitory convergence upon Renshaw cells. J Neurophysiol. 27:1063-79.

Yang JF, Lam T, Pang MY, Lamont E, Musselman K, Seinen E. (2004) Infant stepping: a window to the behaviour of the human pattern generator for walking. Can J Physiol Pharmacol. 82:662-74.

Zagoraiou L, Akay T, Martin JF, Brownstone RM, Jessell TM, Miles GB. (2009) A cluster of cholinergic premotor interneurons modulates mouse locomotor activity. Neuron. 64:645-62.

Zaporozhets E, Cowley KC, Schmidt BJ. (2004) A reliable technique for the induction of locomotor-like activity in the in vitro neonatal rat spinal cord using brainstem electrical stimulation. J Neurosci Methods. 139:33-41.

Zhang J, Lanuza GM, Britz O, Wang Z, Siembab VC, Zhang Y, Velasquez T, Alvarez FJ, Frank E, Goulding M. (2014) V1 and V2b interneurons secure the alternating flexor-extensor motor activity mice require for limbed locomotion. Neuron. 82:138-50.

Zhang Y, Narayan S, Geiman E, Lanuza GM, Velasquez T, Shanks B, Akay T, Dyck J, Pearson K, Gosgnach S, Fan CM, Goulding M. (2008) V3 spinal neurons establish a robust and balanced locomotor rhythm during walking. Neuron. 60:84-96.

Zhong G, Droho S, Crone SA, Dietz S, Kwan AC, Webb WW, Sharma K, Harris-Warrick RM. (2010) Electrophysiological characterization of V2a interneurons and their locomotor-related activity in the neonatal mouse spinal cord. J Neurosci. 30:170-82.

Zhong G, Shevtsova NA, Rybak IA, Harris-Warrick RM. (2012) Neuronal activity in the isolated mouse spinal cord during spontaneous deletions in fictive locomotion: insights into locomotor central pattern generator organization. J Physiol. 590:4735-59.